Dynamic Amplification Effect on Bridges under Traffic Loads: Parametric Study and Novel Design Integration Approach

Amal Pradeep

A thesis

In the Department

of

Building Civil and Environmental Engineering

Presented in Partial Fulfillment of the Requirements

for the degree of Master of Applied Science (Civil Engineering) at

Concordia University

Montreal, Québec, Canada

CONCORDIA UNIVERSITY

SCHOOL OF GRADUATE STUDIES

This is to certify that the thesis prepared

By: Amal Pradeep

Entitled: Dynamic Amplification Effect on Bridges under Traffic Loads: Parametric Study and Novel Design Integration Approach

and submitted in partial fulfillment of the requirements for the degree of

Master of Applied Science (Civil Engineering)

Complies with the regulations of the University and meets the accepted standards with respect to originality and quality.

Signed by the final examining committee:

____ Chair

Dr. Khaled Galal

____ Examiner

Dr. Ramin Sedaghati

____ Examiner

Dr. Anjan Bhowmick

____ Thesis Supervisor

Dr. Ashutosh Bagchi

Approved by ____

Dr. Chunjiang An, Graduate Program Director

Tuesday, January 21, 2025 ______________________________

Dr. Mourad Debbabi,

Dean of Gina Cody School of Engineering and Computer Science

Abstract

Dynamic Amplification Effect on Bridges under Traffic Loads: Parametric Study and Novel Design Integration Approach

Amal Pradeep

Bridges are critical infrastructure that significantly contribute to connectivity and economic growth. Ensuring their durability necessitates addressing dynamic effects from traffic loads, quantified through the Dynamic Amplification Factor (DAF). This factor, influenced by bridge and vehicle parameters, poses challenges for accurate assessment due to the complex interplay of these factors.

This study undertook a comparative analysis of analytical models and revealed that DAF can be reliably estimated using bridge parameters. Results highlighted notable DAF variations even among bridges with similar spans and frequencies, exposing limitations in current design codes. While dynamic amplification generally decreased with increasing bridge span, the reduction also depended on bridge frequency. Higher vehicle velocities elevated DAF, but no consistent trend emerged due to the influence of bridge characteristics.

A 3D Finite Element Model in Abaqus, incorporating skew angles through the Vdload subroutine, showed minimal DAF variation for skew angles up to 30°, with a 20% increase observed at 45°. These findings emphasize the significance of skew angles on dynamic amplification.

The study proposes a DAF estimation approach based on bridge span and frequency. Validation against dynamic load test data showed consistency in 15 of 17 cases, with an error margin below 5%. A regression-based formula was developed, demonstrating alignment with existing codes while identifying inadequacies in DAF values for short to medium-span bridges.

Acknowledgements

First and foremost, I extend my heartfelt gratitude to my supervisor, Dr. Ashutosh Bagchi, for his steadfast support and invaluable guidance throughout my research journey. His encouragement during times of uncertainty has been instrumental in helping me stay focused on my research.

I am also deeply thankful to the examining committee—Dr. Anjan Bhowmick, Dr. Khaled Galal, and Dr. Ramin Sedaghati—for their insightful feedback during the thesis examination. My sincere thanks go to Dr. Alireza Haghighatmamaghani for his support, which has significantly enriched my research.

I would like to express my deepest gratitude to Dr. Bikram Kesharee Patra, Dr. Avirup Sarkar, and Saikat Bagchi for their friendship, support and guidance throughout this journey. My heartfelt thanks also go to Anant Nair, Anupam Menon, and Vaisakh Sreekumar for their friendship and constant encouragement.

Finally, I sincerely thank the Almighty for His abundant blessings, guidance, and strength. I am also profoundly grateful to my family for their unwavering love, support, and encouragement throughout this journey.

Table of Contents

List of figures

List of Tables

Chapter 01

1 Introduction

1.1 Dynamic Amplification Factor

Bridges are essential for maintaining the smooth flow of traffic and for facilitating trade, making them vital to a nation's economy. The long-term performance of a bridge can only be guaranteed by carefully addressing both design and construction aspects. Therefore, in terms of design, it is crucial to accurately account for all different static and dynamic loads into consideration. Among the various dynamic loads acting on a bridge, traffic load is one of the most significant loads acting on the structure.

As a vehicle traverses a bridge, it undergoes oscillations characterized by a specific frequency (AASHTO, 1962). The dynamic forces generated by these oscillations, in addition to the vehicle's weight, continually affect the bridge, causing the dynamic effect of the moving load. This interaction between the bridge and the vehicle leads to an amplified response of the coupled system and the effect is introduced into design in the form of Dynamic Amplification Factor (DAF). This dynamic effect is quantified by treating it as an increment of the static load caused by traffic load. Thus, the dynamic amplification factor (DAF) is defined as the '*ratio of the maximum total response of the structure to the corresponding static load*' (Paeglite, 2013).

$$DAF = \frac{Maximum\ Total\ Load\ Response}{Maximum\ Static\ Load\ Response} \qquad (1)$$

The first attempt to understand the dynamic amplification effect was made by R. Willis in 1849, as he investigated the causes behind a series of railway bridge failures in Britain. However, it took another 78 years before this effect was incorporated into the design of regular bridges. In 1927, the American Association of State Highway and Transportation Officials (AASHTO) was the first to include this dynamic effect in bridge design, using the term "Impact Factor" (Cantieni, 1983). Over time, this concept has been adopted into various design codes under different terminologies. When examining various bridge design codes, it becomes clear that the dynamic amplification effect is integrated into the codes in the form of Dynamic Amplification Factor (DAF), Dynamic Load Allowance (DLA), or Impact Factor (IM) (Deng, 2015). The relationship between these terms is as follows:

$$\mathrm{DLA} = \mathrm{IM} = \mathrm{DAF} - 1 \tag{2}$$

Here, the Dynamic load allowance or Impact factor is the ratio between the maximum dynamic load response to the maximum static load response and thus the values are lesser than 1. To compute the live load effect which is caused due to the design traffic loads on a bridge, the static load is factored by the corresponding dynamic amplification factor of the specific bridge model.

$$\text{Live Load} = \text{Dynamic Amplification Factor} * \text{Static Load effect} \tag{3}$$

The magnitude of the dynamic amplification effect depends on several factors, which can be broadly classified into bridge and vehicle parameters. Key bridge parameters influencing this effect include bridge span, bridge frequency, and road surface irregularities, while major vehicle parameters include vehicle weight, the number of axles, and the characteristics of the suspension system.

1.2 Relevance of the accuracy in computation of Dynamic amplification on bridges

Induced vibrations on bridges primarily stem from factors such as wind, traffic loads, and natural disasters like earthquakes. Vibrations generated by any of these sources pose potential threats to the structural integrity of the bridge and thus failure to adequately account for the dynamic effects in the design process can result in fatigue in bridge components, decreasing bridge lifetime and increase of bridge maintenance cost (McLean, 1998), (Cebon, 1999).

These vibrations are detrimental and thus can even become the root cause for failure in combination with other factors. In the context of traffic loads, amplified dynamic effects may arise from a combination of factors, including braking, acceleration, wind loading, surface irregularities, unbalanced loading and inclined road surfaces (Ludescher, 2009). The critical scenario emerges when these factors combine, leading to an amplification beyond the design criteria. Such vibrations can gradually lead to the failure of various structural components of bridges. Thus, if the dynamic amplification factors are not accurately computed and incorporated, this can lead to fatal accidents.

Underestimating dynamic amplification could potentially lead to the bridge underperforming for the intended span in its design. While overestimating dynamic amplification effects are often seen as conservative, it can also raise concerns. If the factors are overestimated, it may lead to the conclusion that several existing bridges are unsafe for use, as pointed out by

Ludescher et al. (2009). Hence it is always vital to compute the amplification factor with accuracy.

1.3 Challenges in determination of Dynamic Amplification Factor (DAF)

Designing bridges involves a complex dynamic analysis process that encompasses various parameters. To achieve successful and optimized bridge design, it is crucial to comprehend and consider the most critical scenarios during the design phase. A key consideration in bridge design is that traffic loads are the most frequent loads acting on the structure and thus, accurately accounting for the impact of traffic loads is crucial. As vehicles move across a bridge, the forces they exerted on the bridges are amplified by a certain percentage of their static loads and this amplified effect is factored into the design through the Dynamic Amplification Factor (DAF).

Thus, precisely determining the dynamic amplification factor is essential for effectively incorporating traffic loads, which leads to safer and more durable bridge designs. To estimate the dynamic amplification factor, it is crucial to understand the various factors contributing to the dynamic amplification effect. Since this effect is generated due to movement of traffic loads through the bridges, the main contributing factors can be classified into bridge and vehicle parameters. The bridge parameters influencing DAF include bridge span, bridge frequency, road surface irregularities, approach span, and bridge damping. Meanwhile, the contributing vehicle parameters are vehicle weight, number of axles, vehicle velocity, suspension system, and the number of vehicles (Deng, 2015). Additionally, the vehicular bridge interaction also contributes towards the dynamic amplification effect (Azimi et al. 2011). Hence due to these many contributing factors, on considering the different design codes incorporating DAF, it can be observed that a unified approach is still lacking after a century of inclusion of this effect into design.

On considering these bridge and vehicle parameters, it becomes clear that an analytical model capable of accurately estimating DAF values should ideally include a bridge model, a vehicle model, a roughness model, a traffic model, and a surface roughness model. A model that effectively integrates all these aspects may be able to provide precise DAF estimates for various scenarios. However, developing such comprehensive analytical models is challenging, as addressing the complexities involved in solving these models presents significant difficulties.

Therefore, it is crucial to recognize that while all these factors contribute to DAF, their impact may not be equally significant. The key is to identify the most important contributors among the bridge and vehicle parameters and to develop an analytical model that can effectively predict dynamic amplification factors. Additionally, when estimating these effects, it's important to acknowledge that various traffic loading scenarios can occur on bridges. Consequently, models should be designed to account for maximum amplification effects. Regarding analytical models, while several exist that have the potential to incorporate DAF, the results can vary significantly since each model emphasizes different parameter contributions.

Given that several existing analytical models can predict DAF values based on various parameters, this study will focus predominantly on evaluating the variation of DAF values with respect to bridge parameters. Thus, the moving load method introduced by L. Fryba (1972) will be utilized as it incorporates most of the significantly contributing parameter. This method was originally used to calculate the dynamic deflection of a simply supported beam in response to the movement of a point load. However, in this study, it will be adapted to estimate the dynamic amplification factor for bridges subjected to traffic loads.

1.4 Problem statement

The dynamic amplification factor (DAF) is a phenomenon which is observed in all bridges, that results from the movement of vehicles across a bridge structure. This movement amplifies the static load by a specific factor and since both the vehicle and the bridge play a role in this effect, the magnitude of amplification depends on several factors. The major contributing parameters are classified as bridge and vehicle parameters. Despite understanding these contributing factors, a definitive relationship between DAF and factors such as bridge frequency, span length, and vehicle velocity is yet to be established. The moving load method (Fryba, 1972) is an analytical model which does not consider the vehicular bridge interaction and other vehicular characteristics and still can determine the DAF values. Thus, the potential of determination of DAF without accounting for these parameters also needs to be explored.

The Dynamic Amplification Factor (DAF), also referred to as Dynamic Load Allowance (DLA) or Impact Factor (IM), has been incorporated into design practices since 1927. Over time, the terminology and the factors used to account for this effect have evolved. To date, no unified approach has been adopted for incorporating the effect of DAF into design, as various codes have relied on different parameters to account for it. While bridge span and frequency are significant contributors to DAF, no design code has used both of these parameters together as the determining criteria. So, through this study an attempt has been made to propose an approach to incorporate DAF into design by considering both bridge span and bridge frequency as key factors. Thus, the major focus of this thesis is to do a parametric study based on bridge and vehicle parameters and to propose an approach for integrating DAF into design by using both bridge span and bridge frequency as key parameters to reflect their contributions in DAF.

1.5 Research Gap

Although the Dynamic Amplification Factor (DAF) has been considered in design and extensively studied over the past century, several aspects still require further clarification. The key gaps identified in the literature review are as follows:

1. Numerous analytical models have the potential to calculate Dynamic Amplification Factor (DAF) values by considering various influencing parameters. Despite these advancements, there remains uncertainty about the primary contributors to the dynamic amplification effect. Specifically, it is unclear whether the effect is predominantly influenced by bridge parameters, such as its stiffness, span, and natural frequency etc or by the vehicle-related parameters, including its mass, speed, and axle configuration.
2. Several design codes use bridge span as a parameter, with different codes applying various formulas to account for DAF based on span length. A common observation across these codes is the assumption that DAF values decrease as bridge span increases. However, if this assumption holds true, it raises the question of why DAF values for the same bridge spans vary significantly in Bridge Weigh-in-Motion (BWIM) and dynamic load tests conducted.
3. When considering the bridge frequency, it was observed that DAF values differed for bridges with even identical frequencies. A review of design codes that use bridge frequency as a parameter to account for DAF, also revealed significant variations in the values incorporated. Therefore, the relationship between bridge frequency and DAF requires further investigation.
4. Research on vehicle velocity as a contributing factor has shown that the variation of DAF with respect to velocity is not yet fully understood.
5. The skew effect on bridges does impact the distribution of loads on the deck but the effect of skew on the dynamic amplification effect needs further studies.
6. Several design codes integrate the dynamic amplification effect into design but there hasn’t been a unified approach yet. The review showed that few codes use bridge parameters whereas the rest uses vehicle parameters for incorporation of the effect.

1.6 Objectives

This research focuses on comprehending different aspects of dynamic amplification which occurs on bridges under traffic loads. The objectives of the study are as follows:

1. To evaluate whether the dynamic amplification effect is predominantly influenced by bridge parameters or vehicle parameters.
2. Bridge parametric study to comprehend the variation of DAF with respect to bridge span, frequency and skew angle effect.
3. Vehicle parametric study to understand the change in DAF with respect to the variations in vehicle velocity.
4. To devise an approach to integrate DAF into design based on both bridge span and bridge frequency together as parameters.

1.7 Outline of the thesis

The thesis presents the author's effort to provide insight into the key factors influencing the dynamic amplification effect that occurs in bridges subjected to traffic loads and in proposing an approach for integrating this effect into design. Despite over 100 years since its consideration in design, the relationship between Dynamic Amplification Factor (DAF) and parameters such as bridge span, bridge frequency, and vehicle velocity remain unclear. This research aims to explore the variations in these critical factors, enabling a more accurate computation of DAF values. In terms of design integration, DAF is currently incorporated based on either bridge span or bridge frequency, but this approach has limitations and thus a method that combines both factors is proposed through this study.This introductory chapter provides an overview of the dynamic amplification effect caused by traffic loads on bridges and highlights the importance of accurately calculating the DAF. The section also outlines the challenges related to DAF determination and presents the major objectives of this research.

Chapter 02: Literature Review

This chapter starts by introducing the key factors that significantly contribute to the dynamic amplification effect on bridges. It then discusses various methods for determining the Dynamic Amplification Factor (DAF), focusing on analytical approaches and dynamic load testing. After examining the contributing factors and methods for calculating DAF, the chapter concludes with an exploration of how this effect is incorporated into design, referencing design codes such as CSA-S6-19 (Canadian Standards Association, 2019), AASHTO LRFD (2012), IRC6: 2017((Indian Roads Congress, 2017)), and Austroads-5100.2 (Austroads, 2004).

Chapter 03: Methodology

This chapter outlines the methodology employed in the study to determine the dynamic amplification factor on bridges under traffic loads. It begins by evaluating the potential of the moving load method, which is crucial for determining whether the results from this approach can provide valuable insights for the parametric studies and also for the approach attempted in the research. The chapter then explains how the parametric studies will be conducted using the moving load method and highlights the importance of comparing these results with those from dynamic load tests. Following this, the section details the method used to investigate the effect of skew angles on the Dynamic Amplification Factor (DAF) using Abaqus CAE. The final section describes the details of the 72 models used for obtaining DAF values, which will be used for understanding the limitations in the existing process of integration of DAF into design, devise a new formula and support the proposed approach presented in this study.

Chapter 04: Potential of Moving Load Method to determine DAF

This chapter addresses the first critical step of determining whether the moving load method can accurately compute the Dynamic Amplification Factor (DAF), despite neglecting vehicle-bridge interaction and other vehicle characteristics. To assess this, the results from the model are compared against several analytical models to ensure the method's reliability. The comparison involves two complex models and one simpler model, specifically the half-vehicle model (Zhou, 2015), the coupled model (Sadeghi, 2020), and the lumped spring-mass model (Yang, 2009).

Chapter 05: Parametric study and comparison with BWIM Test results

This chapter explores the variation of the Dynamic Amplification Factor (DAF) with respect to bridge span, bridge frequency, bridge damping, and vehicle velocity. The analysis involves eight bridge models and all of them are sourced from literature. Firstly, the study examines whether the results obtained from the moving load method align with the findings from the literature review. Then the study points out the limitations of integrating dynamic amplification factor in design solely based on bridge span or bridge frequency. Additionally, a comparison is also made between the DAF results from the analysis and Bridge Weigh-in-Motion data to gain a preliminary understanding of the consistency between the moving load method results and actual traffic responses on bridges.

Chapter 06: Effect of Skew Angle on DAF using Abaqus CAE

In conducting a parametric study in Chapter 05, the effect of skew angle could not be analyzed, as the moving load method lacks the capability to incorporate the skew angle as a parameter. To investigate the influence of the skew angle on the dynamic amplification effect, the moving load concept is extended to a 3D finite element model using Abaqus CAE. This section explains the process of creating the bridge models and how the Vdload subroutine is written to simulate the moving load effect on these models. Initially, different cases are considered to verify the consistency between the analytical model results and the Abaqus CAE model. After establishing the consistency of the model, the impact of skew angle on the dynamic amplification effect is assessed.

Chapter 07: Proposed approach to DAF estimation and design incorporation

This chapter explores the approach introduced in the study, which combines bridge span and bridge frequency as key factors for incorporating the Dynamic Amplification Factor (DAF) into design, based on results from 72 bridge models. The section also offers new insights into how DAF values vary with bridge span and frequency. To show the potential of the new approach, the results are compared with the BWIM test data and then a formula is also generated using regression analysis. After developing the formula based on the new approach, the chapter compares the proposed method's results with existing design code values. For this comparison, the analysis results are evaluated against guidelines of relevant design codes that consider both bridge and vehicle parameters as factors for including the dynamic amplification effect.

Chapter 08: Summary, Conclusions, and Scope for future works

This chapter outlines the key insights and contributions of the study regarding the Dynamic Amplification Factor (DAF). It presents the results of the parametric study presented here and discusses the potential of the proposed approach for enhancing the understanding of dynamic amplification effects caused by traffic loads on bridges. Lastly, the section addresses the possibilities and necessity for future research on this phenomenon.

Chapter 02

2 Literature Review

2.1 Introduction

This chapter of the thesis presents a comprehensive review aimed at exploring the various aspects of Dynamic Amplification Factors (DAF) on bridges subjected to traffic loads. To understand the variations in dynamic amplification effects on bridges, it is essential to firstly identify the different factors contributing to this phenomenon. Consequently, the section begins by examining the various factors influencing DAF. The different factors that this section focuses on are bridge span, bridge frequency, bridge damping and vehicle velocity.

After identifying these contributing factors, it is important to comprehend the different existing methods that has the potential for determining the DAF values. These values can be determined through both dynamic load tests and analytical models and thus, the review explores the various existing analytical models and dynamic load testing methods.

Once the methods for computing DAF values are also comprehended, it is crucial to understand how these effects are integrated into design practices. Hence to address this, the section discusses the history of DAF incorporation and highlights several currently used codes to enhance understanding. The codes that are explained in the section are CSA-S6-19 (Canadian Standards Association, 2019), AASHTO LRFD (2012), IRC6: 2017 (Indian Road Congress, 2017) and Austroads – 5100.2 (Austroads, 2004).

2.2 Factors affecting Dynamic Amplification

2.2.1 Introduction

To understand the dynamic amplification effect that occurs on a bridge due to traffic loads, the first step is to examine the various parameters that can contribute towards an increase in dynamic loads. In this context, the interaction between the vehicle and the bridge is what leads to the dynamic amplification phenomenon. Thus, the contributing factors to this effect can be broadly categorized into bridge parameters, vehicle or traffic parameters, and construction parameters.

The computation of the dynamic amplification factor becomes challenging as the effect depends on both these parameters. These include traffic parameters (such as axle load, number of axles, mass, vehicular velocity, and suspension system), bridge parameters (such as span, frequency, mass, stiffness), and construction parameters (such as road surface irregularities). The interaction of these parameters also gives rise to vehicular bridge interaction, making the development of an empirical formula a persistent challenge. In addition to recognizing the factors impacting dynamic amplification, another vital consideration is to determine the most influential contributors among them.

Hence, the objective of this section is to evaluate the influence of both bridge and vehicle parameters that contribute to the dynamic amplification effect on bridges under traffic loads. This study focuses on understanding the impact of various bridge and construction parameters and additionally, the effect of vehicular velocity will also be explored. The bridge and construction parameters analyzed in this section include bridge span, natural frequency, road surface irregularities, and bridge approach span.

2.2.2 Bridge span

When designing a bridge, the bridge span is one of the primary parameters considered. Consequently, when evaluating bridge parameters that contribute to dynamic amplification effects, bridge span is typically the first factor analyzed. In fact, when the Dynamic Amplification Factor/Impact factor was first introduced by AASHTO (American Association of State Highway and Transportation Officials) in 1927 (Billing, 1984), the main parameter used for its incorporation was the bridge span(Equation 01). The coefficients in equation (1) was adjusted to limit the impact factor value within a range of 0 to 0.4.

$$IM = \frac{50}{L + 125} \tag{4}$$

Since then, numerous dynamic load tests have been conducted, and various analytical models have been developed to better understand the variation of the dynamic amplification effect in relation to bridge span. Codes such as NZTA (2013), IRC6-2017 (Indian Road Congress, 2017), and Eurocode 1 (EN 1991-2:2003) (European Committee for Standardization, 2003), among others, continue to incorporate Dynamic Amplification Factor (DAF) values based on bridge span.

These codes generally assume that the dynamic amplification effect decreases as the bridge span increases. However, despite using bridge span as a key parameter, the variation of DAF values with respect to bridge span does not follow a uniform pattern. However, a study conducted by Kazi et al. (2011) revealed that for concrete box girder bridges, the dynamic amplification effect exhibits an irregular pattern concerning bridge span. Additionally, research by Chang et al. (1994) found that in long-span bridges, DAF values do not vary significantly with bridge span. Instead, when incorporating DAF into the design of long-span bridges, factors such as vehicular characteristics and surface roughness should be prioritized.

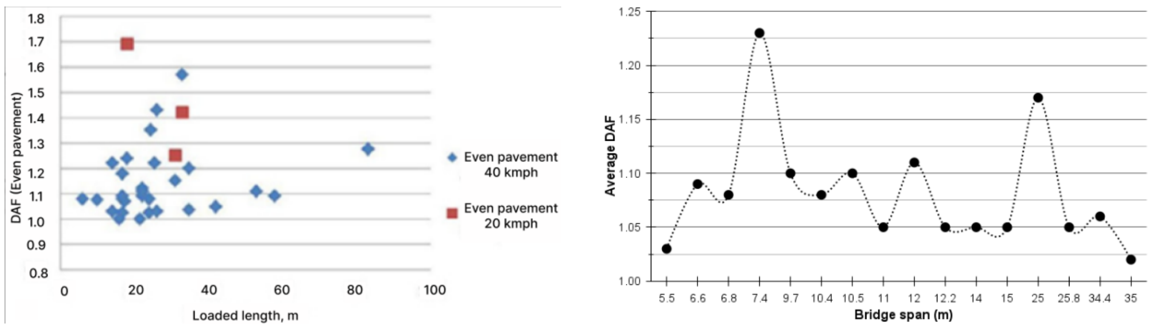

a) b)

Figure 1 a) Extracted from the works of a) (Paeglite, 2013) b) (Kalin, 2022).

Several dynamic load tests have also been conducted in various countries. One of the longest tests was carried out in Latvia from 1990 to 2012 (Paeglite, 2013), aiming to explore the variation of DAF with respect to bridge and vehicle properties (Refer to Figure 1.a). The results indicated no correlation between the dynamic amplification factor and bridge span. A similar trend was observed in a bridge weigh-in-motion test conducted on 15 bridges, where the results also failed to show a consistent relationship between DAF and bridge span (Figure 1.b.). These findings suggest that further research is necessary to better understand the variation of DAF with respect to bridge span.

2.2.3 Bridge Frequency

One of the frequently used parameters for incorporation of dynamic amplification effect into design was bridge frequency. From Figure 2.a, it is quite clear that several bridge design codes like CSA-S6-88, SIA-88, AASHTO-1989 etc. used to incorporate the dynamic amplification effect based on the frequency of bridge span considered in design (Paultre, 1992). But on considering Figure 2.a, it can be observed that there is no unified range for the DAF range incorporated. These itself shows the complexity or rather the importance of having more research done to comprehend the variation of DAF with respect to frequency. Several dynamic load tests were conducted by Eidgenössische Materialprüfungs- und Forschungsanstalt (EMPA) in Switzerland between 1958 and 1981 and Figure 2.b is extracted from the report made on these tests by Cantieni (1983).

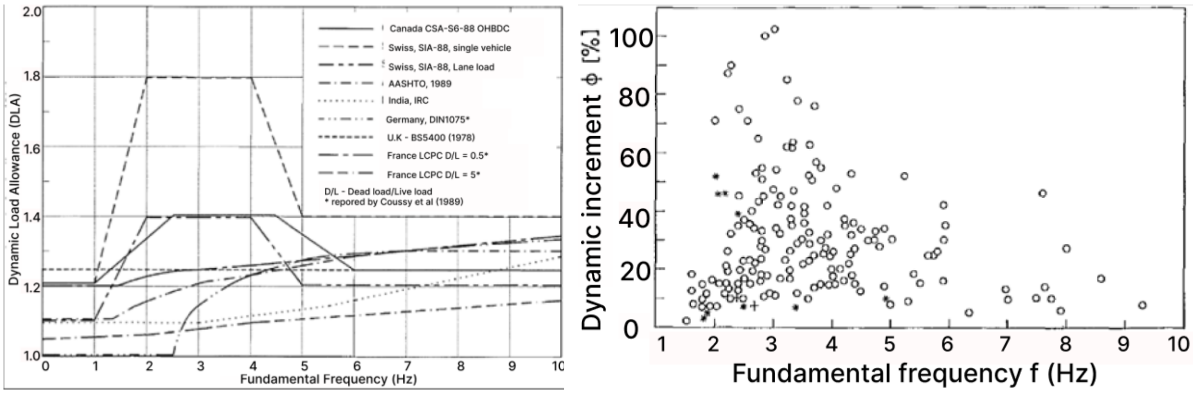

a) b)

Figure 2 Design codes comparisons,Paultre (1992) b) Variation of DAF, (Cantieni, 1984)

These results also indicate that for any particular bridge frequency, the dynamic amplification factor varies. In the relevant bridge code implementation of DAF based on frequency (Figure 2.b), it can be observed that the DAF values are higher for a range of 2 to 5 Hz. This was based on the consideration of vehicular bridge interaction as the body bounce frequency of the vehicle falls in that range. Thus, the probability of amplified dynamic effects could be very high, and thus higher values are provided in that range.

Thus, on considering bridge frequency, the variation of DAF is uncertain as it depends on other contributing factors such as bridge span and vehicular characteristics.

2.2.4 Vehicular velocity

Although the dynamic amplification factor is significantly influenced by various vehicular parameters, the impact of vehicular velocity remains uncertain. Studies suggest that vehicle speed does play a role in the dynamic amplification of traffic loads, but the extent of its contribution has not been conclusively demonstrated. Between 1958-61, AASHTO conducted several dynamic load tests, and the findings published in 1962 revealed a general increase in dynamic effects at higher speeds.

Similar to the tests conducted by AASHTO, EMPA (Eidgenössische Materialprüfungs- und Forschungsanstalt) conducted 356 tests in Switzerland between 1958-81, and the report by Cantieni et al. (1984) illustrates variations in dynamic amplification with respect to the vehicle's velocity. As previously discussed in the context of a vehicle bridge scenario, numerous parameters come into play, and their interaction significantly influences the outcomes. When examining a vehicle, both body bounce and axle hop frequencies are relevant.

The body bounce frequency typically ranges from 1.5 to 4 Hz, while axle hop frequencies fall between 8 and 15 Hz, with the latter becoming significant at speeds exceeding 40 kmph. Thus, bridges with natural frequencies in the 2-5 Hz range exhibit higher amplification as they lie in the body bounce frequency range (DIVINE, 1997). This observation is supported by test results presented by Cantieni et al. (1984), where similar vehicles traversed four bridges at speeds ranging from 10 to 60 kmph. The tests suggest that dynamic amplification neither uniformly increases nor decreases with vehicular velocity, but rather tends to be higher at specific critical velocities.

In the span of 1990-2012, several dynamic loads tests were conducted in (Latvia Ilze Paeglite et al), and the test results aligned with the findings of AASHTO (1962) and EMPA (Cantieni, 1984). While EMPA's tests did not reveal a distinct trend regarding the comparison between velocity and amplifications, the Latvian tests indicated a general increase in amplification for lower velocities. Both tests also indicate the impact of road surface irregularities on dynamic amplification effects and its variations with respect to the vehicle's velocity. Analytical studies conducted by Wekezer et al. (2023), Zhou et al. (2015), and O'Brien et al. (2006) also align with these trends in terms of dynamic effects varying with vehicle speed. However, studies conducted by Azmi et al. (2011) showed that the dynamic amplification effect increases with increase in velocity. Hence, these studies suggest that the relationship between DAF and vehicle velocity is still unclear. The role of vehicle velocity in bridge management would have been crucial if studies were able to suggest a particular velocity or range at which the effect becomes pronounced. However, the test results have not been able to identify such ranges due to the intricate interactions between vehicle velocity, frequencies, and road surface profile.

2.2.5 Road surface irregularities

As mentioned earlier, surface irregularities play a substantial role in amplifying vibrations (Wright, 1964). Studies by Ludescher et al. (2009) indicate that the impact of surface irregularities on the increase of dynamic effects is also influenced by the location of the irregularity. When an irregularity or bump is situated at the midspan, excitations reach their maximum, and as the irregularity shifts away from the midspan, the effect diminishes. Therefore, it is strongly advisable to maintain a smooth profile on bridges to ensure the bridge's structural longevity.

Considering surface irregularities, the presence of expansion joints on bridges becomes a crucial consideration. If the expansion joints are not flush with the roadway, it can lead to amplified bridge response (OHBDC, 1983). Eurocode 1 (EN 1991-2:2003) (European Committee for Standardization, 2003), provides special provisions for the design of spans near expansion joints. It introduces an additional amplification factor formula:

$$\Delta\emptyset = 1.3\left(1 - \frac{D}{26}\right) \tag{5}$$

where (D) corresponds to the distance of the cross section from the expansion joint. This formula indicates that the expansion joint can indeed have an impact, and its influence extends up to a span of 26 meters and the minimum value is 1.

In numerous bridges, a lack of awareness regarding the critical importance of maintaining a uniform bridge deck profile often results in disparities in levels near the expansion joints. When a vehicle traverses these joints at a specific velocity, the irregularities induce the excitation of the vehicle's natural frequency. The resultant increases in either vehicle bounce, or axle hop frequencies are outcomes of the intricate interplay between the vehicle's suspension system and the dynamic response of the bridge (Manning, 1981). The peak vibration amplitude is attained when the frequencies of these interacting systems align, giving rise to a resonance effect.

2.2.6 Approach span

A bridge approach span can be described as the connection between the bridge deck and the road pavement, designed to facilitate a seamless transition between them. However, challenges arise due to differential settlements between the embankment soil and the bridge abutment, leading to the loss of contact between the soil and slab over time. This results in the bending of the approach spans, causing poor deck profiles (Cai, 2007).

Dynamic tests on bridges have clearly demonstrated that irregularities in the road surface of the approach span can amplify the dynamic response of bridges (Wright, 1964). This amplification is attributed to the initial excitation of the vehicle on the bridge approach span, resulting in an additional impact load on the bridges. The dynamic excitation from the surface deterioration of approach spans can be up to 20% more than the Dynamic load allowance (DLA) considered in the design (AASHTO, 2012). Recognizing the significance of smooth bridge approach spans, the Swiss code mandates the inclusion of smooth deck profiles in bridge span approaches (Gonzalez, 2010).

For short-span bridges, approach span conditions play a more significant role in dynamic amplification compared to medium to long-span bridges. This is attributed to the attenuation of vehicle excitation before reaching the critical sections for medium to long span bridges

(DIVINE, 1997). In addition to the bridge profile, the length of the bridge approach span is crucial in terms of dynamic amplification (Liu, 2002) and the analytical tests conducted by O'Brien et al. (2001) indicate that a 100m approach span is necessary for each vehicle to reach a state of steady vibration. Therefore, for optimal bridge structure performance, it is imperative to design and construct approach spans with adequate length and smooth profiles.

2.2.7 Discussion

This section discussed the various bridge, construction, and vehicle parameters that contribute to the dynamic amplification effect on bridges under traffic loads. The literature review covered bridge parameters such as span length, natural frequency, road surface irregularities, approach spans, as well as the influence of vehicle velocity.

When considering bridge span, it was noted that several design codes use span length as a key factor for incorporating dynamic amplification into the design, based on the assumption that DAF values decrease as bridge span increases. However, the specific values used in design vary across different codes. Some studies and dynamic load tests have demonstrated that dynamic amplification does not consistently decrease with increasing span length, showing instead an irregular pattern of variation.

Similarly, for bridge frequency, several design codes have used it as a parameter, but the DAF values assigned across different codes showed significant variation. Results from dynamic load tests were also examined, revealing that even for the same frequency, the DAF values varied. Additionally, it was observed that DAF values tend to be higher within the 2 to 5 Hz range, as this corresponds to the body bounce frequency of vehicles, contributing to greater dynamic amplification.

Regarding vehicle velocity, it was observed that no consistent pattern in DAF variation has been established. Studies have shown that dynamic amplification can either increase or decrease with rising velocity, indicating the need for further research to better understand how variations in vehicle velocity impact dynamic amplification.

Research on the impact of surface irregularities on dynamic amplification has clearly demonstrated that as surface irregularities increase, DAF values also rise. Therefore, it is essential to maintain a smooth surface profile on bridges to mitigate the dynamic amplification effects caused by traffic loads.

Lastly, regarding the approach span, it was observed that ensuring smooth approach spans is crucial for reducing the dynamic amplification effect on bridges due to traffic. Studies have suggested that an ideal approach span length of 100 meters can effectively minimize these dynamic amplification effects.

Overall, this section highlighted the need for more detailed studies to comprehend the variations in dynamic amplification with respect to bridge span, bridge frequency, and vehicular velocity. Additionally, the study emphasized the importance of constructing bridges with smooth profiles and approach spans to mitigate the dynamic amplification effects caused by traffic loads.

2.3 Different methods for determination of DAF

2.3.1 Introduction

As discussed in the previous section, the dynamic amplification factor is influenced by various bridge and vehicle-related factors. Given its dependence on multiple variables, accurately determining the dynamic amplification effect on bridges subjected to traffic loads presents a complex challenge.

Traditionally, the dynamic behaviour of bridges under traffic loads was determined through dynamic load testing. However, due to various constraints, conducting these tests are not always feasible. As an alternative, analytical models have been explored, offering the potential to produce results consistent with dynamic load tests. As discussed in Section 2.2, the dynamic amplification factor (DAF) is influenced by multiple bridge and vehicle parameters. Consequently, many existing models account for certain factors while omitting others, yet still manage to compute the dynamic amplification effect. This section focuses on four different analytical models of varying complexity that incorporate different parameters to calculate DAF: the Moving Load Method (2.3.3.1), Half Vehicle Model (2.3.3.2), Coupled Model (2.3.3.3), and Lumped Spring-Mass Model (2.3.3.4).

The primary objective of this section is to explore various methods for determining DAF values and to examine the methodologies of existing analytical models capable of calculating DAF. The section begins by discussing the history of dynamic load testing, followed by an overview of the Bridge Weigh-in-Motion (BWIM) method for determining DAF, along with results obtained from BWIM tests. The subsequent sections introduce four different analytical models that can effectively determine DAF.

2.3.2 Dynamic Load tests

The dynamic amplification factor is influenced by both the static and dynamic responses of a bridge, with various methods available to evaluate these responses. One of the earliest approaches used to understand the dynamic behavior of bridges involved dynamic load tests, where deflection or strain was measured under moving loads. These tests provide valuable insights into the fundamental responses and characteristics of newly built or existing bridges (Paeglite, 2013).

The first dynamic load test was conducted by R. Willis in 1849, involving the passage of a tracked vehicle over two 2.7-meter-long cast iron beams, with deflections being measured. However, routine load testing did not become common practice until 30 years after Willis's experiments. While dynamic load testing was required for railway bridges, it only became mandatory for highway bridges after 1970 (Cantieni, 1984). Since then, numerous dynamic load tests have been carried out, including major tests conducted by the Eidgenössische Materialprüfungs- und Forschungsanstalt (EMPA) between 1958 and 1981. In the same timeline, between 1958 and 1960, the American Association of State Highway Officials (AASHTO) also conducted a large-scale road test in Ottawa, Illinois (Cebon, 1999). Later, several dynamic load tests were conducted on 65 bridges in Latvia between 1990 and 2012 (Paeglite, 2013). All these test results have indeed provided several valuable insights into comprehending the dynamic behavior of bridges under traffic loads.

Considering the dynamic amplification factor, it is essential to understand and quantify both the static and dynamic behavior of bridges. This requires conducting both static and dynamic load tests. Static load testing can be performed in two ways: the first is a quasi-static test, where the test vehicle moves at a very low speed, and the second involves positioning the vehicle at specific longitudinal points that produce the maximum response. Dynamic load tests, on the other hand, can be carried out by either driving a test vehicle across the bridge to measure the responses or by capturing the dynamic responses while the bridge is open to regular traffic (Deng, 2015).

2.3.2.1 Determination of Dynamic Amplification Factor using Bridge Weigh in Motion

As mentioned in Section 2.3, the dynamic load tests can be conducted by passing test vehicles through a bridge at a particular velocity, through which dynamic responses can be measured. But despite conducting dynamic load tests for bridges involving the passage of a specific design vehicle at varying speeds, it was observed that the obtained results do not align well with reallife scenarios. The values derived from these tests and models offer only qualitative estimates and do not accurately reflect actual conditions (Bakht, 1989). Moreover, dynamic load allowance values in design codes were identified as conservative when compared to the actual dynamic effects on bridges (Kalin, 2015).

Consequently, there arose a need for innovations to obtain precise data on traffic flow and understand how dynamic effects are influenced by vehicular bridge interaction. One of the initial attempts to assess dynamic bridge performance with Bridge Weigh In Motion (B-WIM) was undertaken by Goble, G., Moses, F., & Pavia in 1974. The system gradually found application in measuring stresses on bridges due to traffic loads, which was critical for analysing the reasons for bridge deterioration and also in computation of the bridge load carrying capacity (Paeglite, 2013). The Bridge Weigh In Motion (B-WIM) algorithm utilizes strains measured on a bridge or culvert superstructure to calculate axle loads of crossing vehicles. A distinctive aspect of BWIM analysis is that it computes the structural response first, and then determines the live load responsible for this response (Kalin, 2015). Numerous studies conducted to assess the accuracy of BWIM results and studies by O'Brien et al. (2001) showed BWIM could produce accurate results from traffic studies on bridges.

In this setup, strain measuring devices are affixed along the longitudinal members of the span, typically at intervals of 3 to 5 meters. Since these devices are installed beneath the bridge, they do not impede traffic movement. In cases where axle identification is not achieving accurate results, the sensors may need to be mounted directly on the bridge structure (Kalin, 2022).Within the Bridge Weigh In Motion (B-WIM) framework, the dynamic amplification factor is defined as the ratio between the maximum total strain and the corresponding static load effect observed when a vehicle traverses a bridge span.

$$DAF = \frac{\varepsilon_{tot}}{\varepsilon_{stat}} \tag{6}$$

where ε_{tot} and ε_{stat} represents the maximum total response and the corresponding static load effect (Kalin, 2022). Initially, these values were computed by multiplying the influence line with the sum of the calculated axle loads. However, this method presented challenges, with common occurrences of misidentified axles and system ill-conditioning, often resulting in the underestimation or overestimation of Dynamic Amplification Factor (DAF).

To address this challenge, the signals underwent transformation into the frequency domain using Fourier Transform. Subsequently, the spectrum underwent low pass filtering at a predetermined cut-off frequency. Following this, the signal was transformed back into the time domain, with the remaining signal regarded as the static load effect (Kalin, 2015).

However, this innovation introduced another challenge as the selection of the cut-off frequency required expertise, thereby making the analysis results heavily reliant on individual expertise. Subsequently, to tackle this issue, a new iteration was introduced into the BWIM methodology. This revision involves capturing all loading events twice: firstly, to obtain filter parameters and secondly, for the computation of the DAF (Kalin, 2015). Thus, using this method it is possible to determine the dynamic amplification factor with accuracy without obstructing traffic on the bridges.

2.3.2.2 B-WIM results

Bridge Weight in Motion (B-WIM) systems were deployed in 15 bridges, with 10 installations in Slovenia and the rest in the USA (Kalin, 2022). The tests were conducted over a period of 9 to 13 days in Slovenia, while in the USA, they were completed within 16 to 23 days. Bridges S101 to S107 were slab-type bridges, whereas the others were beam-and-slab (B&S) type (Table 1). Bridges S101 to S105 were located on primary and secondary state roads in Slovenia, while S106 was tested as part of a research project. S107 served as a permanent test site on a motorway bridge, S108 and S109 were two parallel highway bridges, and S110 was a long single-span motorway bridge. In contrast, all the bridges tested in the US were multi-span, older highway bridges.

Table 1 Extracted from the works of Znidaric et al. (Kalin, 2022)

Site	Bridge Type	Bridge span (m)	Vehicles	Mean DAF
S101	Slab	7.4	202	1.23
S102	Slab	10.5	4590	1.10
S103	Slab	12.0	1850	1.11
S104a	Slab	5.5	516	1.03
S104b	Slab	5.5	318	1.04

S105	Slab	6.8	617	1.08
S106a	Slab	9.7	865	1.10
S106b	Slab	9.7	474	1.19
S107	Slab	6.6	746594	1.09
S108	B&S	34.4	432307	1.06
S109	B&S	35.0	402595	1.02
S110	B&S	25.8	28533	1.05
US01	B&S	12.2	1,979	1.05
US02	B&S	10.4	15295	1.08
US03	B&S	11.0	7398	1.05
US04	B&S	10.4	1608	1.08
US05	B&S	25.0	25219	1.17

Table 1 shows the results obtained from BWIM tests that were conducted on bridge spans ranging from 5.5 to 35 meters. The mean Dynamic Amplification Factor (DAF) obtained from the testing varied, with a minimum value of 1.02 for the 35-meter span bridge (S109) and a maximum of 1.23 for the 7.4-meter span bridge (US05). These results clearly demonstrate that longer span bridges experience significantly lower DAF compared to shorter span bridges.

2.3.3 Analytical Models

Although dynamic load tests are highly effective, they are not always feasible due to physical and financial constraints. These limitations arise because such tests require multiple steps, including instrumentation, data collection, processing, analysis, and interpretation. As a result, alternative approaches became a necessity for understanding the dynamic behavior of bridges. Hence, several studies began to explore the potential of analytical models to determine the dynamic characteristics of bridges. The goal was to develop models that could produce results consistent with those of load tests, allowing dynamic responses to be predicted without the need for costly and time-consuming testing. The following sections provide a detailed discussion of several analytical models capable of determining the dynamic amplification factor for bridges under traffic loads.

2.3.3.1 Moving Load Method – (Fryba, 1972)

In the analytical model, a simply supported beam is considered with a moving load traversing through it. When the mass of the load is smaller in comparison to the beam, its inertial forces due to mass can be neglected and hence the load is considered as a concentrated point load moving through the beam as shown in Figure 3.

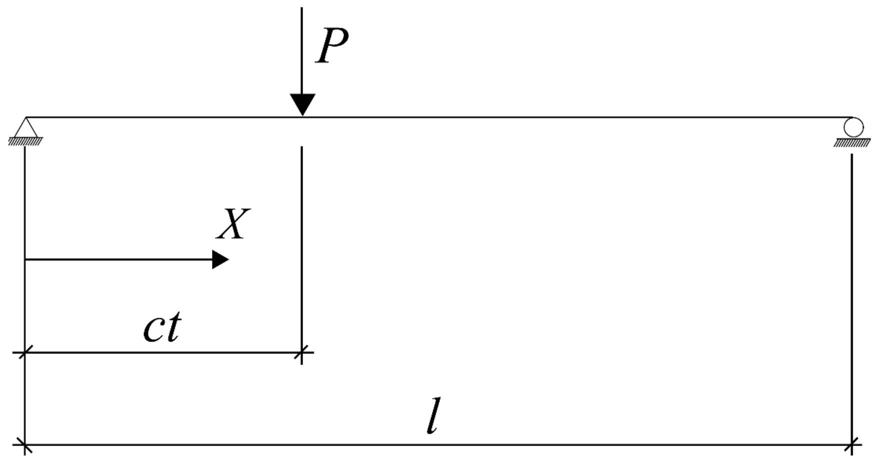

Figure 3 Based on the work of L. Fryba (Fryba, 1972)

The assumptions considered in this method are as follows:

1. The beam behavior is based on Bernoulli-Euler's differential equation derived on the assumptions that the theory of small deformations, Hooke's law, Navier's hypothesis and Saint-Venant's principle can be applied. The cross section and mass per unit length are constant for the entire beam.
2. Since the mass of the moving load is comparatively less compared to the mass of the bridge, only the gravitational effects of the load are considered.
3. For each case, the load moves at constant speed from one end of the beam to the other.
4. Beam damping is considered to be proportional to the velocity of vibration.
5. The beam is considered to be in a simply supported condition and to be at rest when the moving load enters the beam.

The simply supported beam has a uniform cross section with uniformly distributed mass, constant flexural stiffness (EI) and the moving load has a constant velocity (c). The moving load problem is defined as:

$$EJ\frac{\partial^4 v(x,t)}{\partial x^4} + \mu\frac{\partial^2 v(x,t)}{\partial t^2} + 2\mu\omega_b\frac{\partial v(x,t)}{\partial t} = \zeta(x - ct)P \tag{7}$$

The boundary conditions are:

$$\vartheta(0,t) = 0; \qquad \vartheta(l,t) = 0, \qquad \left.\frac{\partial^2 v(x,t)}{\partial x^2}\right|_{x=0} = 0 \qquad \left.\frac{\partial^2 v(x,t)}{\partial x^2}\right|_{x=l} = 0$$

The initial conditions are:

$$\vartheta(x,0) = 0 \qquad \left.\frac{\partial v(x,t)}{\partial t}\right|_{t=0} = 0$$

where x - length coordinate with the reference to origin, $v(x,t)$- beam deflection at point x and time t, E-modulus of elasticity of beam, J - moment of inertia of beam, μ - constant mass per unit length, ω_b - circular frequency of damping of the beam, P - concentrated force, - span of the beam and C- constant speed of the load motion.

This equation is solved using Laplace - Carlson integral transformation and beam deflection $v(x,t)$ can be computed as:

$$v(x,t) = v_o\sum_{j=1}^{a}\frac{1}{j^2[j^2(j^2-\alpha^2)^2+4\alpha^2\beta^2]}[j^2(j^2-\alpha^2)\sin j\omega t$$
$$-\frac{j\alpha[j^2(j^2-\alpha^2)-2\beta^2]}{(j^4-\beta^2)^{\frac{1}{2}}}\alpha e^{-\omega_b t}\sin\omega'_{(j)}t - 2j\alpha\beta(\cos j\omega t - \tag{8}$$
$$- e^{-\omega_b t} cos\omega'_{(j)}t\,)]sin\frac{j\pi x}{l}$$

Where v_o - midspan deflection, j - mode number, $\alpha = \frac{cl}{\pi}(\frac{\mu}{EJ})^{1/2}$, $\beta = \frac{\omega_b l^2}{\pi^2}(\frac{\mu}{EJ})^{1/2}$, $\omega = \frac{\pi c}{l}$, $\omega_{(j)} = \frac{j^2\pi^2}{l^2}\sqrt{\frac{EI}{\overline{m}}}$, $\omega_b = \xi\omega_{(j)}$ and $\omega'_{(j)} = \omega_{(j)} * \sqrt{1-\xi^2}$.

These equations clearly show a relationship between bridge span and frequency, indicating that as the bridge span increases, its natural frequency decreases. From equation (8), the total deflection of the load under the moving load would be computed for the total duration and the maximum deflection is utilized for the determination of the dynamic amplification factor. Thus, equation 3 would be used to find the DAF values for each velocity case, where the maximum deflection from equation 2 would be divided by the maximum static deflection (v_o).

2.3.3.2 Half vehicle Model - (Zhou, 2015)

This approach builds on the work of Zhou et al. (2015), which utilizes a model of a half-vehicle traversing a smooth profile simply supported beam. The model incorporates the vehicle's suspension system and inertial forces, with the vehicle represented by four degrees of freedom. The mass, stiffness, and damping characteristics of the vehicle are considered and to capture the beam's time history, the vehicle-bridge interaction method is applied. The vehicle's properties used in the model are as follows: M=mass of the vehicle, Z = vertical displacement of the vehicle, α = rotational DOF of vehicle, I_a = rotational moment of inertia of vehicle, m_i(i=1,2) = the axle mass of tire and suspension, Z_i(i=1,2) = vertical displacements of axle, k_{si}(i=1,2) = stiffness of upper spring, k_{ti}(i=1,2) = stiffness of lower spring, c_{si}(i=1,2) = damping coefficient of upper spring, c_{ti}(i=1,2) = damping coefficient of lower spring, z'_i (i=1,2) = vehicle body displacement and l_u = axle distance, β_i(i=1,2) = ratio of axle distance from mass centre to the distance l_u and $Z_b(x_i, t)$ = bridge displacement.

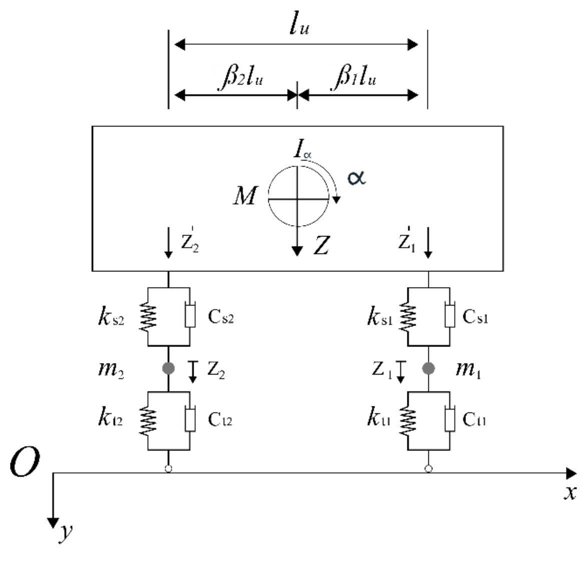

Figure 4 Half vehicle model based on Zhou et al. (2015)

The half vehicle model as shown in Figure 4, the bridge is considered as multi degree of freedom system and the vibration equations are as follows:

$$[M_b]\{\ddot{Z}_b\} + [C_b]\{\dot{Z}_b\} + [K_b]\{Z_b\} = \{F_b\} \tag{9}$$

$[M_b]$, $[K_b]$ and $[C_b]$ are the mass, stiffness and damping matrices of the bridge model and $\{\ddot{Z}_b\}$, $\{\dot{Z}_b\}$, $\{Z_b\}$ are the acceleration, velocity and displacement of the bridge model. The vector of the vehicular bridge interaction forces are incorporated through $\{F_b\}$.

By utilizing the displacement and interaction force relationships at the contact points between the vehicle and bridge, the vibration equations for both systems were combined, forming the vehicle-bridge coupling model. The vibration data was then processed using the fourth-order Runge-Kutta method in the time domain. Then, total dynamic displacement of the bridge was computed and using equation(1) the dynamic amplification factors are determined.

2.3.3.3 Coupled model – (Sadeghi, 2020)

This method, proposed by Sadeghi et al. (2020), calculates the total amplitude of harmonic vibrations in a bridge model. It incorporates the vehicle-bridge interaction by representing the vehicle as a mass-spring system positioned at the center of the simply supported bridge (beam). In this approach, the vehicle does not traverse the bridge; instead, the vehicle and bridge properties are combined. The total vibration amplitude is then determined based on the mass, stiffness, and frequency ratios. Compared to previously used methods, this is a simplified approach. Since the vehicle remains stationary, the time history of the structure is not calculated, and only the total vibration amplitude for each case is determined. A representation of the model is shown in the figure 5.

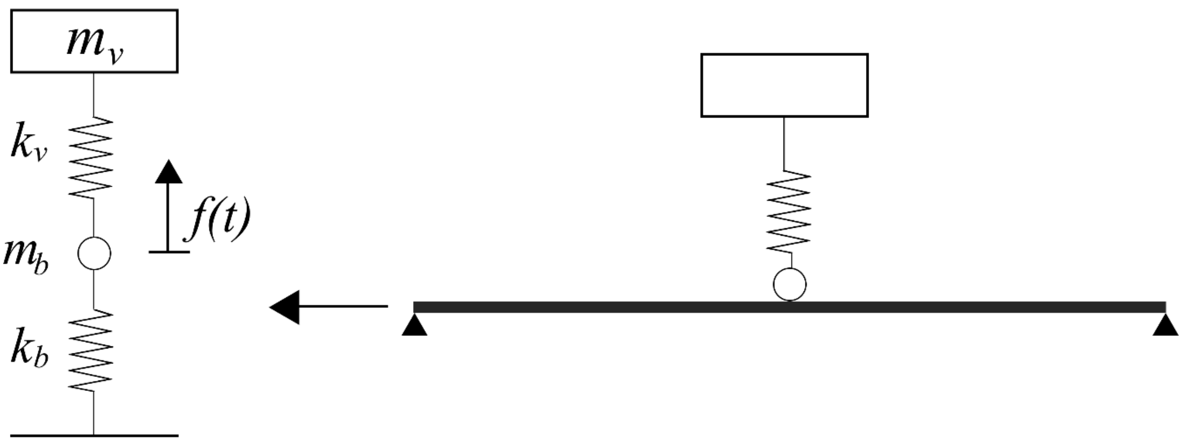

Figure 5 Extracted from the work of (Sadeghi, 2020)

The equation of motion:

$$\begin{bmatrix} m_b & 0 \\ 0 & m_v \end{bmatrix} \begin{pmatrix} \ddot{x_b} \\ \ddot{x_v} \end{pmatrix} + \begin{bmatrix} k_b + k_v & -k_v \\ -k_v & k_v \end{bmatrix} \begin{pmatrix} x_b \\ x_v \end{pmatrix} = \begin{pmatrix} f(t) \\ 0 \end{pmatrix} \quad (10)$$

where m_b, m_v, $k_b$and k_v are the mass and stiffness of the bridge and vehicle, respectively. The acceleration and displacement of the bridge and vehicle are represented as $\ddot{x}_b$, $\ddot{x}_v$ and x_b, x_v respectively. The equation is then solved with eigenvalue analysis to determine the amplitude of bridge vibration (amp (x_b)):

$$\text{amp } (x_b) = \frac{1}{k}\left[\frac{1}{(\gamma^2-1)(\alpha^2-2\alpha\beta-4\alpha+\beta^2+3\beta+2)} + \frac{(\alpha-\beta)^2}{(\beta-\alpha\gamma^2)(\alpha^2-2\alpha\beta+\beta^2+\beta)}\right] \tag{11}$$

where α - ratio of mass of bridge and vehicle, β - ratio of stiffness of bridge and vehicle and γ - ratio of frequency of external force and frequency of the vehicle. The model also states a condition that the mass ratio should be more than the stiffness ratio. Finally, to obtain DAF, equation (4) is divided by the static vibration of the bridge.

2.3.3.4 Lumped spring mass model – (Yang, 2009)

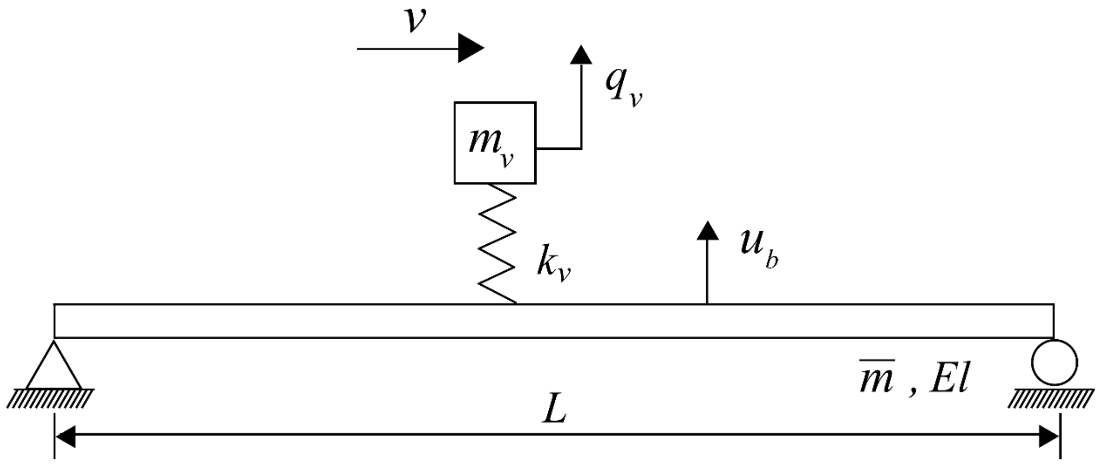

Figure 6 Based on the work of Yang et al.(2009)

This method was proposed by Yang et al. (Deng, 2015) to determine the dynamic response of vehicle bridge coupled model. In this method, the vehicular bridge interaction phenomenon is considered with the vehicle defined by a spring-mass system which traverses through a simply supported beam with a smooth profile represented in Figure 6.

A Bernoulli-Euler beam with a span of L and uniform cross section is considered in this model. The equation of motion of the bridge and vehicle are as follows:

$$\bar{m}\ddot{u} + EIu'''' = f_c(t)\delta(x - vt) \tag{12}$$

Where $\bar{m}$ represents mass per unit length of the bridge, $\ddot{u}$ is second order differential of bridge displacement with respect to time, E is the modulus of elasticity, I is the moment of inertia, u'''' is the fourth order differential with respect to space, f_c is the contact force between vehicle and the bridge and v is the vehicular velocity. The equation of motion of the vehicle is as follows:

$$m_v \ddot{q}_v + k_v (q_v - u_{x=vt}|) = 0 \tag{13}$$

where m_v and k_v are the respective mass and stiffness of the vehicle, $\ddot{q}_v$ is the acceleration of the vehicle and q_v is the displacement of the vehicle.

The contact force (f_c) between the bridge and vehicle is defined through the summation of the total weight of the vehicle and the elastic force of the suspension system. The equation for the contact force is given below:

$$f_c(t) = -m_v g + k_v (q_v - u_{x=vt}|) \tag{14}$$

The vibration equations are solved using the modal superposition method and the dynamic displacement of the beam when the vehicle moves through it with a constant velocity (v) for zero initial condition is as given below:

$$q_{b,n} = \frac{\Delta_{st,n}}{1 - S_n^2} \left[\sin \frac{n\pi v t}{L} - S_n \sin \omega_{b,n} t \right] \tag{15}$$

where the natural frequency of nth mode of the bridge is :

$$\omega_n = \frac{n^2 \pi^2}{L^2} \sqrt{\frac{EI}{\bar{m}}} \tag{16}$$

where static deflection of the nth mode induced by the vehicle is represented by:

$$\Delta_{st,n} = \frac{-2 m_v g L^3}{n^4 \pi^4 EI} \tag{17}$$

and the non-dimensional speed parameter represented by:

$$S_n = \frac{n\pi v}{L \omega_{b,n}} \tag{18}$$

Using this equation the total dynamic response of the system can be determined and then through dividing the maximum response with the maximum static response, the dynamic amplification is determined for each case.

2.3.4 Discussion

This section discussed various methods for determining the dynamic amplification factor (DAF) for bridges under traffic loads. It provided an overview of the history of dynamic load tests and elaborated on the Bridge Weigh-in-Motion (BWIM) methodology for calculating DAF, along with the results obtained from BWIM tests. The section also explored four analytical models of varying complexity that can determine DAF. Among these models, the coupled model was found to be the simplest, as it considers only a few input parameters, while the half vehicle model was identified as the most complex due to its incorporation of both the physical parameters of the vehicle and vehicular bridge interaction. The moving load method (Fryba, 1972) was noted as the oldest analytical model capable of computing DAF within the compared models, but it does not account for the physical characteristics of vehicles or vehicular-bridge interactions. Thus, the subsequent sections will evaluate the potential of this method to accurately determine DAF values despite these omissions.

2.4 Incorporation of DAF into design

2.4.1 Introduction

The previous sections have demonstrated that the dynamic amplification effects caused by traffic loads are influenced by various bridge as well as vehicular parameters. These dependencies have consistently made it challenging to integrate these effects into design practices. Due to the wide range of factors involved, different design codes have adopted distinct criteria for accounting for dynamic effects, with these factors evolving over time.

In this section, the historical inclusion of dynamic effects from traffic loads in design codes will be examined, with a detailed review of few current design standards, such as CSA S6-19 (Canadian Standards Association, 2019), AASHTO LRFD 2012 (AASHTO 2012), IRC 6-2017 (Indian Road Congress, 2017), and Austroads 5100.2 (Austroads, 2004). The objective is to explore the key parameters used to incorporate the Dynamic Amplification Factor (DAF) into design and to determine whether a uniform approach has yet been established for addressing the dynamic amplification effect in bridge design.

2.4.2 History of incorporation of DAF into design

Table 2 Incorporation of Dynamic amplification in Design Codes

#	Region	Design Code	Year	Parameter	Min DLA	Max DLA
1	USA	AASHTO	1927	Bridge span	0	0.3
2	Canada	OHBDC	1983	Bridge frequency	0.2	0.4
3	Latvia	SNIP 2.05.03	1984	Bridge type and span	0	0.4
4	Switzerland	SIA	1988	Bridge frequency	0.2	0.8
5	Canada	CSA-S6	1988	Bridge frequency	0.21	0.4
6	India	IRC:6	1988	Bridge frequency	0.1	0.22
7	USA	AASHTO	1989	Surface condition	0.1	0.3
8	China	MTPRC	1989	Bridge span	0	0.3
9	Canada	OHBDC	1991	Vehicle characteristics - axle	0.25	0.4
10	USA	AASHTO	1992	Bridge span	0	0.3
11	Japan	JRA	1996	Bridge type and span	0	0.4
12	USA	AASHTO	2003	Surface condition	0.1	0.2
13	Europe	CEN	2003	Bridge span	0.4	0.7
14	China	MTPRC	2004	Bridge frequency	0.05	0.45
15	Britain	BS5400-2	2006	Traffic configuration	0.25	0.25
16	New Zealand	NZTA	2013	Bridge span	0	0.3

AASHTO (1927) pioneered the incorporation of dynamic effects caused by traffic loads into design, prompting the global adoption of this practice in standard design codes. But as DAF depends on bridge as well as vehicular factors, the parameter based on which the effect was incorporated were various in different codes. Even the codes which were using a particular factor as a deciding criterion changed the parameter into a different one in few years. For instance, in the case of AASHTO (1927), dynamic amplification was initially based on the bridge span parameter, but subsequently shifted the governing factor to roughness (AASHTO 1989), bridge span (1992), and back to surface roughness (AASHTO 2003). Such alterations are widespread across most of the standard design codes.

The data shown in Table 2, compiled from the works of (Paeglite, 2013), (Deng, 2015), and (Paultre, 1992), highlights the variation in how dynamic amplification has been incorporated into design across different codes in time. It is evident that there is no consistent approach to integrating the dynamic amplification effect into design standards. Some codes, such as AASHTO-1927, rely on bridge parameters, while others, like OHBDC (1991), consider vehicle characteristics as the primary factor. Even when focusing on bridge parameters, there is significant variation, with some codes using bridge span, while others account for bridge frequency or surface conditions. As shown in Table 2, the highest dynamic effect was incorporated by SIA (1988), with a value of 0.8 based on bridge frequency, whereas the lowest maximum Dynamic Load Allowance (DLA) was used by AASHTO-2003 (0.2), which considered surface irregularities.

On observing Table 2, it is comprehended that most design codes have predominantly used bridge properties as the key factor, with bridge span and bridge frequencies being the most prominent parameters. Even today, codes such as NZTA (2013) continue to base the incorporation of Dynamic Amplification Factor (DAF) on bridge span. To provide a clearer understanding of how dynamic amplification is integrated into design, a review of few current design codes is presented in the following sections.

2.4.3 Canadian Highway Bridge Design Code - CSA S6 – 19

The Canadian Highway Bridge Design Code (CHBDC) of the Canadian Standard Association (CSA) - S6 – 2019 (Canadian Standards Association, 2019), includes the dynamic amplification effect in the form of dynamic load allowance (DLA). According to CSA-S6-19, the dynamic load allowance is defined as "*an equivalent static load that is expressed as a fraction of the traffic load and is considered to be equivalent to the dynamic and vibratory effects of the interaction of the moving vehicle and the bridge, including the vehicle response to irregularity in the riding surface*."

The magnitudes of DLA considered are based on the type of components being designed and the number of axles in standard CL-W trucks, which are utilized for the design process. The allocation of dynamic allowance also varies depending on the type of components, as the response characteristics of different components vary (Paultre, 1992). For example, DLA is omitted in the design of elements such as traffic barriers. However, in the assessment of dynamic effects induced by vehicles, it is imperative to incorporate the DLA. The Dynamic Load Allowance specified in this code also relies on whether the components are buried, and, in this section, we will focus exclusively on the DLA for non-buried structures. It can be inferred from Table 3 that the factors considered for dynamic load allowance vary in direct proportion to the number of axles utilized in the design.

Table 3 Incorporation of DLA - CSA-S6-19 (Canadian Standards Association, 2019)

#	Description	Dynamic Load Allowance (DLA)
1	Deck joints	0.5
2	Only 1 axle of CLW truck is used	0.4
3	Only 2 axles of CLW truck is used	0.3
4	3 or more axles of CLW Truck is used	0.25

P.F. Csagoly et al. (1971) noted that when multiple lanes are considered for design loading, it is improbable for multiple trucks to be dynamically identical and synchronized. Consequently, the maximum dynamic effects of one truck are likely to exceed those of a multiple trucks. Hence, these dynamic allowance factors are adjusted by multiplying them with the appropriate modification factor specified in the code.

Table 4 DLA of permit vehicles based on velocity

#	Description	Dynamic Load Allowance (DLA)
1	Velocity - 10 kmph	0.3
2	10 kmph < Velocity 25 kmph	0.5
3	25 kmph < Velocity 40 kmph	0.75
4	Velocity 40 kmph	1.0

Additionally, when addressing the design of wood components and evaluating their dynamic effects, the DLA factors are subject to multiplication by 0.7. This adjustment is made due to the significantly higher damping properties exhibited by wood when compared to steel or concrete, as highlighted by P.F. Csagoly et al. (1971). Furthermore, the code also categorizes dynamic load allowance of permit vehicles according to vehicle speed, indicating the significant impact of vehicle velocity on dynamic load allowance. (Table 4)

2.4.4 AASHTO LRFD (2012)

AASHTO has consistently played a pivotal role in advancing the understanding of the dynamic behaviour of bridges. Being among the pioneers, AASHTO was one of the first organizations to integrate dynamic effects caused by traffic loads into bridge design (AASHTO 1927). Furthermore, during the period from 1958 to 1961, AASHTO also conducted a series of dynamic load tests, and the findings from these tests significantly enhanced the comprehension of dynamic effects resulting from traffic loads on bridges (Cantieni, 1984).

Regarding the dynamic amplification factor, dynamic effects were initially accounted for using the impact factor until 1994 when it was superseded by the Dynamic Load Allowance. On considering AASHTO (2012), the dynamic load allowance is determined based on the design component and the limit state of design and expressed as DLA = 1 + IM (Impact factor).

Table 5 Impact factor (IM) - AASHTO (2012)

#	Description	Impact Factor (IM)
1	Deck joints – All limit states	0.75
2	All other components	
3	Fatigue and fracture limit states	0.15
4	All other limit states	0.33

According to the code, the maximum increase in static load resulting from the passage of a single design truck is 25%, excluding deck joints. However, when accounting for both the design truck and lane loads, the effect is set to be at least 4/3 of the impact observed in the single design truck scenario, resulting in a 33% dynamic load allowance.

The code also outlines conditions for conducting dynamic analysis on bridges, specifying that the surface profile, velocity, and vehicular characteristics need approval and that the impact factor is defined as the ratio of the maximum dynamic effect to its corresponding static force effect. Furthermore, an additional clause is that the calculated value for Dynamic Load Allowance (DLA) should not be less than 50% of the values specified in the Table 5.

On comparing with CSA-S6-19 (Canadian Standards Association, 2019), AASHTO also incorporates the multiple presence factor while considering Impact Factor. However, in the context of designing wood components, the code specifies that the dynamic load allowance is not required. The rationale behind this omission lies in the understanding that wood structures tend to exhibit diminished dynamic wheel load effects due to internal friction among components and the damping characteristics inherent in wood. Moreover, wood demonstrates greater strength for short-duration loads compared to longer-duration loads, and this increase in strength surpasses the rise in force effect attributed to the dynamic load allowance.

2.4.5 Indian Road Congress IRC:6 – 2017

The Indian design code (Indian Road Congress, 2017) integrates dynamic effects through Impact factor (IM), which are contingent upon the several factors like loading category, bridge span, vehicle category (tracked or wheeled) and material type (reinforced concrete or steel). The code encompasses various loading types such as Class A, Class B, Class AA, Class 70R, and Class SV. Notably, dynamic effects are excluded only in Special Vehicle loading. Class B pertains to loading on timber bridges, while Class AA and Class 70R are specialized categories within Class A loading designated for permanent bridges and culverts.

The impact factor formulas incorporated shows that on considering Load Classes A and B, only the bridge length is accounted for in determining the impact factor. However, for Class AA and Class 70R, if the bridge span is less than 9m, the impact factor depends on both the bridge span and vehicle type. Furthermore, when the bridge span exceeds 9m, the factor also considers the bridge material category, in addition to the factors mentioned for bridge spans less than 9m.

Figure 7 distinctly demonstrates that the highest dynamic impact factor is assigned to steel bridges, followed by reinforced concrete bridges, particularly for Class A/Class B loading. Upon analysing the impact factors for Class AA/Class 70R loading, it becomes evident that the dynamic impact is comparatively lower than that observed for Class A/Class B loading.

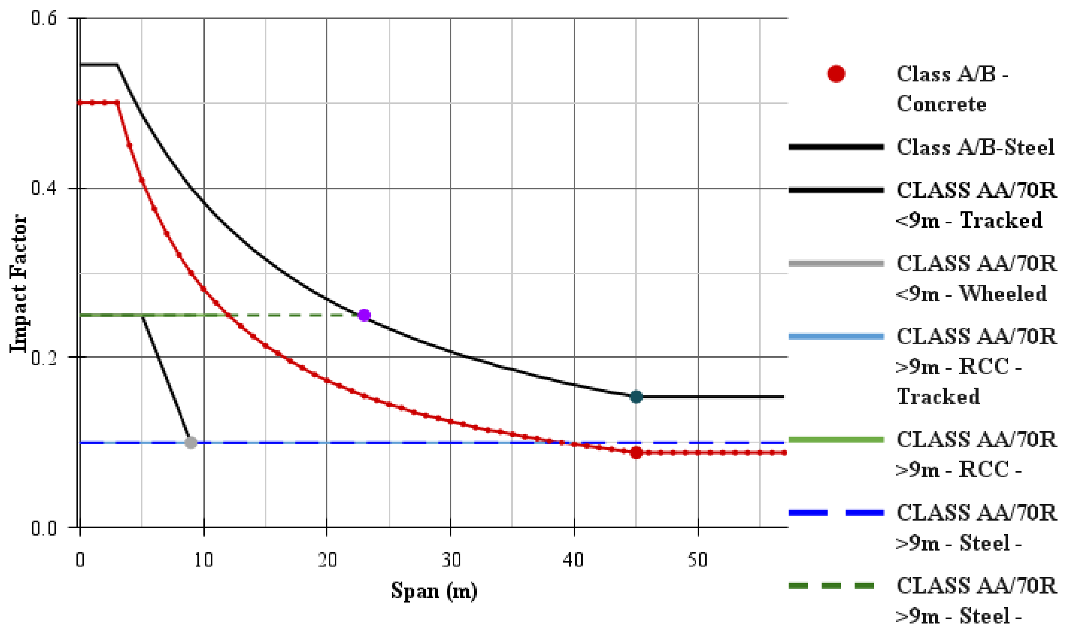

Figure 7 Impact factor incorporation in IRC6 (Indian Road Congress, 2017)

The graph distinctly demonstrates that the highest dynamic impact factor is assigned to steel bridges, followed by reinforced concrete bridges, particularly for Class A/Class B loading. Upon analysing the impact factors for Class AA/Class 70R loading, it becomes evident that the dynamic impact is comparatively lower than that observed for Class A/Class B loading.

Furthermore, when analyzing the inclusion of dynamic effects for tracked and wheeled vehicles, a noticeable distinction is that the dynamic effects are significantly more pronounced in the case of wheeled vehicles compared to tracked vehicles. In summary, the incorporation of dynamic impact factors in the Indian code explicitly indicates a diminishing effect with an increase in bridge span, alongside being influenced by other above-mentioned factors.

2.4.6 Austroads Part 2 - AS 5100.2 - Design Loads

Within the Austroads (2004) AS 5100 Bridge Design Standard—Part 2: Design Load (Austroads, 2004), dynamic effects are accounted for through Dynamic Load Allowance (DLA), and this is contingent upon the traffic configuration. The traffic loads are represented by W80 wheel load, A160 axle load, M1600 moving traffic, tri-axle group load, S1600 stationary traffic load, and HLP320 or HLP400 load. Furthermore, the inclusion of a Heavy Loaded platform load, traveling at 10 kmph, is also considered, with a corresponding DLA of 10%. In scenarios where multiple lanes are loaded to design for critical conditions, an additional factor must be multiplied along with vehicular loading, akin to the approach in CHBDC (CSA-S6-19) (Canadian Standards Association, 2019).

Table 6 Impact Factor incorporation in Austroads – AS 5100.2

#	Description	Impact Factor (IM)
1	W80 Axle Load	0.4
2	A160 Axle Load	0.4
3	M1600 Tri Axle Group	0.35
4	M1600 Axle Load	0.3
5	Heavy Load Platform	0.1

When analysing the dynamic load allowances prescribed for design, it is notable that these values typically range between 30% and 40%. Significantly, these allowances are rendered independent of extraneous factors, and it may be to adopt a conservative stance in design. This approach ensures the provision of surplus structural strength for bridges.

2.4.7 Discussion

This section highlights that the Dynamic Amplification Factor (DAF) has been incorporated into design based on various bridge and vehicular characteristics. AASHTO first introduced the dynamic effects of traffic loads in 1927, and since then, design codes around the world have gradually adopted similar approaches. However, despite nearly 100 years of incorporation, no uniform approach has been yet established. The most used parameters for determining dynamic amplification were inferred to be bridge span and frequency. Additionally, it was observed that the highest Dynamic Load Allowance (DLA) value historically used by any code was 0.8 (SIA-88), while the lowest was 0.2, suggested by AASHTO-2003, where surface irregularities were considered the determining factor.

While road surface irregularities play a crucial role in the dynamic amplification of traffic loads, the current design codes currently do not consider them as a parameter and instead assume a smooth profile for the bridge deck. This omission may be attributed to the difficulty of accurately incorporating road surface irregularities, given their random nature. Furthermore, the location and type of these irregularities are significant factors, making their inclusion as parameters complex, especially considering their potential to change over time. Consequently, design codes opt for a conservative approach when integrating (DAF) or (DLA) into the design.

On reviewing CSA-S6-19 in detail, one of the key observations was that DLA was a design aspect which is used frequently in the code. The DLA was found to be utilised in design of the traffic loads to analysis of decks to even for the consideration of transport and delivery. Thus, one of the key takeaways from this section was also that DLA plays a crucial role in design of bridges.

On considering the parameter for inclusion of DLA into design, Indian code IRC 6-2017 stands out as the only code that allocates DAF based on the consideration of bridge as well vehicular characteristics. Upon reviewing CSA S6-19 and AASHTO 2012 code, they present conflicting approaches to wood components. The Canadian code suggests providing a reduced DLA, whereas the American code completely neglects the effect.

While the dynamic load allowance (DLA) is an integral component of bridge design, there is currently no unified criterion for incorporating dynamic effects into the design process. Therefore, further in-depth research is needed to identify the most critical factors that should be considered as design parameters.

2.5 Summary

This section outlined the contributions of various bridge, vehicle, and construction parameters to the dynamic amplification effect. It was evident that more detailed studies are needed to understand the variations in DAF related to bridge span, bridge frequency, and vehicle velocity. Additionally, it became clear that maintaining a smooth profile and approach span is essential for reducing dynamic amplification effects on bridges. The review highlighted the potential of existing dynamic load testing technologies, such as bridge weigh-in-motion systems. Regarding analytical models, it was noted that while the moving load method does not account for the physical characteristics of vehicles and their interactions with bridges, it remains capable of determining the dynamic amplification factor for bridges. Finally, a study on the history of DAF incorporation revealed that various parameters have been utilized in design codes and that bridge span, bridge frequency, and traffic configuration were the most used parameters. Although this effect has been integrated into design practices for nearly a century, a unified approach is yet to be established. Therefore, further detailed studies are necessary to identify the factors on which DAF should be based for effective design integration.

Chapter 3

3 Methodology

3.1 Introduction

This thesis adopts a structured approach to understanding the various aspects of dynamic amplification of traffic loads on bridges. The dynamic amplification effect is influenced by a variety of bridge and vehicle parameters. To discern whether the effect is predominantly governed by bridge or vehicle parameters, it is crucial to consider a model that isolates either bridge or vehicle characteristics. A review of existing literature indicates that the moving load method has the potential to predict the Dynamic Amplification Factor (DAF) based solely on bridge parameters. While vehicle-bridge interactions and numerous vehicle-specific factors play a role in DAF, it is essential to assess whether the moving load method (Fryba, 1972) can deliver reliable results even when these influences are excluded. To explore this potential, the results from the moving load method are first compared with those from models that account for these effects.

To understand the influence of parameters such as bridge span, frequency, and vehicle velocity, multiple test results are necessary. Therefore, eight bridge models from existing literature are selected, and their results were analyzed to assess the variation in DAF with respect to these parameters. In addition, these comparisons would also highlight the limitations of using bridge span or frequency as sole parameters. Finally, the results from the preliminary analysis are compared with BWIM test data (Kalin, 2022) to evaluate the consistency of the moving load method with dynamic load test outcomes.

After demonstrating the potential of the moving load method through these results, the concept is expanded to a 3D finite element model using Abaqus CAE. Through this method, the analysis investigates the effect of skew angle on the dynamic amplification effect. Finally, a new approach utilizing bridge span and frequency is developed by collecting data from the analysis of 72 bridge models with varying spans and frequencies across a velocity range of 10 to 120 kmph. The results are then compared with the BWIM test data and the consistency with all bridge data are comprehended. In addition, a formula will also be devised to incorporate DAF into design based on bridge and bridge fundamental frequency. Based on these findings, conclusions are drawn regarding the effectiveness of this approach and the limitations of current design codes. The illustration of the approach employed in the study (Figure 8) and details of the sections are as follows:

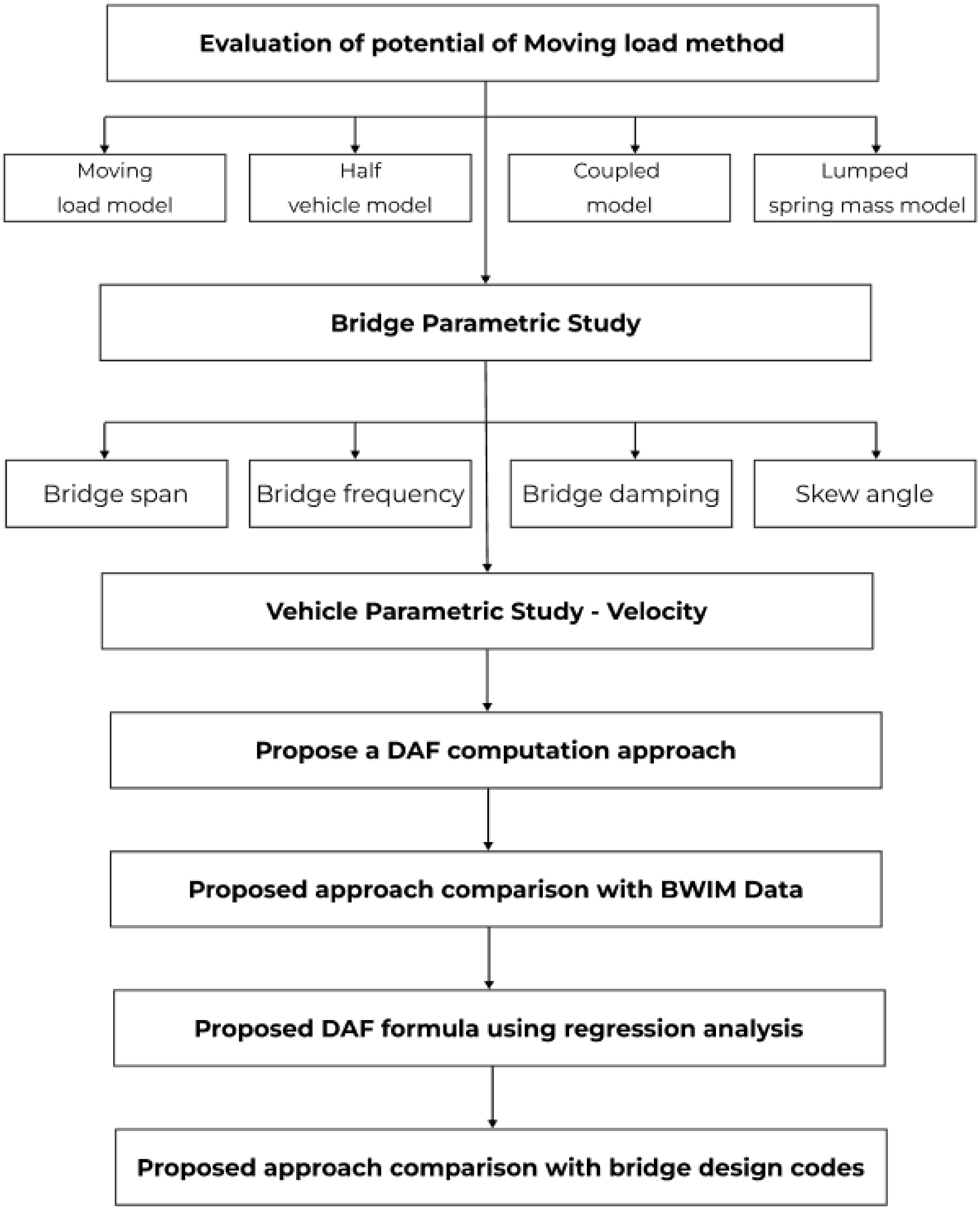

Figure 8 Illustration of methodology utilized in the study

3.2 Evaluation of potential of Moving load method

The literature review showed that the relationship between dynamic amplification factor and bridge span, frequency and vehicle velocity is not yet established clearly. Thus, to establish a relationship between these factors and DAF, either by doing dynamic load tests or by using analytical model. Due to physical and financial constraints, it is not possible to acquire data from the dynamic load tests and thus analytical models would be considered for the determination of the dynamic amplification values. In the literature review, four different analytical models were discussed, and they were moving load model, half vehicle model, coupled model and lumped spring mass model. The moving load model was one model which incorporated the largest number of bridge parameters among the models considered and neglected VBI and other vehicle parameters. This makes the moving load model less complex but then the focus is to understand whether this model can produce accurate results after simplification. Along with this arises a question, that is, if this model can produce consistent results even after neglecting vehicle characteristics, would it be possible to simplify the model further. So, to comprehend the potential of moving load method and to understand if further simplification of the model can produce consistent results, the moving load method needs to be compared with the results of other models. The half vehicle model is the most complex model as it incorporates the maximum number of input parameters. Thus, the half vehicle model results would be used as benchmark for comparison. This would ideally provide an insight on the potential of the moving load in determination of Dynamic Amplification Factor.

3.3 Parametric study and comparison with BWIM test results

To comprehend the effect of parameters which contribute towards the Dynamic amplification effect, a few bridge models are selected from the existing literature and the parameters are inputted into the moving load method for analysis. The different parameters explored in the study are bridge span, bridge frequency, bridge damping and vehicular velocity. A total of eight different bridge models are considered in the study where four of them have rectangular cross sections and the remaining are I sections. To consider the bridge span as a parameter, the models are selected to have a span range of 14 to 50 m. This ensures that short to long span bridges are considered in the analysis. With respect to the bridge frequency, a frequency range of 0.75 to 8.03 Hz is considered in the analysis. With respect to bridge damping, a single case of 3% is utilized to get an understanding regarding the effect of bridge damping on dynamic amplification factor. Since normal traffic moves at a velocity range of 10 to 120 kmph, this range is considered in the study.

On considering a particular bridge model, the parameters would be inputted into the moving load method and the analysis would be done separately for each of velocities within the velocity range of 10 to 120 kmph. From these 12 results, the average, maximum and minimum dynamic amplification factors are initially determined. Once these values are determined, then the parametric studies based on bridge span, frequency, bridge damping and vehicle velocity is conducted. Along with the aim of parametric study, insights regarding the limitation of considering bridge span or frequency solely as parameters is also comprehended from this analysis. Thus, through this analysis, the limitation of incorporating DAF into design using either of these parameters is also explored. From the earlier section, the potential of Moving load method was analyzed only by comparing the results with other complex analytical models. However, to incorporate the values obtained from the moving load method into the new approach, it is vital to ensure that the value from this method is comparable with the actual traffic scenarios on a bridge. Thus, to comprehend whether Moving load method (Fryba, 1972) produces results which are comparable with dynamic load test results, the analysis results from the section is compared with the Bridge Weigh in Motion data.

3.4 Parametric study including Skew angle effect using Abaqus CAE

On observing the moving load method, it can be comprehended that this method does not have the capability to incorporate skew angle effect. Thus, another alternative to get an understanding regarding the variation of DAF values due to the skew angle, the moving load method is extended as a 3D finite element model. A software like SAP2000 cannot be used for this purpose as dynamic amplification factor is an user inputted parameter in the software. Thus, the Abaqus CAE software is used for determination of DAF values using moving load method concept. The moving load is assigned on the model using Vdload coding for the user-defined subroutine.

3.5 New approach for estimation and design integration of DAF

The fact that the results from the moving load method is consistent with complex models, BWIM data and Finite element model results help to show the authenticity of the results from the method. In the earlier section, only a few bridge models were considered in the study but to elaborately understand the effect of variation of DAF with respect to various parameters, it is vital to consider several bridge models. Thus in the section, bridge models with a span ranging from 10 to 50m and 8 bridge frequencies ranging from 2.0 to 5.5 Hz is considered (72 models). Each of these models would be analyzed for velocities in the range of 10 to 120 kmph and then the maximum and average DAF values are determined for the parametric study conducted here. From these results, the effect of bridge span and bridge frequency on the dynamic amplification effect can be comprehended. This analysis also provides an insight on the limitations of considering bridge span or frequency as deciding parameters for integrating DAF values into design.

3.6 Proposed approach comparison with BWIM data

To evaluate the potential of the proposed approach, it is essential to compare its results with the dynamic amplification effects observed on bridges under real traffic conditions. For this purpose, the DAF values obtained from Bridge Weigh-in-Motion tests conducted on 17 bridges will be analyzed. This comparison will help determine whether the DAF values proposed by the approach are safe. Additionally, it will provide insights into whether the values derived from the proposed method are optimized or if they tend to be underestimated or overestimated.

3.7 Proposed DAF formula is regression analysis

Once the reliability of the results from the proposed approach has been established, the next critical step is to develop a formula that can effectively incorporate the DAF values into bridge design practices. This formula would serve as a practical tool for engineers to account for the dynamic amplification effect in their calculations. To achieve this, data derived from the analysis of 72 bridge models will be employed in a comprehensive linear regression analysis. By identifying trends and relationships within the dataset, the regression process will help formulate a precise and reliable equation for integrating DAF values, ensuring their applicability and accuracy in bridge design scenarios.

3.8 Proposed approach comparison with bridge design codes

After assessing the reliability of the model results and deriving a DAF formula, it is equally important to compare the outcomes with existing bridge design codes. To this end, the results from the proposed approach are compared with codes such as IRC 6-2017 and NZTA 2013, which define DAF based on bridge parameters, as well as CSA-S6-19 and AASHTO (2012), which incorporate DAF based on vehicle parameters. This comparison aims to evaluate whether the values determined through the proposed approach are aligned with the codes, offering valuable insights into their adequacy and potential areas for refinement.

Chapter 04

4 Potential of Moving Load Method to determine DAF

4.1 Introduction

The literature review showed that there are several existing analytical models that have the capability to determine the Dynamic Amplification Factor (DAF) resulting from traffic loads on bridges. Among the models reviewed, the moving load method (Fryba, 1972) was unique, as it focuses solely on bridge parameters and reduces the complexity of the analysis by considering a point load moving across the bridge span. This approach assumes that the moving mass is negligible compared to the bridge, allowing the inertial forces generated by the mass to be ignored. However, neglecting vehicle parameters and omitting vehicle-bridge interaction raises the question of whether this method can still provide accurate results for dynamic deflection and, consequently, for the precise determination of the DAF.

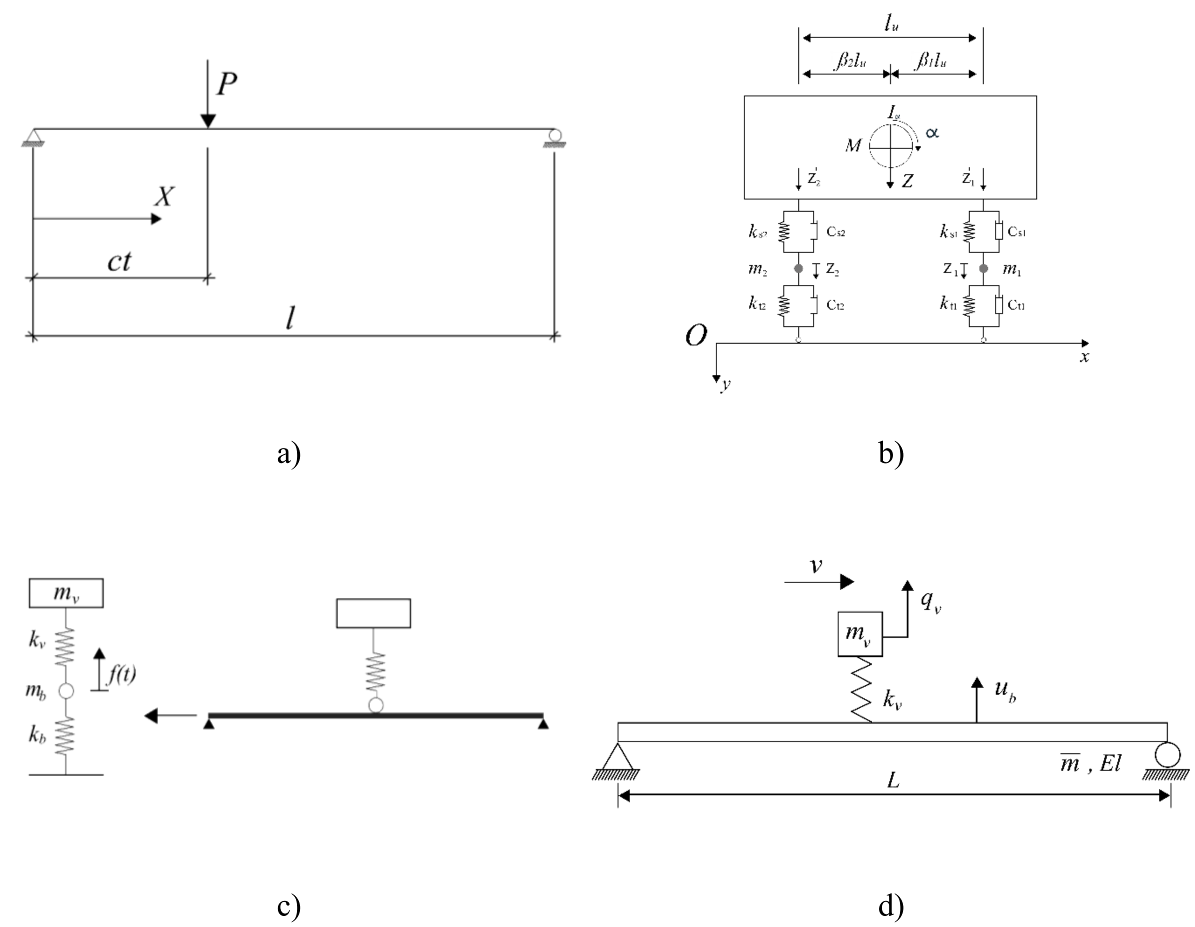

Figure 9 a) Moving load model b) Half vehicle model c) Coupled model d) Lumped Spring mass model

Furthermore, if this method can consistently produce accurate results, it raises the question of whether an even more simplified model could yield similar DAF values. Hence, to explore the potential of the moving load method in determining the Dynamic Amplification Factor and to assess whether simpler models can deliver reliable outcomes, three other analytical models of varying complexities are considered in this section for comparison.

The models used for comparison are based on the works of Zhou et al. (2015), Sadeghi et al. (2020), and Yang et al. (2009). Among these four models, the model from Zhou et al. (2015) includes the most input parameters, making it the benchmark for comparison and to evaluate whether simplified models can produce consistent results, the model from Sadeghi et al. (2020) is included in the analysis. Additionally, to gain a preliminary understanding of whether vehicle-bridge interaction can be neglected in determining the DAF, models based on the works of Zhou et al. (2015) and Yang et al. (2009) are used in this study.

For determining the dynamic amplification factor, both the dynamic and static deflections from the models are found and the values are inputted into Equation (1). The velocity range for all analyses is set between 10 and 120 kmph and damping is not included as a parameter in this analysis since the benchmark model does not account for it. A part of the study was presented in Pradeep and Bagchi (2024).

4.1.1 Half vehicle model (Zhou, 2015)

This model, developed by Zhou et al. (2015), involves coupling a half-vehicle model with a simply supported bridge. The vibration equations are formulated and solved using the fourth-order Runge-Kutta method in the time domain. Among the analytical models considered, this model incorporates the most input parameters and thus serves as the benchmark. Results from other models are compared against this benchmark to evaluate their accuracy.

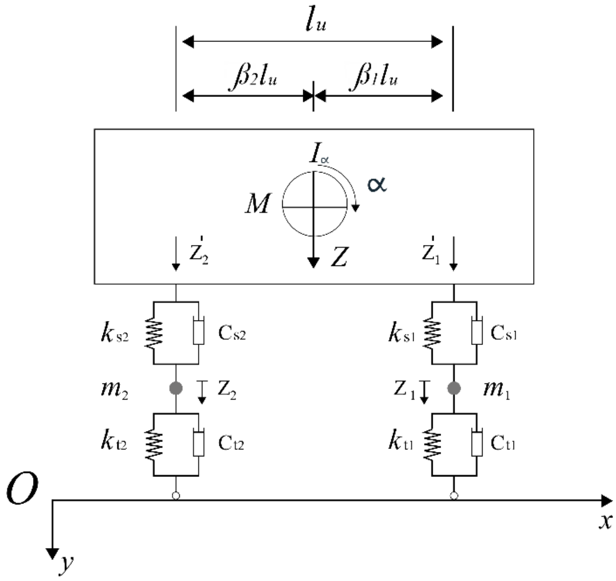

Figure 10 Based on the work of Zhou et al. (2015)

The bridge and vehicle parameters that was considered in the work of Zhou et al. (2015) are as follows:Bridge parameters: The span L is 40 m, the stiffness of the bridge EI is 1.28x10^{11} N/m^2, with a constant mass per unit length of the bridge of 1.20×10^4 kg/m, and the deck surface is assumed to be smooth. Vehicle parameters: m1=m2=4330kg, M=24790kg, l_u =3.625m, $\beta_1 l_u$ =1.787 m, $\beta_2 l_u$ =1.838 m, k_{ti}=4.28×10^6 N/m, C_{ti} =9.8×10^5 N·S/m, k_{Si} =2.54×10^6 N/m, C_{Si}=1.96×10^6 N·S/m, and I_α =3.258×10^6 kg.

The results for comparison using this method are sourced from the findings reported in (Zhou, 2015) and thus additional analysis was not conducted for this model. The velocity range considered in the analysis ranges from 10 to 120 kmph, and the variation of the Dynamic Amplification Factor with respect to velocity is shown in Figure 10.

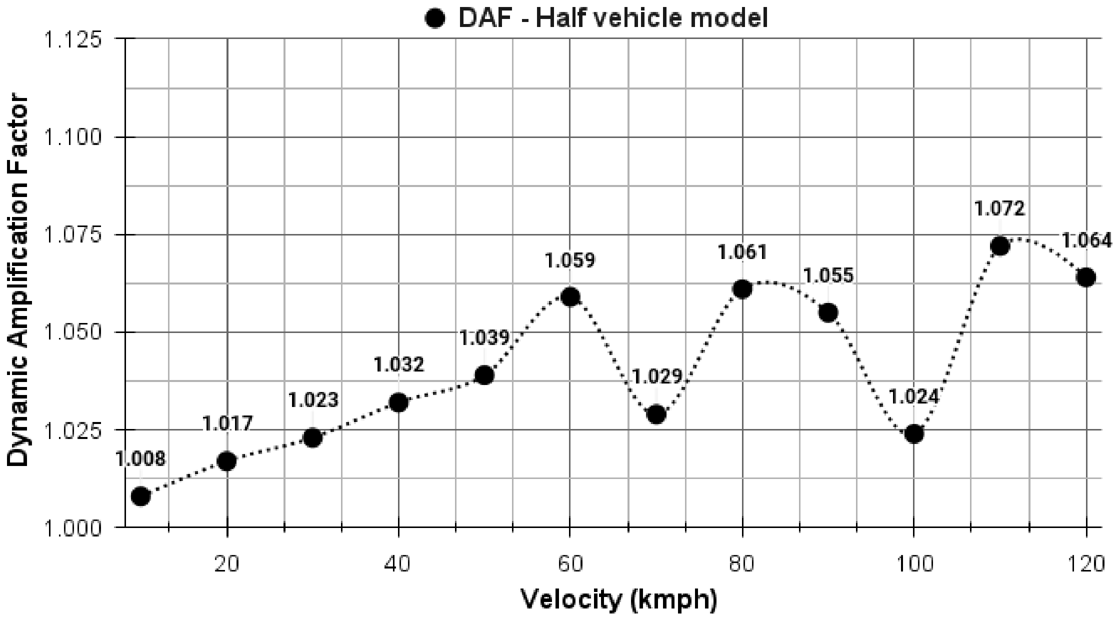

Figure 11 The Dynamic amplification factor results (Zhou, 2015).

The results shown in Figure 11 indicate that the average and maximum Dynamic Amplification Factors were 1.04 and 1.072, respectively. The data demonstrates that dynamic amplification varies with vehicle speed, with the highest amplification observed at a velocity of 110 kmph. On considering the pattern of variation of DAF values with respect to velocity, it can be observed that the dynamic amplification increased proportionally with velocity up to 50 kmph. But, beyond this point, the trend shifted, with amplification exhibiting fluctuations as velocity continued to increase. Additionally, the results also showed that for a 40-meter span bridge, the dynamic amplification remained quite low, with values below 1.10.

4.1.2 Moving load method (Fryba, 1972)

As discussed in the literature review section, the moving load method was introduced by L. Fryba in the year 1972. It was utilized to determine the dynamic deflection that resulted from the movement of the point load across a simply supported beam, idealized as a bridge model (Figure 12). In this method, the vibration equations are solved using Laplace - Carlson integral transformation and beam deflections were computed.

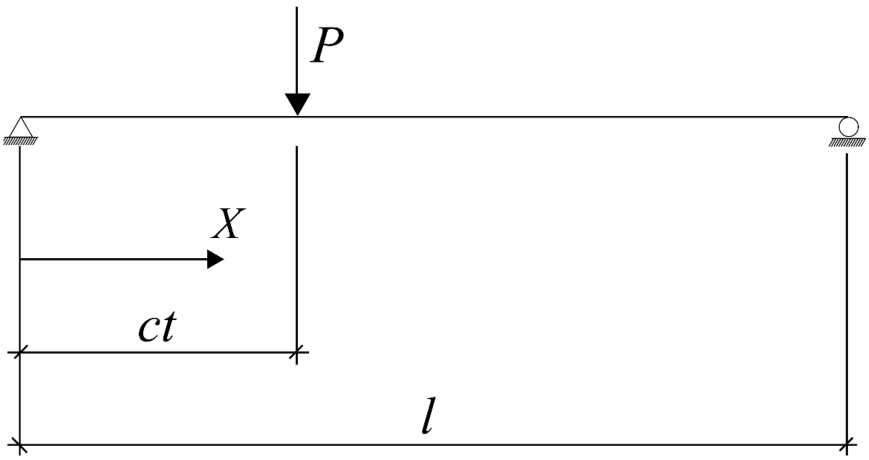

Figure 12 Based on the work of L. Fryba (1972)

Since the results from this analysis are compared with the Half Vehicle Model (Zhou, 2015), the parameters used in (Zhou, 2015) will be utilized here. The analysis considers a velocity range of 10 to 120 kmph, and damping is neglected as it was not a parameter in the Half Vehicle Model (Zhou, 2015).

In the moving load method, the effect of velocity is incorporated by the utilization of load circular frequency (ω) which is computed based on the formula ($\frac{\pi * c}{l}$) where 'c' is constant speed in m/s^2 and 'l' is the bridge span. The load circular frequency for the velocity range of 10 to 120 kmph can be referred to in Table 7.

Table 7 The different load circular frequencies utilized in the analysis.

#	Velocity (m/s^2)	Velocity (kmph)	Load Circular Frequency (rad/sec)
1	2.78	10	0.218
2	5.56	20	0.436
3	8.33	30	0.654
4	11.11	40	0.873
5	13.89	50	1.091
6	16.67	60	1.309
7	19.44	70	1.527

8	22.22	80	1.745
9	25.00	90	1.963
10	27.78	100	2.182
11	30.56	110	2.400
12	33.33	120	2.618

A total of 20 modes are considered for each velocity case to determine the Dynamic Amplification Factor (DAF) values. The constants α and β were computed based on the bridge and velocity parameters for each case. The time duration of each analysis varies depending on the velocity considered in the simulation and to ensure maximum accuracy in the dynamic amplification calculations, a time step of 0.001 seconds is considered. The dynamic deflection is calculated using Equation (2), and the corresponding DAF is determined using Equation (1). The coding for the analysis was done using MATLAB, while the plotting was performed with Microsoft Excel.

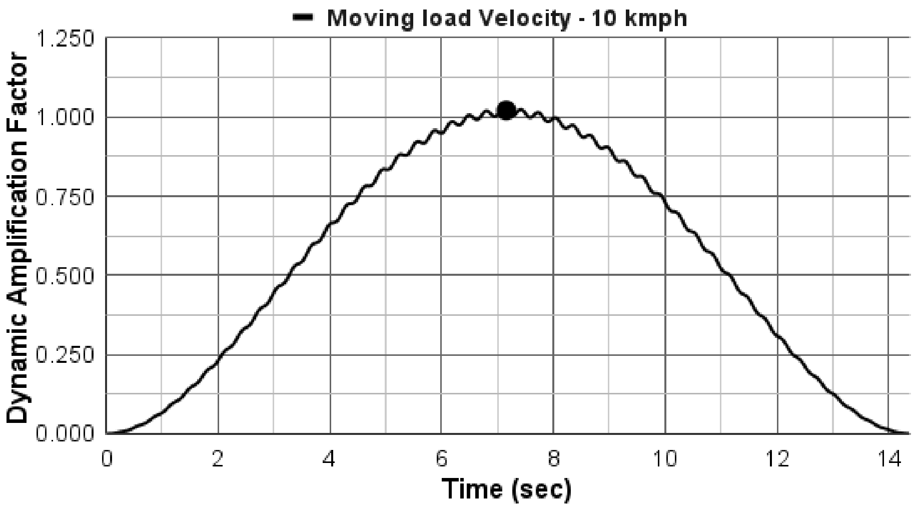

Figure 13 Variation of dynamic amplification factor for a velocity of 10 kmph.

For the first analysis of the moving load method, let us consider a velocity of 10 kmph (Figure 13) with a corresponding load circular frequency $\left(\frac{\pi * c}{l}\right)$ of 0.218 rad/sec. At this velocity, the time taken for the load to traverse the beam model is 14.38 seconds. The dynamic response is computed at each time step of 0.001 seconds, and the corresponding Dynamic Amplification Factor (DAF) is determined.

The maximum amplification observed during the entire loading duration is utilized as the DAF value for each velocity scenario. For a velocity of 10 kmph, the DAF was found to be 1.025 and this result indicates that at very low velocities, there is minimal amplification of the loads. The small oscillations present at the peaks are due to the variation of the sine function of the damped circular frequency of the beam.

The total dynamic amplification occurs as a result of the contributions from each of the 20 modes as shown in Figure 14. It can be clearly seen that it's the fundamental mode that predominantly contributes towards the dynamic amplification effect. The contributions from the fundamental mode was determined to be 98% and the rest comes from other modes.

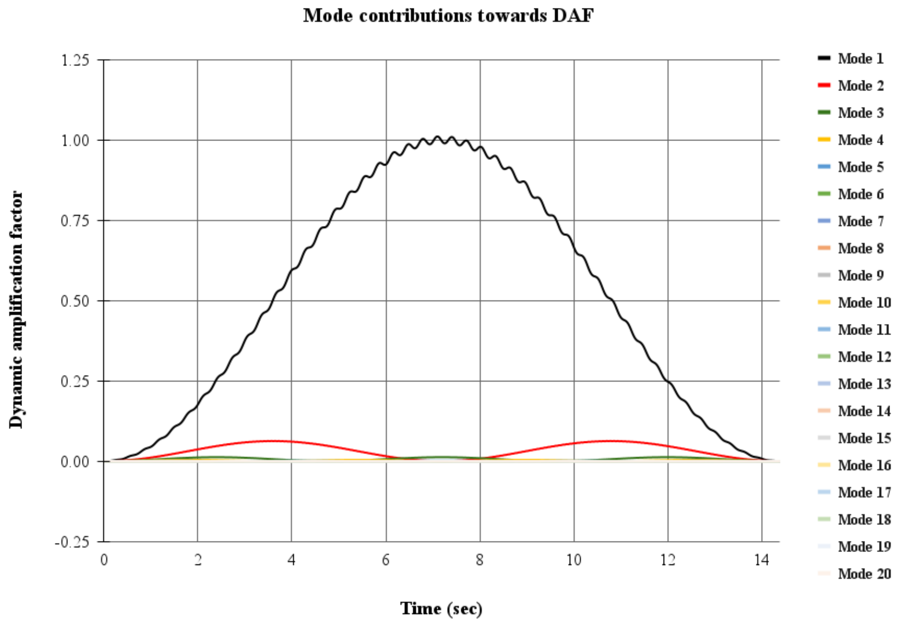

Figure 14 Mode contributions towards DAF for velocity of 10kmph

It was noted that the maximum dynamic amplification did not occur when the load was at the midspan of the beam model. Instead, the peak dynamic amplification happened shortly after the load had passed the midspan. While the maximum static load deflection occurs at midspan, this analysis shows that maximum dynamic deflection does not necessarily align with the load's position at midspan.

Analyses were similarly conducted for velocities ranging from 10 to 120 kmph. As the velocity increased, the time duration required for the load to traverse the bridge decreased. The amplification observed at each time step for the different velocities is shown in Figure 15.

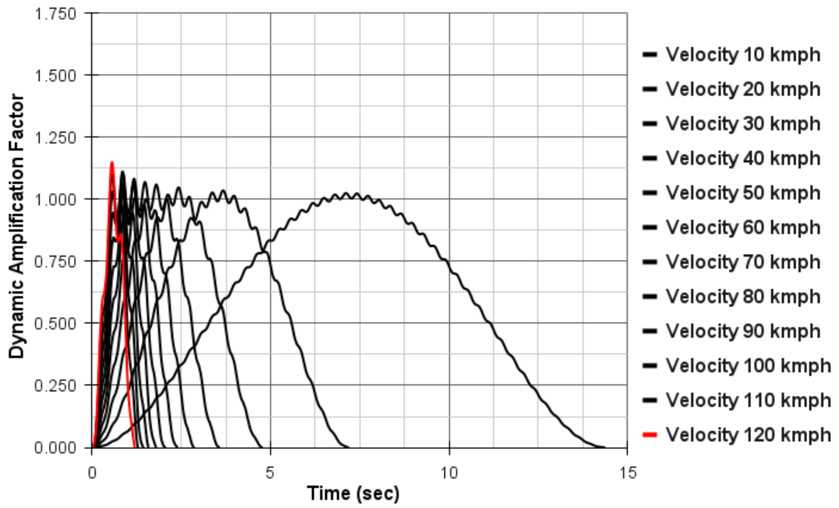

Figure 15 Variation of DAF for each time step at a velocity range of 10-120 kmph

From the analysis results, the maximum Dynamic Amplification Factor (DAF) for each velocity case was determined and plotted in Figure 16. The results showed that the maximum dynamic amplification of 1.149 occurred at a velocity of 120 kmph, with an average dynamic amplification of 1.076 for this model. The results indicate a proportional increase in DAF values with respect to velocity up to 60 kmph, after which the trend starts to vary with further increases in velocity.

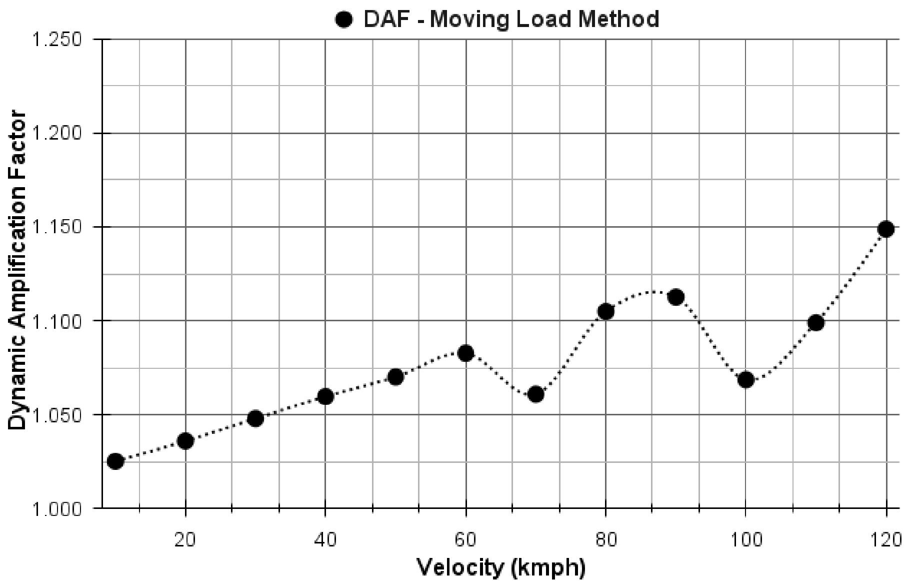

Figure 16 Variation of DAF values for velocity range of 10 to 120 kmph

In Figure 16, it can be observed that the dynamic amplification factor is showing inconsistent variations with the increase in velocity. This is due to the contribution of the damped circular frequency of the beam. For certain beam frequencies, the contribution towards the dynamic amplification effect is much more pronounced than other beam frequencies and thus leads to the higher dynamic amplification and this is being illustrated in figure 17.

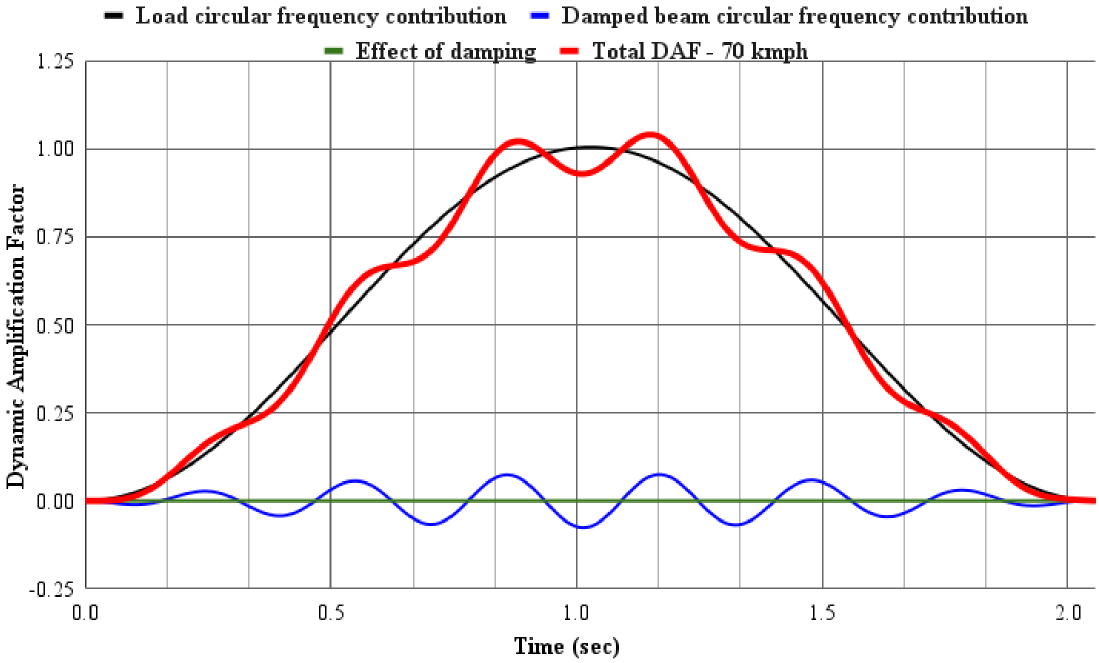

Figure 17 Contributions of different factors towards DAF

Figure 17 illustrates the contributions of the load circular frequency, the damped beam frequency, and the effect of damping on the DAF for a constant velocity of 70 kmph. In this case, damping was neglected, resulting in no observed contributions. For a velocity of 70 kmph, the contribution of the damped circular frequency is significantly lower compared to velocities such as 60 kmph. Consequently, the DAF value is lower at 70 kmph than at 60 kmph. This indicates that for certain critical damped circular frequencies of beams, the dynamic amplification factors are reduced, leading to variations in DAF values as velocity increases.

4.1.3 Coupled model – (Sadeghi, 2020)

In the model proposed by Soheil et al., the considered parameters include mass ratio, stiffness ratio, and frequency ratio. Notably, damping is not accounted for as a parameter in this model. To establish the ratios, the total mass of the vehicle and bridge is treated as lumped. The bridge's stiffness of the model is computed by incorporating parameters from the Half vehicle model (Zhou, 2015) model into the formula ($\frac{48\,EI}{L^3}$) where EI and L are the bridge stiffness and span respectively. This model has the limitation that it does not show the variation of DAF with time and can only predict a single value. The model does not have the potential to show the time at which the maximum dynamic amplification effect occurs.

The mass and stiffness of the half vehicle model were aggregated, and they amount to 33,450 kg and $6.82*10^6$ N/m, respectively. Similarly, the bridge's mass and stiffness are specified as 480,000 kg and 96,000,000 N/m.

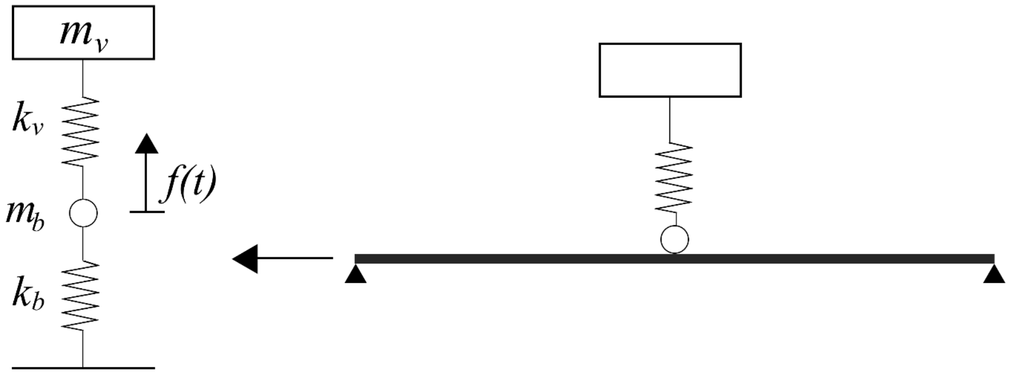

Figure 18 Based on the works of Sadeghi et al. (2020)

The velocity parameter is included in the form of load circular frequency ($\frac{\pi c}{l}$) as modeled in the moving load model. The velocity is restricted to the range of 10-120 kmph, and the peak dynamic amplification of (1.12) is observed at a speed of 120 kmph. It's important to note that, in this specific model, the Dynamic Amplification Factor (DAF) cannot be computed with respect to time. However, the amplification factor can be determined for respective vehicular velocities. Furthermore, in contrast to the findings of the previous model, the dynamic amplification factor was observed to be increasing

Table 8 Variation of DAF values based on the work of Sadeghi et al.(2020)

Description	Values	Units	Velocity (kmph)	Load Circular Frequency (We)	Frequency Ratio (We/Wv)	DAF
Bridge span	40	M	10	0.218	0.015	1.08
Mass of bridge	480000	Kg	20	0.436	0.031	1.08
Mass of vehicle	33450	Kg	30	0.654	0.046	1.08
Stiffness of bridge	96000000	N/m	40	0.873	0.061	1.09
Stiffness of vehicle	6820000	N/m	50	1.091	0.076	1.09

Mass ratio	14.35		60	1.309	0.092	1.09
Stiffness ratio	14.08		70	1.527	0.107	1.09
Frequency of vehicle	14.28	rad/sec	80	1.745	0.122	1.10
			90	1.963	0.137	1.10
			100	2.182	0.153	1.11
			110	2.400	0.168	1.11
			120	2.618	0.183	1.12

4.1.4 Lumped spring mass model – (Yang, 2009)

In this model, a vehicle of lumped mass 'm_v' and stiffness 'k_v' is considered to move across a simply supported beam of span 'L' with a constant velocity of 'v'. The modulus of elasticity and moment of inertia of the beam model is represented as 'E' and 'I' respectively. The displacement of the bridge and vehicle are represented as 'u_b' and 'q_v' and the mass per unit length is represented as '$\overline{m}$'. In this model, the vehicular bridge interaction is considered and thus comparison of this results with the moving load method will indeed give insights regarding the potential of the moving load method to determine the dynamic amplification factor.

In this model, a vehicle with lumped mass 'm_v' and stiffness 'k_v' moves across a simply supported beam of span 'L' with a constant velocity 'v'. The modulus of elasticity and moment of inertia of the beam are denoted by 'E' and 'I' respectively. The displacements of the bridge and vehicle are represented by 'u_b' and 'q_v', and the mass per unit length of the beam is '$\overline{m}$'. This model takes into account vehicular-bridge interaction and comparing these results with those from the moving load method will definitely provide insights into the effectiveness of the moving load method in the determination of Dynamic Amplification Factor.

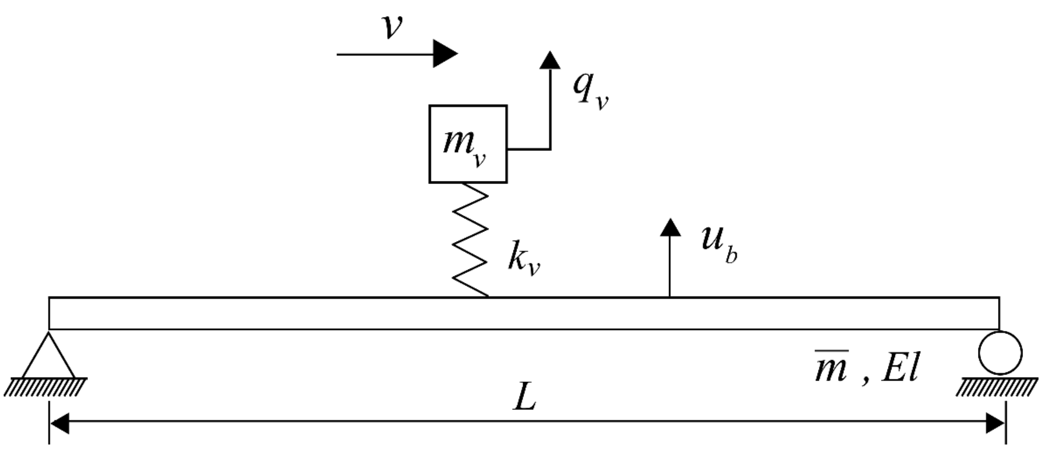

Figure 19 Based on the work of Yang et al. (2009)

The dynamic deflection of the bridge model, caused by the vehicle moving across it at a specific velocity, was calculated using Equation (5). For this analysis, the bridge and vehicle parameters from (Zhou, 2015) were employed. The mass and stiffness properties of the half-vehicle model were lumped to integrate them into this model. Thus, the mass (m_v) and stiffness (k_v) of the vehicle were 33450 kg and 6.82 x 10^6 N/m.

The average and maximum Dynamic Amplification Factors (DAF) from this model were 1.061 and 1.032, respectively. The maximum dynamic amplification was observed at a velocity of 120 kmph, indicating that peak amplifications might be occurring at higher velocities. The results also demonstrated an increase in DAF with increasing velocity up to 60 kmph, after which the trend varied. The analysis revealed that dynamic amplification was lower at lower velocities, with the minimum amplification recorded at 1.01.

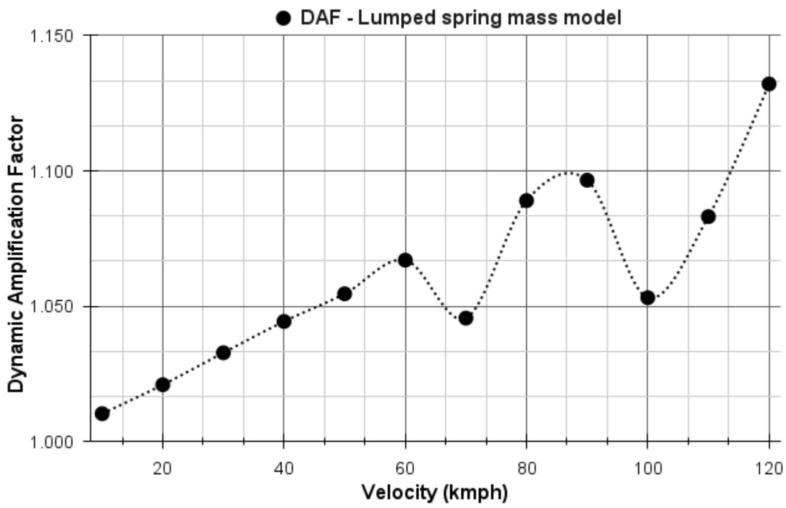

Figure 20 Variation of DAF for the velocity range based on the work of Yang et al. (2009)

4.2 Analysis result comparison between mathematical models

Comparison between the models reveals that the outcomes of the moving load model (Fryba, 1972) as well as the lumped spring mass model (Deng, 2015) align well with the intricate model proposed by Zhou et al. (2015). But, considering the coupled model put forth by Sadeghi et al. (2020), it is notable that the results from this model is not well aligned with the other model results. On considering the results from the model (Sadeghi, 2020), minimal variations were seen in Dynamic Amplification Factor (DAF) values with changing velocities. The model only exhibits a range of 1.08 to 1.12 across velocities ranging from 10 to 120 kmph. Furthermore, unlike other models, this model displays an increase in DAF with rising velocities, indicating a flaw in its accuracy and the rationale for this is that as the vehicle velocity rises, the frequency ratio also increases. When this ratio approaches one, the amplification likewise intensifies. (Refer Table 8)

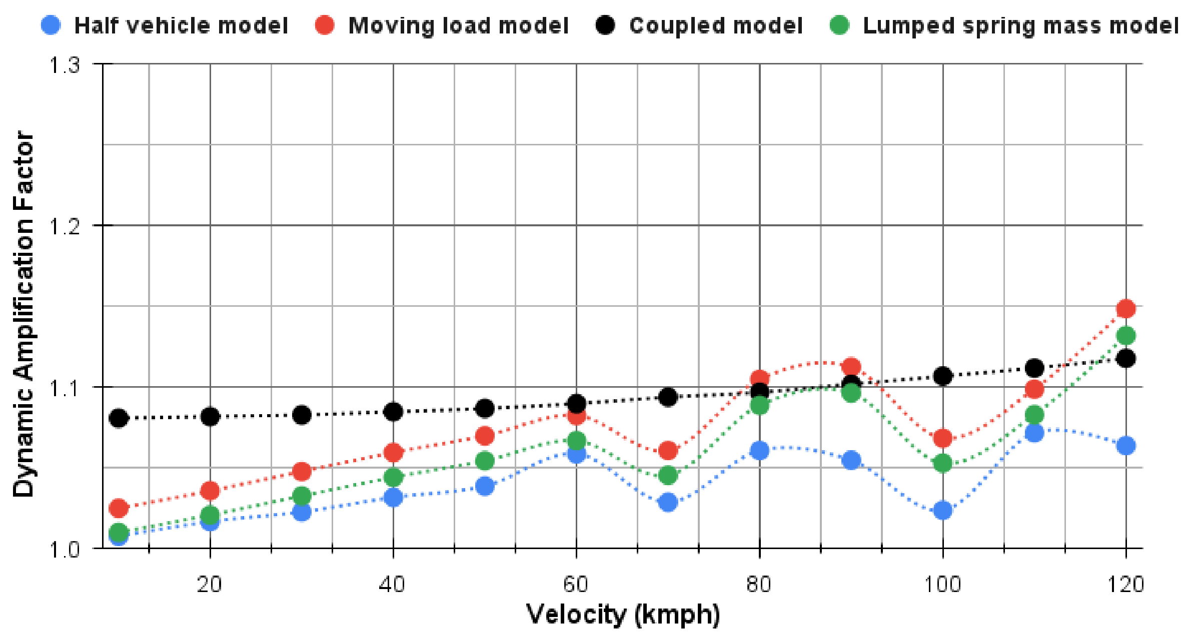

Figure 21 Comparison of DAF values between analytical models for the velocity range

The comparative analysis results (Figure 21) indicate that only two of the compared models align with the half vehicle model (Zhou, 2015). Both the moving load method and the lumped mass spring model exhibited a similar trend in the variation of the Dynamic Amplification Factor (DAF) with velocity. In these models, like in (Zhou, 2015), the DAF increased with velocity up to 60 kmph. Beyond this point, the trend varied, with DAF values both increasing and decreasing as velocity increased.

Table 9 Maximum, Minimum and Average DAF of the analytical models

#	Model description	Minimum DAF	Maximum DAF	Average DAF
1	Moving load model (Fryba,1972)	1.03	1.149	1.076
2	Half vehicle model (Zhou, 2015)	1.01	1.072	1.040
3	Coupled model (Sadeghi, 2020)	1.08	1.12	1.095
4	Lumped spring mass model (Yang, 2009)	1.01	1.132	1.061

However, Models (Fryba, 1972) and (Yang, 2009) diverged from this trend at a velocity of 120 kmph. Model (Zhou, 2015) showed a decrease in DAF from 110 kmph to 120 kmph, whereas models (Fryba, 1972) and (Yang, 2009) displayed an opposite pattern, with increasing DAF values. Despite this variation, all three models (Fryba, 1972), (Zhou, 2015), and (Yang, 2009)) generally demonstrated consistency in DAF values relative to changes in velocity.From Table 9, the average DAF values for the moving load model and the lumped spring mass model are 1.76 and 1.061, respectively. When compared to the average DAF value of 1.04 from the half-vehicle model (Zhou, 2015), these variations are minimal. Specifically, the average DAF values for models (Fryba, 1972) and (Yang, 2009) show differences of only 3.48% and 1.98%, compared to model (Zhou, 2015).

4.3 Discussion

In this section, the results from various analytical models—specifically the half-vehicle model (Zhou, 2015), the coupled model (Sadeghi, 2020), and the lumped spring mass model (Yang, 2009)—were compared to evaluate the potential of the moving load method. The results indicated that models (Fryba, 1972) and (Yang, 2009) were consistent with the half-vehicle model (Zhou, 2015). With respect to velocity parameter, the study examined the variation of dynamic amplification across different velocities, revealing a consistent increasing pattern up to 60 kmph. Furthermore, the results showed that the dynamic amplification was very low at a velocity of around 10 kmph and the rationale is that at such low velocities, the moving vehicle or load behaves similarly to a static load, leading to minimal dynamic amplification.

The analysis revealed that the results from the coupled model (Sadeghi, 2020) were not consistent with those of the other models, as the DAF values from this model showed a different trend where the DAF values continuously increased with velocity, which contrasts with the results of the other models. This suggests that further simplification of parameters beyond those used in the moving load method would result in inaccurate outcomes and cannot be relied upon for determining DAF values. When comparing the results from the moving load method with those from the half-vehicle model and the lumped spring mass model, the variation in outcomes was minimal, with the moving load method yielding more conservative results than the other models. From the analysis, it can be concluded that, despite not accounting for vehicle characteristics or vehicle-bridge interaction, the moving load method can still produce results that closely align with models that do include these factors. Furthermore, among all the analytical models considered, only the moving load method has the potential to incorporate bridge damping as a parameter. Therefore, these analysis results clearly indicate that the moving load method is a viable approach for determining the Dynamic Amplification Factor (DAF).

Chapter 05

5 Parametric study and comparison with BWIM Test results

5.1 Introduction

From Chapter 4, it was seen that the results from the moving load method are consistent with those from more intricate models. This highlights the potential of using the moving load method to determine the dynamic amplification factor, even though it does not account for physical vehicle characteristics or vehicle-bridge interaction.

In this section, a parametric study will be presented, focusing on bridge span, natural frequency, damping, and vehicle or load velocity as key parameters. A total of eight bridges with varying properties will be considered, with four models having rectangular cross sections and the remaining four featuring I-shaped cross sections. All bridge models used in this study are sourced from existing literature, and their parameters will serve as inputs for the moving load method. The spans of the models range from 14 to 100m, with natural frequencies between 0.75 and 8.03 Hz.

A comparison of various design codes in the literature review indicated that bridge frequency was traditionally used to incorporate the dynamic amplification factor (DAF) into design, while many modern codes now use bridge span as a parameter. Hence, this study also explores whether DAF can be incorporated into design using either bridge span or bridge frequency as a single parameter. To investigate this, two models with the same span but different frequencies, and two models with the same frequency but different spans, are analyzed.

After examining whether bridge frequency or span can serve as a single parameter for incorporating DAF into design, a comparison will be made between the model results and Bridge Weigh-in-Motion (BWIM) data (Kalin, 2022) to evaluate the consistency of the moving load method with actual dynamic test results. Additionally, a preliminary analysis using BWIM data will be conducted to assess whether bridge span alone can be used to incorporate DAF into design.

5.2 Different bridge models and corresponding DAF values

The literature review revealed that the dynamic amplification factor (DAF) is influenced by multiple parameters, including both bridge and vehicle characteristics. However, the moving load method accounts only for bridge parameters and hence, the parametric study will focus on the relevant bridge factors. The major bridge parameters that influence DAF include span length, natural frequency, bridge damping, and road surface irregularities. All of these, except road surface irregularities, will be considered, as the moving load method does not incorporate it as a parameter. Regarding vehicle characteristics, only vehicle velocity is included in the moving load method, the study will examine how variations in velocity impact the DAF.

To examine the effects of these parameters, the study analyzes eight bridge models with varying properties. Four of these models have rectangular cross-sections, while the other four have I-shaped cross-sections. The bridge models are numbered from 01 to 08, and these numbers will be used for referencing the models. The parameters for the rectangular and I-shaped sections are detailed in Table 10 and Table 11, respectively.

Table 10 Properties of bridge models with rectangular cross sections

Bridge no	Units	01	02	03	04
Bridge span	(m)	14	25	25	40
Bridge width	(m)	10	8.5	2.36	1.71
Bridge depth	(m)	0.625	1.25	0.85	2.92
Moment of Inertia (I)	(m)	0.2035	1.3835	0.12	3.555
Density (d)	(m)	2420	2446	2400	2400
Mod of Elasticity (E)	(m^4)	$35x10^9$	$36x10^9$	$27.5x10^9$	$36x10^9$
Mass per unit length	(m^2)	15125	26201.25	4814.4	12000
Bridge Frequency	(Hz)	5.5	3.48	2.08	3.206

The bridge models used in this study are adapted from established models found in the literature, specifically cited in references (Zhou, 2015), (Sadeghi, 2020), (Brady, 2006), (Shokravi, 2024), and (Malekjafarian, 2022). The bridge span considered in the study ranges from 14 to 100 meters, with frequencies between 0.75 Hz and 8.03 Hz. Bridge damping is not considered in the initial analysis but is utilized for the bridge damping parametric study.

Table 11 Properties of bridge models with I cross sections

Bridge no	Units	05	06	07	08
Bridge span	(m)	15	30	50	100
Outside depth	(m)	0.6	1.1	1.6	2.4
Outside width	(m)	0.3	0.5	1.3	2
Flange thickness	(m)	0.04	0.05	0.1	0.15
Web thickness	(m)	0.02	0.03	0.05	0.1
Moment of Inertia (I)	(m^4)	0.0021	0.0163	0.1579	0.8376
Area	(m^2)	0.034	0.08	0.33	0.81
Density (d)	(kg/m^3)	2400	2400	2400	2400
Mod of Elasticity (E)	(N/m^2)	$5.0978*10^{10}$	$5.0978*10^{10}$	$5.0978*10^{10}$	$5.0978*10^{10}$
Bridge Frequency	(Hz)	8.03	3.63	2.05	0.75

Initially, the parameters for bridge models 01 to 08 are applied to equation (1) to calculate the dynamic deflection for each model as a moving load passes over the bridge at velocities ranging from 10 to 120 kmph. The effect of damping was not considered in this analysis. Then, the static deflection for the same moving load is computed, and the dynamic amplification factor (DAF) for each velocity scenario is determined using equation (2). The DAF values across the velocity range of 10 to 120 kmph for all models are presented in Table 12.

Table 12 DAF values for bridge model 01 to 08 for the velocity range of 10 - 120 kmph

#	Velocity (kmph)	Bridge 01	Bridge 02	Bridge 03	Bridge 04	Bridge 05	Bridge 06	Bridge 07	Bridge 08
1	10	1.033	1.031	1.039	1.025	1.026	1.027	1.028	1.031
2	20	1.051	1.047	1.070	1.036	1.038	1.041	1.041	1.053
3	30	1.070	1.049	1.073	1.048	1.044	1.052	1.054	1.064

4	40	1.079	1.079	1.080	1.060	1.053	1.066	1.068	1.063
5	50	1.113	1.073	1.159	1.070	1.054	1.079	1.086	1.116
6	60	1.069	1.115	1.179	1.083	1.085	1.056	1.092	1.064
7	70	1.134	1.054	1.088	1.061	1.083	1.112	1.113	1.156
8	80	1.183	1.140	1.074	1.105	1.116	1.100	1.051	1.186
9	90	1.175	1.182	1.196	1.113	1.088	1.073	1.128	1.156
10	100	1.115	1.179	1.307	1.069	1.084	1.139	1.174	1.076
11	110	1.020	1.135	1.403	1.099	1.142	1.177	1.186	1.048
12	120	1.091	1.060	1.480	1.149	1.176	1.186	1.165	1.137

From the analysis, the average, maximum and minimum DAF were determined for each of the bridge models, and they are mentioned in Table 13. These dynamic amplification values would be utilized in the parametric study which starts with bridge span followed by bridge frequency, bridge damping and vehicle velocity.

Table 13 Maximum, Minimum and Average DAF values for the bridge models.

Description	Bridge 01	Bridge 02	Bridge 03	Bridge 04	Bridge 05	Bridge 06	Bridge 07	Bridge 08
Span (m)	14	25	25	40	15	30	50	100
Frequency (Hz)	5.5	3.48	2.08	3.206	8.03	3.63	2.05	0.75
Maximum DAF	1.183	1.182	1.480	1.149	1.176	1.186	1.186	1.186
Minimum DAF	1.020	1.031	1.039	1.025	1.026	1.027	1.028	1.031
Average DAF	1.094	1.095	1.179	1.076	1.083	1.092	1.099	1.096

5.3 Parametric study – Bridge span

This section focusses on comprehending the effect of variation in dynamic amplification with respect to the change in bridge span. The variation of DAF with respect to bridge span is studied here as several design codes utilize bridge span as the parameter based on which the dynamic amplification factor is incorporated, and the critical aspect is to comprehend whether bridge span alone is sufficient to determine dynamic amplification.

Thus, to gain a clear understanding of the influence of span on dynamic amplification, bridge models with spans ranging from 14 m to 100 m are analyzed in this study. Additionally, to further explore how other factors might affect DAF for a fixed span, two models (Models 03 and 04) with identical spans of 25 m but varying other parameters are considered. These results will shed light on whether parameters beyond bridge span significantly impact DAF.

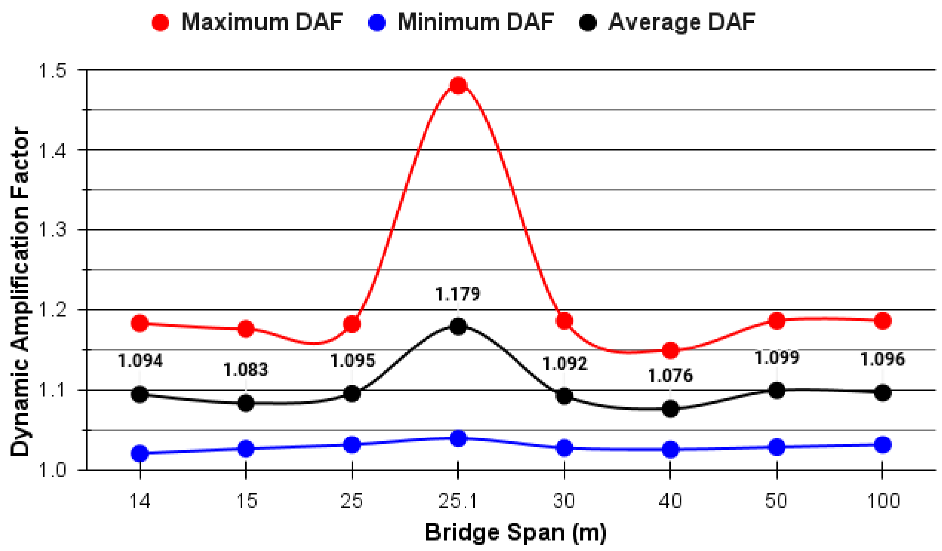

Figure 22 Variation of DAF with respect to bridge span

For representation purposes, Bridge Model 03, with a 25 m span, is plotted as 25.1m. From Figure 22, it is evident that for all the bridge spans considered, the minimum DAF values remain well within 10%, indicating that the minimum DAF does not vary significantly across different spans, whether small or large.

Despite considering a wide span range from 14 to 100 meters in this analysis, the results do not show a clear pattern of variation in DAF values with respect to bridge span. The average DAF for a 14-meter span was found to be 1.094, while for a 100-meter span, it was 1.096. The literature review indicates that many design codes include bridge span as a factor, based on the theory that dynamic amplification decreases with increasing span length. However, the preliminary analysis results did not reveal any distinct pattern. Therefore, to establish a relationship between DAF and bridge span, more analysis results would be required.

A key observation from the results is that, despite having the same 25m span, the dynamic amplifications recorded were 1.179 and 1.095 for models 3 and 4. Furthermore, comparing the maximum dynamic amplification for these models revealed a significant 35% variation in DAF values. When examining the average dynamic amplifications across the range of spans from 14 m to 100 m, it was found that a notable change in DAF occurred only in Model 04 with a 25 m span (1.179). For the remaining spans, the average DAF value ranged from 1.076 to 1. 099.These findings suggest that bridge span should not be the sole criterion for incorporating DAF, as the dynamic amplification varies considerably with changes in other model properties. Therefore, this preliminary study indicates that relying solely on bridge span to determine the dynamic amplification factor in design could lead to inaccuracies.

5.4 Parametric study – Bridge frequency

Bridge frequency was traditionally used to incorporate DAF into design. However, over time, a shift occurred, and bridge span became the primary parameter for incorporating DAF in several design codes. From the previous analysis, it was comprehended that relying solely on bridge span is insufficient for accurately incorporating DAF into design. Thus, this section evaluates the effectiveness of using bridge frequency alone as a parameter for incorporating DAF into design. In this study, two bridge models with nearly identical frequencies are also examined to assess whether the DAF values would significantly differ for models with similar frequencies. Bridge Models 03 and 07, with frequencies of 2.08 Hz and 2.05 Hz, are utilized for this purpose.

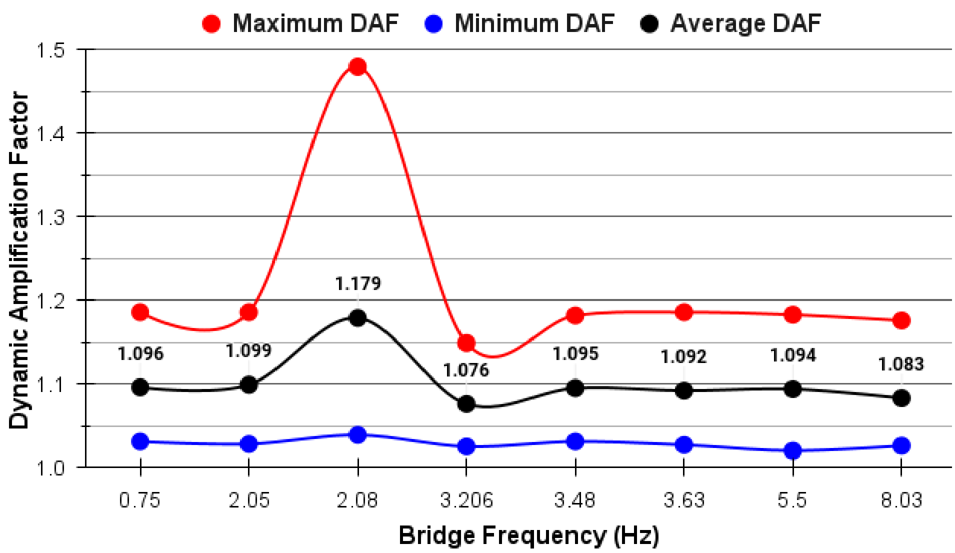

Figure 23 Variation of DAF with respect to bridge frequency

Figure 23 shows the variation minimum, maximum and average DAF for all the bridge models with respect to bridge frequency. A broad frequency range was considered in the study to understand the variation of DAF with respect to bridge frequency. However, like the case with bridge span, the effect of frequency variations did not show significant changes in DAF values. For instance, the DAF values for bridges with frequencies of 0.75 Hz and 8.03 Hz were 1.096 and 1.083, respectively. Thus, more analysis needs to be done for establishing a relationship between bridge frequency and DAF.When comparing DAF values across the frequency range of 0.75 Hz to 8.03 Hz, significant variation occurs primarily at 2.08 Hz relative to the other frequencies considered in the study. Additionally, comparison of results of bridge models with frequencies 2.08 Hz and 2.05 Hz shows that DAF values for nearly identical spans varies up to 35% in terms of maximum DAF values.

These results suggest that much like bridge span, bridge frequency should not be used as the sole parameter for incorporating DAF into design, as dynamic amplification effects vary even at identical frequencies. This variation could be attributed to differences in bridge span, as the spans of the models with identical frequencies were 25m and 50m, respectively. Thus, these studies give a preliminary indication that a coupled approach where both bridge frequency as well bridge span being considered as parameters might be the right approach to estimate the dynamic amplification effect with accuracy.

5.5 Parametric study – Bridge damping

The literature review indicated that bridge damping influences the dynamic amplification effect on bridges. To evaluate its impact on the dynamic amplification factor, a 3% damping ratio was applied to all eight bridge models, and DAF values were calculated for velocities ranging from 10 to 120 kmph. The maximum, minimum, and average DAF values for each bridge model were then determined and presented in Table 14.

Table 14 Maximum, Minimum and Average DAF values with 3% damping.

Description	Bridge 01	Bridge 02	Bridge 03	Bridge 04	Bridge 05	Bridge 06	Bridge 07	Bridge 08
Span (m)	14	25	25	40	15	30	50	100
Frequency (Hz)	5.5	3.48	2.08	3.206	8.03	3.63	2.05	0.75
Maximum DAF	1.142	1.141	1.433	1.113	1.136	1.143	1.143	1.144
Minimum DAF	1.010	1.016	1.017	1.015	1.015	1.015	1.015	1.015
Average DAF	1.062	1.063	1.146	1.047	1.053	1.061	1.067	1.065

The results in Table 13 were used to conduct comparative analysis with the DAF results from bridge models where damping was not considered. Table 14 provided the results for the 3% damping case across all eight bridge models and the variations in maximum, minimum, and average dynamic amplification between these scenarios are detailed in Table 15.

Table 15 Variation in DAF values between 0% and 3% damping

Description	Bridge 01	Bridge 02	Bridge 03	Bridge 04	Bridge 05	Bridge 06	Bridge 07	Bridge 08
Span (m)	14	25	25	40	15	30	50	100
Frequency (Hz)	5.5	3.48	2.08	3.206	8.03	3.63	2.05	0.75
Variation % - Max DAF	3.60%	3.58%	3.24%	3.20%	3.49%	3.77%	3.76%	3.73%
Variation % - Min DAF	3.05%	0.99%	2.14%	1.03%	1.10%	1.22%	1.30%	1.61%
Variation % - Avg DAF	3.02%	3.00%	2.88%	2.83%	2.84%	2.92%	2.99%	2.85%

From Table 15, it is observed that the average DAF values with a 3% damping consideration ranged from 2.85% to 3%. These results clearly indicated that when bridge damping is considered, the magnitude of the dynamic amplification effect reduces. The results showed that the maximum amplification values had a variation of around 4% whereas the average DAF values had a difference of around 3%.

Thus, from these results it can be concluded that the bridge damping does have an impact on the dynamic amplification effect and that the results from moving load on incorporating DAF is consistent with the studies mentioned in the literature review.

5.6 Parametric study – Vehicle velocity

From previous studies, it was clear that no clear correlation has yet been established between dynamic amplification and vehicle velocity. Whether a bridge experiences higher DAF values at high or low vehicle speeds remains an unresolved question.

In this analysis, an attempt is made to gain a basic understanding of the variation in DAF at different velocities, both high and low. Additionally, in earlier sections where comparisons between different analytical models were made, it was observed that DAF increased with vehicle speed up to 60 kmph, after which the trend shifted. Thus, this study also aims to determine whether dynamic amplification follows a similar pattern in line with the previous analysis.

Table 16 Maximum DAF for bridge models and their corresponding velocities

#	Bridge no	Velocity (kmph)	Maximum DAF
1	01	80	1.183
2	02	90	1.182
3	03	120	1.480
4	04	120	1.149
5	05	110	1.176
6	06	120	1.186
7	07	80	1.186
8	08	120	1.186

Table 16 shows that the dynamic amplification factor (DAF) values were higher at high velocities across all eight bridge models. The lowest velocity at which the maximum DAF occurred was 80 kmph, while 25% of the models experienced their maximum DAF at 120 kmph. These findings suggest that dynamic amplification tends to be greater at higher velocities. Additionally, the results from Table 16 indicate that dynamic amplification is minimal when the velocity is 10 kmph or less, as the moving load behaves similarly to a static load at low speeds.

Comparing the maximum DAF results from Table 16 reveals that the maximum DAF values are identical for bridge models 06, 07, and 08. However, the velocities at which these maximum DAF values were attained differ: 120 kmph for models 06 and 08, and 80 kmph for model 07. To better understand any trends in the variation of DAF with respect to velocity, the DAF values for these models are plotted in Figure 24.

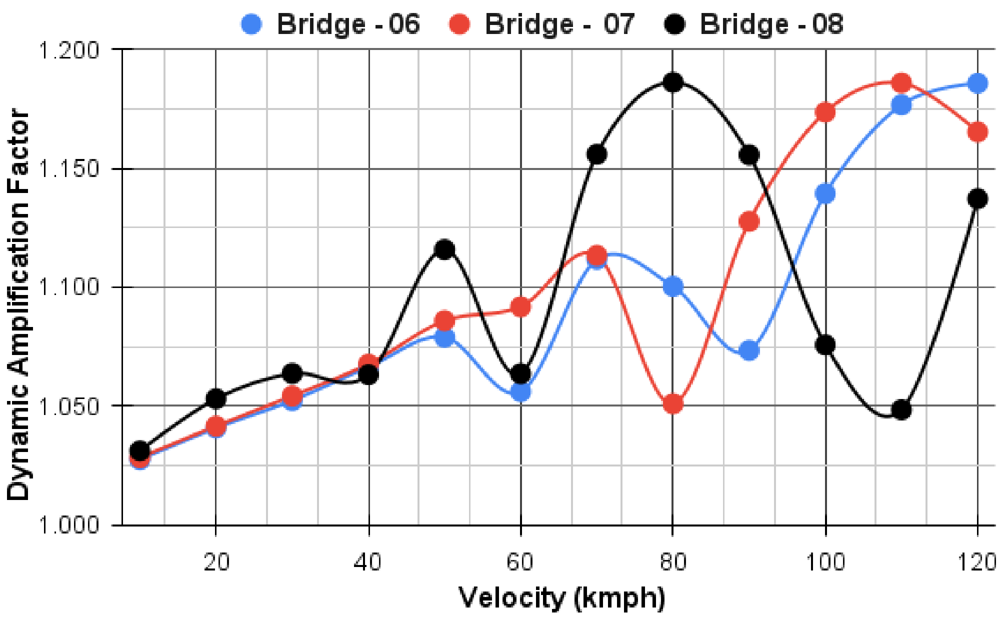

Figure 24 DAF values of bridge models 06, 07 and 08

Figure 24 indicates that DAF values increase with velocity up to 30 kmph for model 08 and up to 50 kmph for models 06 and 07. However, previous analysis showed an increase in DAF with velocity up to 60 kmph. Comparing these results suggests that the trend of DAF variation with velocity fluctuates, and no definitive conclusion can be drawn regarding this trend, as it significantly depends on other bridge model parameters.

Thus, it can be concluded that while dynamic amplification generally increases with velocity up to a certain point, but this trend cannot be estimated as the dynamic amplification effect is significantly influenced by specific bridge model characteristics like bridge span and frequency.

5.7 Comparison between Moving load model and BWIM results

The bridge weigh in motion data was collected from the actual testing done on 16 bridges throughout the US. The results used here are based on the work of Kalin et al. (2022) and the method of computation of DAF from BWIM data were detailed in the literature review section. Thus, the dynamic amplification factors obtained from the bridge weight in motion data are mentioned in Table 17.

Observing the data from Table 17, obtained through actual site tests, it is evident that the average dynamic amplifications were relatively low, ranging from 1.02 to 1.23. A comparison between bridge spans of 6.8 m and 7.4 m reveals a significant change in average dynamic amplification, with values of 1.08 and 1.23 respectively, despite the difference in span being only 0.6 m. Similarly, for spans of 25 m and 25.8 m, a notable difference in dynamic amplification is observed. Thus, these results provide an indication that if the bridge span is the only parameter considered in DAF, the results might not be accurate. These raises questions on which parameters need to be considered along with bridge span for a more precise estimation of the dynamic load effect on bridges.

Table 17 Data extracted from the work of (Kalin, 2022)

#	Bridge span (m)	Average DAF
1	5.5	1.03
2	6.6	1.09
3	6.8	1.08
4	7.4	1.23
5	9.7	1.1
6	10.4	1.08
7	10.5	1.1
8	11	1.05
9	12	1.11
10	12.2	1.05
11	14	1.05
12	15	1.05
13	25	1.17
14	25.8	1.05
15	34.4	1.06
16	35	1.02

In addition, to evaluate if the moving load method can address these differences, comparisons will be made using results from earlier analyses. Although earlier sections covered models with bridge spans ranging from 14 m to 100 m, only results from the models within the range of 5.5 m to 35 m will be considered, as this range corresponds to the test results from BWIM data.

The results from 17 are used to compare the BWIM test data (Kalin, 2022) with those from the moving load method. For the bridge span of 25.8 m, the results from bridge Model 04 are considered, while for the 25 m span, the results from bridge Model 03 are used. Although the moving load method was not applied to a 34 m span, the results from bridge Model 06 (with a 30 m span) are used to provide a preliminary comparison to assess whether the values fall within a reasonable range.

Figure 25 shows that the DAF values from the moving load model were on the conservative side compared to the actual load test results. However, the results indicate that the moving load method has the potential to accurately predict dynamic amplification, as the values were consistent on comparison with BWIM data.

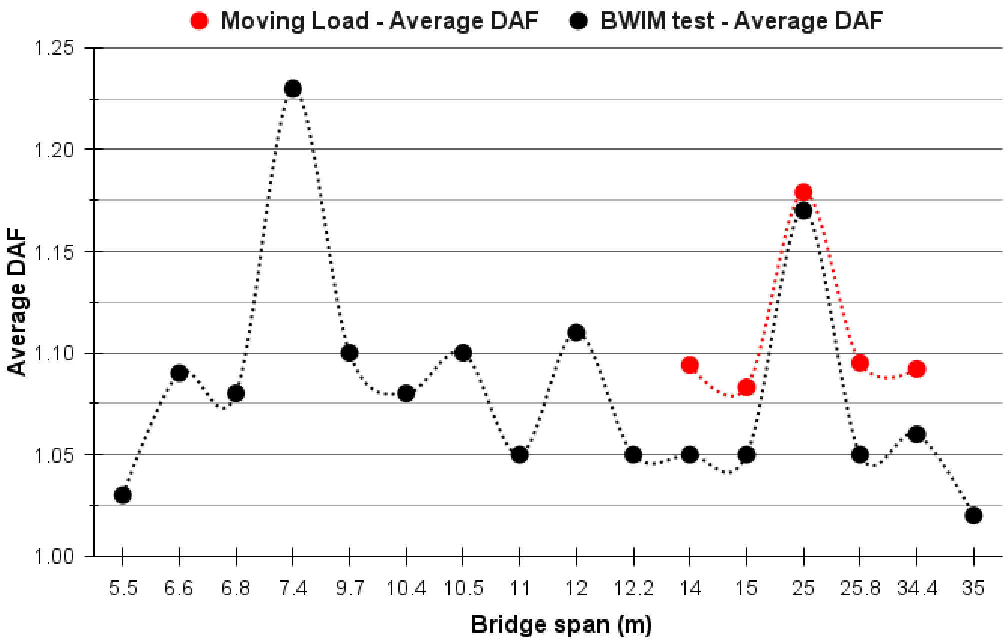

Figure 25 Comparison of BWIM test results (Kalin, 2022) and Preliminary analysis results.

The comparison of the BWIM results with those from preliminary moving load method analysis indicates that the moving load method is quite accurate in predicting dynamic amplification, with variations between test data and moving load results being relatively small, which is about 4.2% at a peak value. Additionally, the moving load results were slightly higher than the actual test data, suggesting that these results are safe for design inclusion.

5.8 Discussion

In this section, eight different bridge models with spans ranging from 14 m to 100 m were initially introduced. Using the parameters of these bridge models, the moving load method was employed to determine the dynamic amplification factor (DAF) for each model, calculating the corresponding maximum, average, and minimum DAF values. A parametric study was then conducted focusing on the effects of bridge span, bridge frequency, bridge damping, and vehicle velocity on the Dynamic amplification factor.

The bridge models considered in this study had spans ranging from 14 to 100 meters, selected to capture the variation of the dynamic amplification effect on both short and long-span bridges. However, the results showed no significant changes in DAF values across the span range, except for the 25-meter bridge model. Similarly, with respect to frequency, the models were chosen to cover both high and low frequencies (0.75 to 8.03 Hz), but the preliminary analysis did not reveal any clear pattern, as the values remained largely unchanged, except for one model. Therefore, to establish a definitive relationship between DAF and bridge span or frequency, further analytical investigation would be necessary.

Since bridge span and frequency are among the key parameters contributing to the dynamic amplification effect, several design codes use these factors to incorporate DAF into structural design. However, design codes typically consider either bridge span or frequency as the deciding parameter for the incorporation. Thus, the present study also aims to determine whether bridge span or bridge frequency could independently be used to incorporate DAF into the design process. The results clearly indicated that neither bridge span nor bridge frequency can serve as a single parameter for this purpose as the results showed significant variations in DAF when comparing bridge models with the same span or the same frequency. These results clearly demonstrated that both parameters alone are insufficient for accurately incorporating DAF into design.

A parametric study was then conducted based on bridge damping, incorporating a 3% damping ratio into all the models. The results from this analysis were then compared to those from the 0% damping case. The results showed that incorporating damping affects in the analysis, the dynamic amplification, with DAF values decrease as the damping increase. Specifically, the maximum DAF values are found to be reduced by approximately 4%, and the average DAF values decreased by 3%.

A parametric study has also been conducted for vehicle velocity to determine if a consistent pattern in DAF values could be identified. One critical observation from the study was that dynamic amplification effect occurs at high velocities. The study also clearly indicated that no uniform trend exists with respect to velocity, as DAF patterns vary with each model. This occurs as the dynamic amplification effect is significantly influenced by other model parameters like bridge span or bridge frequency, making it difficult to establish a consistent pattern based solely on vehicle velocity.

Finally, to get an understanding whether the results from the moving load method are reliable, the results are compared with the actual site test results. For this purpose, the BWIM data based on the works of Kalin et al. (2022) was utilized and the comparison clearly showed the potential of moving load method in determining accurate dynamic amplification factors. Furthermore, on observing the data, it was also clear that considering bridge span alone as a parameter for inclusion of DAF into design might not yield accurate results, as the DAF values for bridge with almost similar span lengths were showing significant variations. Thus, through this section the potential of moving load method in determining dynamic amplification factor on bridges under traffic loads has been once again proved to be useful, and the limitation in using the bridge span or bridge frequency alone as a factor for incorporating DAF into design is understood.

Chapter 06

6 Effect of Skew Angle on DAF using Abaqus CAE

6.1 Introduction

Skew deck bridges are integral components of transportation networks, especially in scenarios where geometric constraints demand unconventional bridge alignments. These structures are engineered to facilitate high-speed traffic and accommodate intricate roadway layouts, serving as critical links within the transportation infrastructure. The skew angle on bridge decks refers to the angle between the longitudinal axis of the bridge and the alignment of the road or structure it spans, typically resulting from geometric constraints that create an oblique intersection. However, the distinct geometry of skew deck bridges introduces complexities in their structural analysis and design, necessitating tailored methodologies to guarantee their safety and reliability under diverse loading scenarios (Patra et al., 2013).

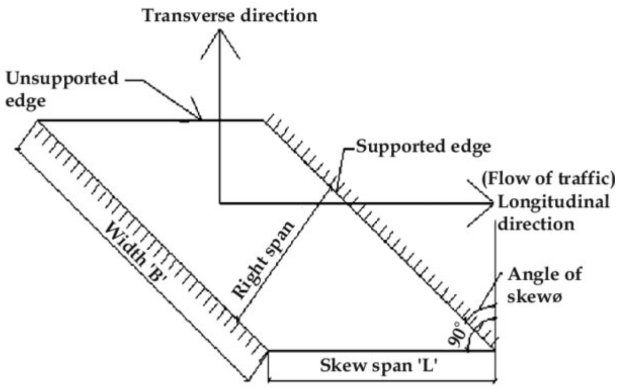

Figure 26 Skew deck slab bridges

Studies conducted by Patra et al. (2024) have shown that the skew angle effect can lead to the redistribution of forces. Hence, this can also lead to the variation on DAF values and needs to be explored. However, on considering the analytical model, it can be comprehended that the method does not have the potential to incorporate skew angle effect. In this regard, to comprehend the effect of skew angle on DAF values, it become imperative to extend the concept into a 3 D Finite Element Model which can determine the variation of Dynamic Amplification Effect with respect to the skew angles.

The crucial aspect was to select a suitable finite element software for determining the dynamic amplification factor (DAF). While software like SAP2000 can define moving load models, it cannot compute the DAF directly, as it requires the amplification factor to be provided as a user-defined parameter. To address the limitations and to accurately determine the DAF, Abaqus CAE software was utilised in the study. Consequently, this section extends the 2D problem to a 3D model using Abaqus CAE 6.22.0.

The input parameters of Bridge Model-01 utilised in the parametric study using moving load method will be considered in the analysis using Abaqus. The bridge will be modelled using solid elements, and the moving load will be applied using the standard explicit method. The skew angles considered in the study are 15^0, 30^0 and 45^0.

6.2 Abaqus CAE modelling

6.2.1 The bridge model:

Abaqus CAE 6.22.0 software was used for the 3-dimensional analysis of the moving load method. All the bridge models were modelled as solid homogeneous sections with properties based on the models utilised in the analytical moving load method. The nonlinear geometric effects were considered in all the models and time periods were fixed based on the moving load velocity incorporated.

The unit system followed in the model is SI and the bridge properties considered in the model were the modulus of elasticity, Poisson's ratio, mass density and material damping. Meshing size of 0.1 is considered for accuracy of the results and hex element shape along with structured technique was utilised for meshing. Since the analytical model doesn't consider the vehicular bridge interactions, the same has been neglected in the Abaqus models. The moving load is applied as a user-defined pressure load, with its magnitude and path defined by a user-defined subroutine in Abaqus.

The bridge deck was modelled using 5000 solid elements (C3D8R). In this study, solid elements were chosen over shell elements to model the bridge structure in Abaqus. While shell elements are computationally efficient and well-suited for thin-walled structures, their primary assumptions make them less effective for accurately capturing three-dimensional stress states in complex geometries or thicker sections. The solid elements, in contrast, allow for a more detailed representation of the bridge's 3D geometry, providing higher accuracy in stress, strain, and deflection analysis (Cook, 2002).

All the bridge models considered are simply supported where one end of the bridge model is supported by a 3D hinge and the opposite end by a 3D roller. At one end of the bridge, a 3D hinge was modeled by constraining translational degrees of freedom in the longitudinal (U_1)

and vertical (U_3) directions, while rotational degrees of freedom (UR_1,UR_2,UR_3) were left unconstrained. The opposite end was modeled as a 3D roller, allowing translational movement in the longitudinal direction (U_1) while constraining vertical (U_3) and transverse (U_2) displacements. These boundary conditions were applied directly to the nodes at the ends of the bridge's span.

The 3D hinge allows rotational freedom around all axes, with restraints applied only in the longitudinal and vertical directions. This configuration permits movement in the transverse direction, while preventing any displacement along the longitudinal and vertical directions whereas the 3D roller support allows movement along the longitudinal direction while restricting movement in the transverse and vertical directions. It permits rotational freedom around all axes but prevents any displacement in the transverse and vertical directions.

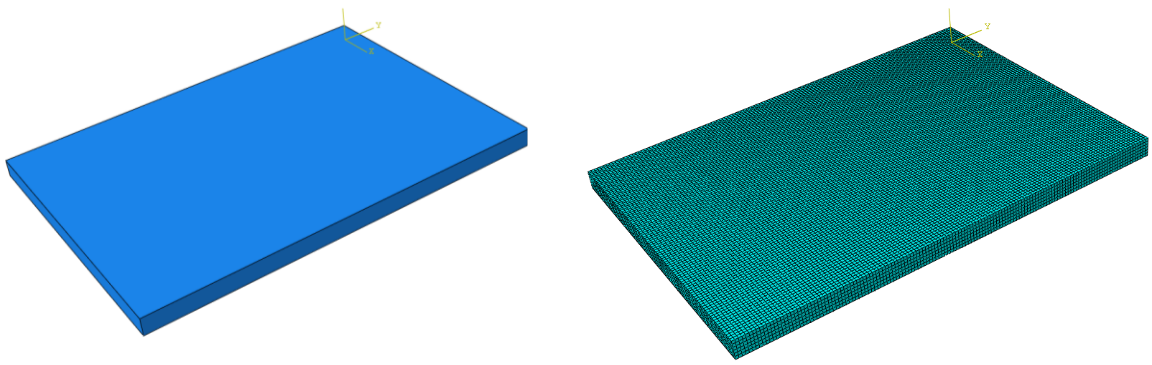

a) Bridge deck model b) Meshed Bridge deck

Figure 27 Abaqus model of bridge deck- rectangular cross-section

6.2.2 The moving load force using Vdload subroutine

After creating the bridge model in the Abaqus environment, the next essential step is to define the moving load that traverses a specific path across the bridge. The geometric and material properties of the bridge, along with the meshing, can be handled within Abaqus. But, the moving load can defined and incorporated in the analysis only by a user defined subroutine and in this study, the task was performed using the 'Vdload' subroutine.

The Vdload subroutine is one of several subroutines utilized by Abaqus CAE software and incorporates both read-only and write-only variables. The read-only variables, defined using the `dimension` command, include `nblock`, `ndim`, `stepTime`, `totalTime`, `amplitude`, `curCoords`, `velocity`, `dirCos`, `jltype`, and `sname`. These variables provide critical information for the subroutine input parameters from the Abaqus bridge mode. While all of the variables could potentially be utilized in code generation, not all are employed in the specific code developed for this analysis. Details on the function of each read-only variable are described in Appendix A.

The only write-only variable in the Vdload subroutine is `value`, which stores the magnitude of the load to be applied at each integration point. This variable is assigned the value based on user-defined conditions and is the only parameter returned by the subroutine, defining the load magnitude for the integration points in the analysis.

6.2.3 Overview of the Vdload subroutine coding

In the Abaqus CAE implementation for moving load analysis, the Vdload subroutine utilizes the following read-only variables, `curCoords`, `nblock`, `ndim`, `velocity`, `sname`, and `dirCos`. These variable inputs are passed on from the Abaqus model during each iteration. The contact surface of the load is defined within the subroutine and is done by defining two variables, a and b as real numbers, 8 bytes - 64 bits in size. The pressure load is assigned to the write-only variable 'value' using a variable P which is again defined as a real number 8 bytes - 64 bits in size. Along with these variables, beamwidth and velocity are incorporated through variables such as 'slabWidth' and 'vehicleVelocity'.

After initializing these variables, a do loop combined with if-else conditions determines whether the load should be assigned to a particular block. The loop index variable km initiates the loop, which iterates from 1 to nblock. For instance, if nblock is 10, indicating 10 integration points in the input parameters, the loop will execute 10 times to evaluate the conditions. When conditions meet the user-defined criterions, the pressure load is assigned and returned to the Abaqus model through the 'value' variable.

6.3 Determination of DAF values for Bridge Model - 01

6.3.1 Bridge model:

Bridge model -01 with 14m span, 10m width, 0.625m depth, modulus of elasticity of 35×10^9 N/m^2 and Poissons ratio of 0.3 is being utilized in this analysis. The bridge is modelled with a simply supported condition and material damping is neglected in this scenario.

6.3.2 Vdload subroutine coding explanation:

According to CSA-S6 2019 (Canadian Standards Association, 2019), when the width of the bridge falls in the range of 6 to 10 m, the maximum number of lanes to be considered in 2 and thus in this analysis, Bridge Model-01 is considered as a two-lane bridge with a lane width of 5m. The load moves through the center of one of the lanes of the bridge model. To achieve this, the width of the bridge is inputted, and the if-else conditions in the code are structured to ensure the load moves along the middle of the lane (Figure 28). The load's contact area is defined as 0.3 m × 0.3 m and using the if-else loop, when an integration point falls within the contact area for a time step, a load of 1000 N or 1 kN is applied. The duration of the loading varies with the velocity of the moving load in each analysis.

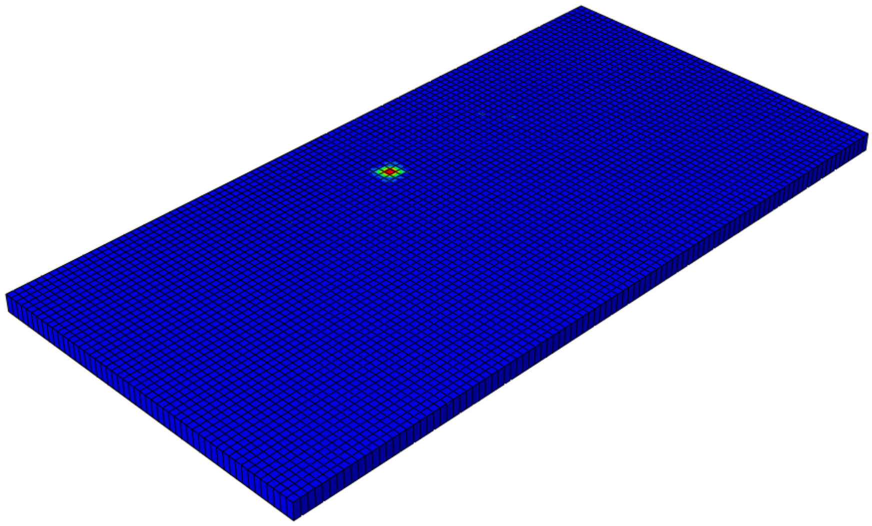

Figure 28 Bridge deck with moving load on the center of the left lane

6.3.3 Analysis Results:

The initial step involves determining the static deflection of the bridge model under a 1000 N/m^2 pressure load applied at the midspan. After obtaining the static deflection, the next step is to compute the dynamic deflection caused by the same 1000 N/m^2 moving load, applied over a contact surface area of 0.3 m × 0.3 m. The Vdload subroutine is employed to execute the moving load traversing from one end to the opposite end with a definite velocity. The analysis is conducted for a velocity range of 20 to 120 kmph and constant velocity maintained throughout each simulation. Once the dynamic deflection is obtained for each velocity from the 3D model analysis, the dynamic amplification factor is determined using equation (1). The static and dynamic deflections for the bridge model are shown in Figure 29.a and Figure 29.b, respectively.

From the static analysis of Bridge Model-01, the static deflection was found to be 9.878 x10^{-7} m. For the dynamic deflection, the moving load analysis was performed for velocities ranging from 20 to 120 kmph and the results indicated that the maximum dynamic amplification occurred at a velocity of 20 kmph, with a magnitude of 1.22. The corresponding maximum dynamic deflection at this velocity was 1.21×10^{-6} m.

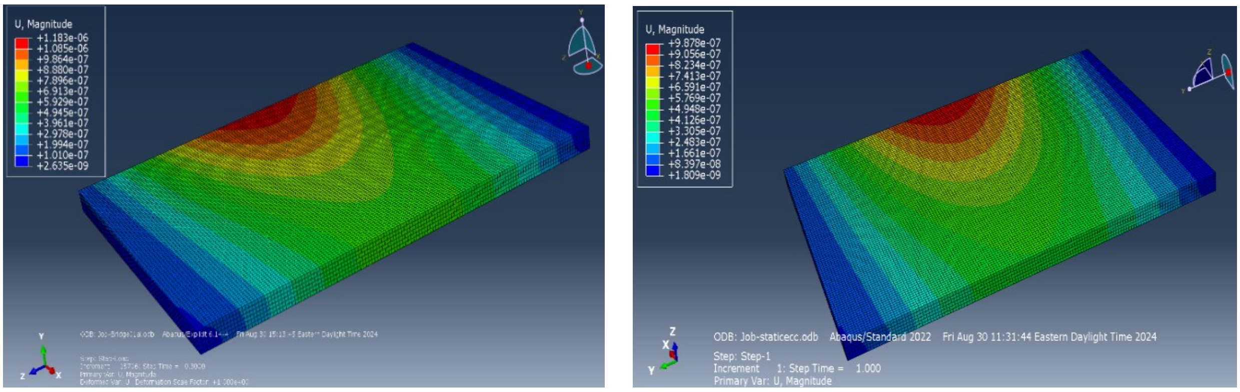

Figure 29 Bridge-01 model a) Static deflection b) Dynamic deflection

The analysis showed that the minimum dynamic amplification factor was 1.09, when the velocity of the moving load was 110 kmph. One of the key observations from the analysis was that dynamic amplification was found not to be proportional to velocity. These results also validate the analytical observation that velocity impacts the dynamic amplification of moving loads on bridges and that the dynamic amplification factor (DAF) does not vary proportionally with velocity.

Table 18 DAF Values – Bridge 01 - Abaqus Model

#	Velocity (kmph)	DAF
1	20	1.22
2	30	1.19
3	40	1.14

4	50	1.17
5	60	1.11
6	70	1.13
7	80	1.2
8	90	1.2
9	100	1.17
10	110	1.09
11	120	1.15

6.4 Consistency of Moving Load and 3D Abaqus Model

The comparison between the results of the Bridge model – 01 from Abaqus and the analytical moving load method has been carried out to evaluate the consistency between the two approaches. The selection of the position of the moving load to be on the center of the left lane would be the first consideration and if the comparison between the moving load analytical model results and Abaqus model, then this scenario could be utilized for the incorporation of the skew angles. This would confirms that a 3D model can serve as an extension of the analytical method, allowing its results to be utilized for comprehending the variation of DAF with respect to the skew angle of bridge deck. The establishment of consistency also helps to validate the results from the analytical moving load method.

The moving load analysis was implemented using the Vdload subroutine, and results were obtained for a velocity range of 20 to 120 kmph. The comparison revealed that, although the 3D model results were slightly higher, the average Dynamic Amplification Factors (DAF) for the analytical and 3D models were 1.10 and 1.16, respectively. When examining the maximum DAF values, the analytical model yielded 1.183, while the 3D model produced 1.22. Both models consistently highlighted the significant influence of velocity on DAF, demonstrating that DAF values fluctuate as velocity changes, reflecting the dynamic interaction between the moving load and the structural response.

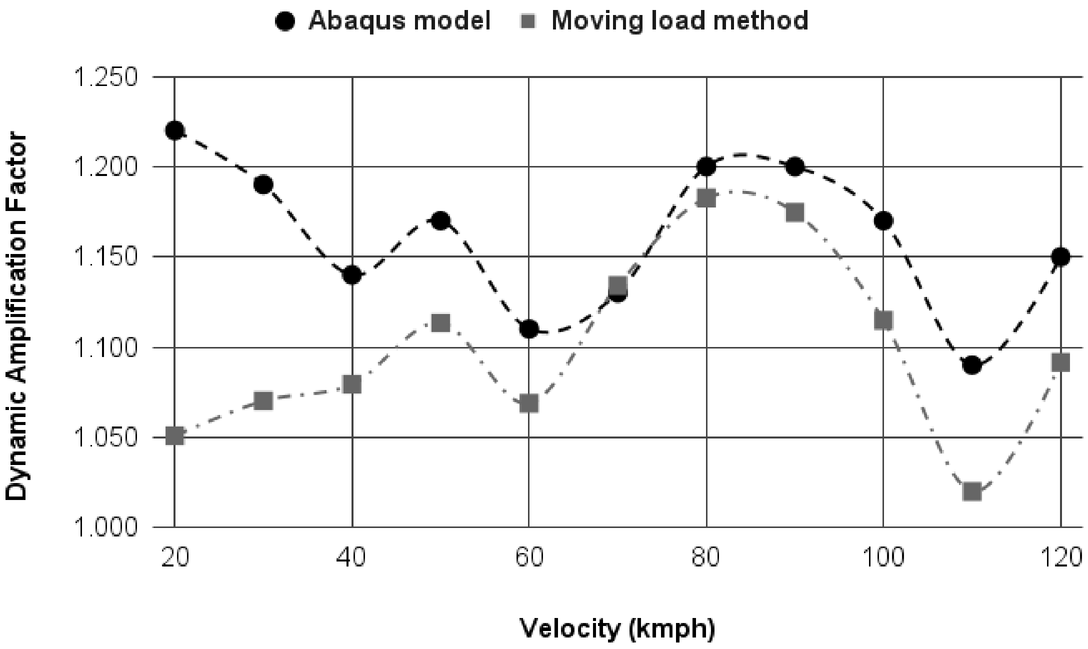

Figure 30 Comparison between the moving load method and the Abaqus model

Although the models are consistent, some variations in the results were observed. In the analytical model, the dynamic amplification was lower at lower velocities, with the highest amplification occurring at 80 kmph. However, in the 3D model, higher amplifications were observed at both low as well high velocities.

Since the analysis demonstrates that the 3D model results align with the analytical model, this scenario would be employed for the comprehension of the effect of variation of the DAF with the increase in the skew angle.

6.5 Effect of skew angle on dynamic amplification factor

The skew angle of bridge decks can influence load distribution (Patra et al., 2024) and these load distributions can affect the dynamic amplification effect on bridges. However, upon reviewing various design codes, it was found that the Dynamic Amplification Factor (DAF) is incorporated in the bridge codes without accounting for the skew angle as a parameter. Therefore, this analysis aims to investigate the effect of skew angle on the DAF. In this analysis, four different scenarios of bridge model 01 are examined, corresponding to skew angles of 0°, 15°, 30°, and 45°. The skew angle is limited to 45°, as per CSA S6-19 (Canadian Standards Association, 2019), which sets 45° as the maximum permitted skew angle for bridges. The bridge dimensions are 14 m by 10 m, with only the right (straight) span varying. Damping was not considered in this analysis, and the structure is modelled as simply supported.

For each of the four cases, a velocity range of 20 to 120 kmph was considered, resulting in a total of 44 simulations for this analysis. The moving load model was implemented using the Vdload subroutine as discussed earlier, with different codes applied for each model. The moving loads were positioned to travel along the center of one of the lanes, and the duration of loading varied according to the velocity in each simulation. The maximum deflection from each simulation was used to determine the Dynamic Amplification Factor (DAF).

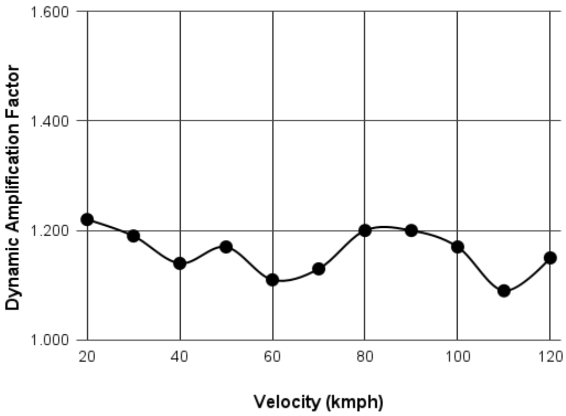

a) DAF – 0^0 Skew

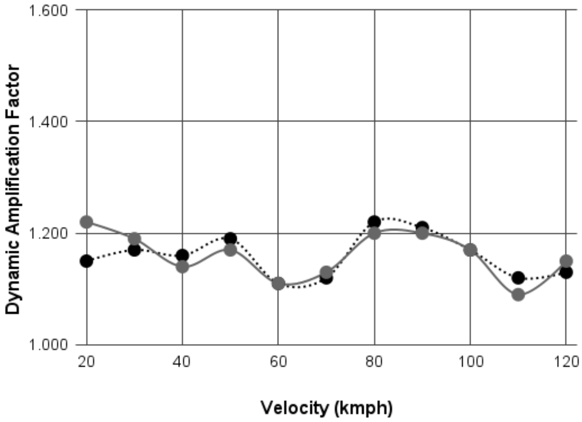

b) DAF – 15^0 Skew vs 0^0 Skew

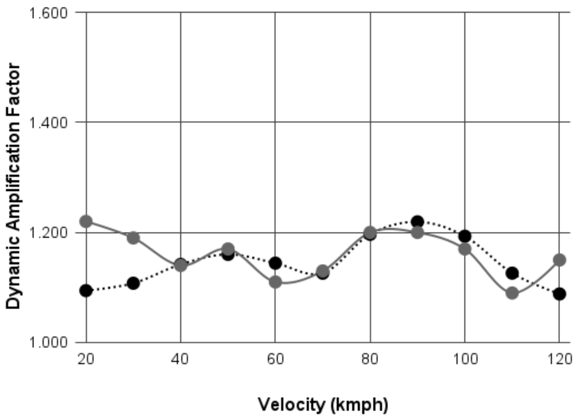

c) DAF – 30^0 Skew vs 0^0 Skew

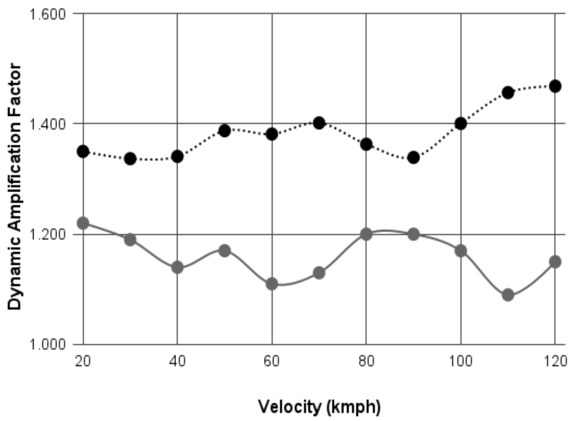

d) DAF – 45^0 Skew vs 0^0 Skew

Figure 31 Comparison of DAF for different skew angles

For each model, the static deflection was first determined from the Abaqus model by applying a load at midspan along the longitudinal direction and 2.5 m from the edge in the transverse direction. A pressure load of 1000 N/m² was applied over a contact area of 0.3 m x 0.3 m. After computing the static deflection, the dynamic deflection was obtained by applying a moving pressure load of 1000 N/m², which traveled along the center of one lane of Model-01. The dynamic deflection was calculated for each velocity, and the corresponding Dynamic Amplification Factor (DAF) was determined. Figure 31.a presents the DAF values for each velocity case at a skew angle of 0°, while the subsequent figures compare the 0° skew angle values to those at 15°, 30°, and 45° for each velocity case.

Figure 31.b shows that the dynamic amplification effect for a 15° skew angle shows little variation compared to the scenario with no skew. While there are minor differences in a few velocity cases, the overall DAF values are generally aligned with those of the zero-skew angle case. In Figure 31.c, a similar trend can be observed, with the DAF values closely following the pattern of the zero-skew scenario. However, for the 20 kmph velocity, the DAF values for the 0° and 30° skew angles were 1.09 and 1.22, respectively, representing 11% variation. Aside from this, the results for both models are comparable. In contrast, Figure 31.d reveals that the dynamic amplification for the 45° skew angle is significantly higher than the previous cases. The DAF follows a distinct trend, with the highest amplification occurring at a velocity of 120 kmph. In addition, the DAF values corresponding to all the velocities were observed to be higher than that of the scenarios where lower skew angles were considered.

Table 19 Comparison of Minimum, Maximum and Average DAF Values for the 4 models.

Skew Angle	Minimum DAF	Maximum DAF	Average DAF
0^0	1.11	1.22	1.16
15^0	1.11	1.22	1.16
30^0	1.09	1.22	1.15
45^0	1.34	1.47	1.38

From Table 19, it can be observed that the maximum dynamic amplification effect for the 0°, 15°, and 30° skew angle scenarios is significantly lower than the minimum DAF values for the case of 45° skew angle. The results indicate that skew angle up to 30° has marginal impact on the dynamic amplification effect as compared to the case of zero-skew angle. However, in the case of 45° skew angle, the results differ noticeably, with an average DAF of 1.38, as compared to 1.16 for the 0° skew angle, showing variation of approximately 20%. Currently, no design code accounts for the effect of skew angle variation on the DAF, yet the results clearly show that skew angles of 45° or more significantly influence DAF values. Therefore, from a bridge structural design perspective, it is recommended to account for skew angle effects to ensure the dynamic amplification effect is properly addressed in the design.

6.6 Discussion

In the previous section, the moving load method was applied for the parametric study. However, since the analytical model cannot account for the effect of skew angles, the study was extended to a 3D Finite Element Model using Abaqus CAE to evaluate the variation of DAF with changes in skew angle. As an initial step, it was imperative to verify the consistency between the analytical model results and the Abaqus model results. For this validation, the properties of Bridge Model-01 were considered. A comparative analysis demonstrated that the results from both methods were consistent.

Subsequently, skew angles of 15°, 30°, and 45° were incorporated into the bridge model to analyse the variation in DAF. The findings revealed that skew angles do influence the Dynamic Amplification Effect. However, the effect is minimal for skew angles up to 30°. When the skew angle exceeded 30°, the DAF values showed a significant increase of more than 20% for the case of skew 45°angle. These results underscore the need for design codes to account for the effect of skew angles when incorporating DAF values. Although the skew angle is not considered in the bridge design codes, it should also be noted that some codes (e.g. the Canadian code, CSA S6-19) restricts the skew angle to a certain limit (e.g. 45°).

Chapter 07

7 Proposed new approach to DAF estimation and design incorporation

7.1 Introduction

Dynamic amplification factor (DAF) is one the key aspects for the design of a bridge and thus it is imperative to compute it with accuracy and to incorporate it into design. However, since DAF depends on various bridge and vehicular factors, selecting the appropriate parameter for its incorporation in design itself is a challenge.

From literature review, it was observed that the major bridge parameters which affects the dynamic amplification factor was bridge span, bridge frequency and surface irregularities and on reviewing various design codes, it became apparent that these three factors are commonly used to incorporate DAF into design. However, an interesting finding was that none of the codes considered all three parameters together when determining the incorporation of DAF.

When considering the above-mentioned parameters in the design of a new bridge, the bridge span and bridge frequencies are the only definitive factors known to the designer. While the literature review emphasizes the importance of surface irregularities as a significant factor that can amplify dynamic loads, predicting how these irregularities will develop over time during the initial design phase is challenging. Furthermore, the locations of these irregularities are critical, as the amplification caused by irregularities at midspan differs significantly from that at the ends of the span (Ludescher, 2009). Therefore, incorporating surface irregularity as a primary parameter may not be the most effective approach. Instead, the DAF values integrated into the design should be structured to account for the dynamic amplification resulting from surface irregularities to some extent but should be incorporated based on other parameters.

Therefore, focusing on the remaining bridge parameters—bridge span and bridge frequency—it is evident that many design codes utilize these parameters individually for incorporating DAF into the design, but never together. But the analysis results from previous sections indicated that using either bridge frequency or bridge span as the sole parameter for DAF incorporation may lead to inaccurate values. This conclusion was supported by the analysis results, which showed significant variations in DAF values for similar spans and frequencies.

Thus, this section proposes an approach that accounts for both bridge frequency and span as parameters for estimating dynamic amplification on bridges under traffic loads. By employing the moving load method, both bridge span and frequency will serve as determining factors for computing DAF values. This method seeks to understand the influence of bridge span and frequency on the DAF and to determine whether both factors should be considered together as parameters for short to long span bridges. In addition, from literature review, it was clear that the influence of both bridge span and frequency is still ambiguous and thus this study would also provide insights into the contribution of these parameters towards dynamic amplification.

Furthermore, to comprehend the variations of the newly proposed approach with the existing codes, the analysis results are compared with the codes that incorporates DAF using bridge, vehicle and other parameters. This comparison would give insights into the limitations of the DAF values suggested in the existing bridge codes and also help to comprehend the effectiveness of this method.

7.2 Bridge span and Bridge frequency as parameters for DAF estimation

To incorporate the dynamic amplification effect into the design using bridge span and frequency as key parameters, the initial step involved identifying an analytical model capable of accurately calculating the dynamic amplification factor while considering these parameters.

In the previous sections, the moving load method's potential for determining the Dynamic Amplification Factor (DAF) was explored, which accounts for both bridge span and frequency as parameters. Additionally, the results from this method were found to align with other intricate models and Bridge Weigh-in-Motion data. Therefore, in this section, the moving load method will be applied to compute the dynamic amplification factors.

The literature review revealed that the dynamic amplification effect tends to vary for short to long span bridges. Therefore, this study considers bridge spans ranging from 10 to 50 meters, providing insights into the effect on both long-span and short-to-medium-span bridges. Regarding frequency, it was noted that the maximum dynamic amplification typically occurs when the bridge frequency falls between 2 and 5 Hz. However, to explore variations beyond this range, the study extends the frequency range slightly, from 2 to 5.5 Hz.

This analysis offers an approach in incorporating the Dynamic Amplification Factor (DAF), as it will provide insights into how DAF varies for a fixed span under different bridge frequencies. The results will clarify whether it is feasible to use only bridge span as a parameter within a certain span range or if it is consistently necessary to account for both bridge span and frequency in the design process.

To explore these possibilities, the moving load method was employed, incorporating the parameters so that bridge models with all combinations within the specified span and frequency ranges were utilized. The analysis included a total of 8 bridge spans, ranging from 10 to 50 meters, and 8 bridge frequencies, ranging from 2 to 5.5 Hz. For instance, a bridge span of 10 meters was analysed with 8 different frequencies within this range.

In reviewing the various bridge parameters that contribute to the Dynamic Amplification Factor (DAF), it became clear from the literature that bridge span, bridge frequency, and road surface irregularities are the primary factors influencing DAF. However, the moving load method assumes a smooth road profile and does not account for the impact of surface irregularities. To ensure conservative results, the bridge damping parameter, which has been shown in previous analyses to reduce the dynamic amplification effect, is set to 0%.

In the case of a bridge, typical traffic moves at velocities ranging from 10 to 120 kmph. Accordingly, this velocity range was applied to each of the 72 bridge models, resulting in a total of 864 sets of results (*9 bridge spans × 8 bridge frequencies × 12 velocities = 864 sets*). From these results, the average and maximum Dynamic Amplification Factors (DAF) were calculated for each of the 72 models. These results were then compared to analyse the variation of DAF with both bridge span and frequency considered together. The average DAF values for the respective models are given in Table 20.

From Table 20, the DAF values corresponding to each frequency (2.0 to 5.5 Hz) for a given bridge span can be observed. For example, in the first row, the variation in DAF values as the frequency changes from 5.5 to 2.0 Hz for a 10 m bridge span can be determined. The results clearly show that the highest average DAF value (1.385) occurred when the bridge span was 10 m, and the frequency was 2.5 Hz. Conversely, the lowest DAF value (1.044) was recorded for a 50 m bridge span with a frequency of 5.5 Hz. These findings suggest that higher DAF values tend to occur in short bridges with low natural frequencies. To further understand this trend, refer to Figure 32.

Table 20 Average DAF values from moving load method analysis for 72 bridge models

#	Bridge span (m)	5.5 Hz	5 Hz	4.5 Hz	4 Hz	3.5 Hz	3.0 Hz	2.5 Hz	2.0 Hz
1	10	1.160	1.192	1.238	1.281	1.321	1.372	1.385	1.354
2	15	1.095	1.094	1.109	1.137	1.177	1.238	1.300	1.372
3	20	1.091	1.099	1.097	1.096	1.100	1.137	1.192	1.281
4	25	1.068	1.077	1.088	1.099	1.095	1.094	1.122	1.192
5	30	1.065	1.065	1.071	1.082	1.096	1.097	1.094	1.137
6	35	1.058	1.058	1.067	1.067	1.080	1.096	1.095	1.100
7	40	1.052	1.054	1.061	1.066	1.067	1.082	1.099	1.096
8	45	1.050	1.052	1.052	1.061	1.067	1.071	1.088	1.097
9	50	1.044	1.049	1.052	1.054	1.063	1.066	1.077	1.099

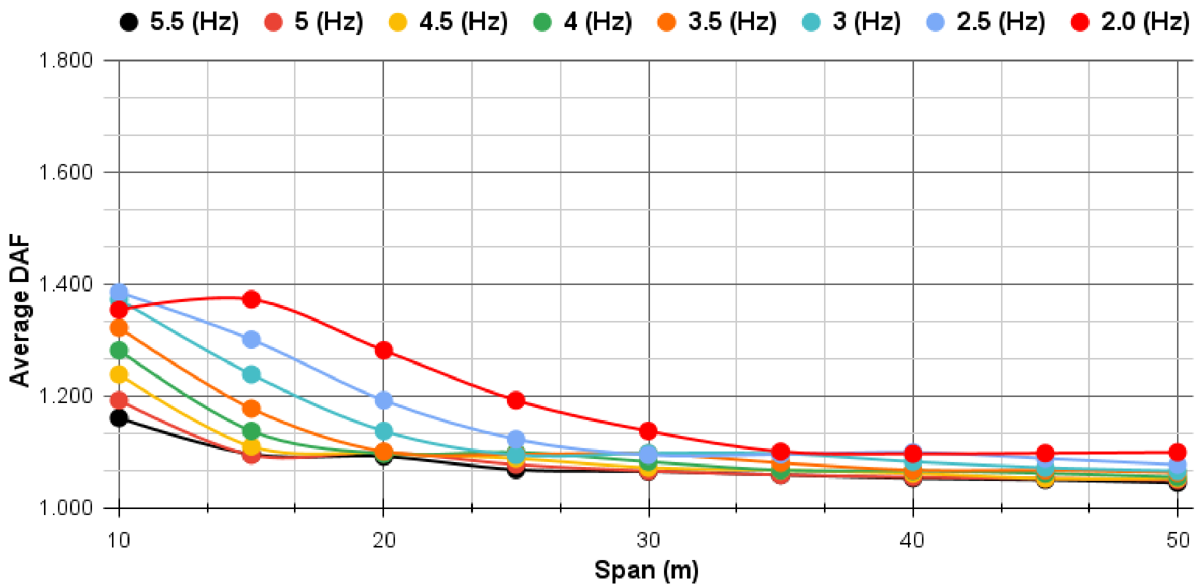

Figure 32 Variation of Average DAF values based on bridge span and frequency

Figure 32 clearly illustrates the variations in Dynamic Amplification Factor (DAF) values across different spans as frequencies change. A key insight from these results is that frequency variation has a significant impact on short to medium-span bridges. For spans up to 25 meters, the variation in DAF values with respect to bridge frequency is pronounced, whereas for spans beyond 25 meters, this variation becomes minimal.

From Figure 32, with respect to the bridge frequency, it is evident that the dynamic amplification effect is more pronounced at lower frequencies compared to higher frequencies. The analysis results clearly indicate that when the frequency range is between 2.0 and 2.5 Hz, the DAF values are significantly higher than those at higher frequencies. This trend continues up to a bridge span of 25 meters, beyond which the variations become negligible. Spans exceeding 30 meters do not exhibit high DAF values, with the maximum DAF recorded beyond this point being 1.137 (around 14%).

Table 21 Maximum DAF values from Moving load method analysis for 72 bridge models

#	Bridge span (m)	5.5 Hz	5 Hz	4.5 Hz	4 Hz	3.5 Hz	3.0 Hz	2.5 Hz	2.0 Hz
1	10	1.435	1.513	1.581	1.623	1.628	1.628	1.629	1.625
2	15	1.186	1.186	1.228	1.351	1.475	1.581	1.629	1.628
3	20	1.186	1.186	1.185	1.184	1.189	1.351	1.513	1.623
4	25	1.114	1.160	1.186	1.186	1.181	1.186	1.309	1.513
5	30	1.116	1.116	1.121	1.174	1.184	1.185	1.186	1.351
6	35	1.105	1.105	1.113	1.112	1.168	1.184	1.181	1.190
7	40	1.086	1.092	1.116	1.115	1.112	1.174	1.186	1.184
8	45	1.086	1.087	1.087	1.116	1.113	1.121	1.186	1.185
9	50	1.067	1.086	1.087	1.092	1.115	1.116	1.160	1.186

The variation in average DAF values was found to be greatest for a bridge span of 10 meters, with a variation of 20%, while the smallest variation (4%) occurred for a bridge span of 35 meters. These results highlight the importance of incorporating both bridge span and frequency in determining DAF values for short to medium-span bridges. The analysis suggests that even if frequency is not considered as a parameter in DAF calculations, the results would remain accurate due to the negligible variations observed for longer spans. To fully understand the importance of considering both bridge span and bridge frequency together as parameters, it is vital to consider the maximum DAF values for each of the 72 models as well. Thus, maximum DAF values for each of the 72 models are shown in Table 21.

From Table 21, it can be observed that the maximum DAF value of 1.628 occurred for a combination of bridge span of 15 m and bridge frequency of 2.5 Hz. On comparing the maximum DAF values, the results follow the trend shown in the average DAF results analysis where the maximum DAF values were observed for short to medium span bridges for low frequencies in the range of 2 to 2.5 Hz.

From Figure 33, the relationship between maximum DAF and frequency for a specific bridge span is clearly illustrated. The variation in DAF values is most pronounced for the 15 m bridge span, with a minimum value of 1.186 at a frequency of 5.5 Hz and a maximum value of 1.629 at 2.5 Hz. Additionally, the variation in DAF with frequency diminishes as the bridge span increases, similar to the trends observed in the average DAF. These findings also suggest that for bridge spans exceeding 30 m, the dynamic amplification remains relatively low.

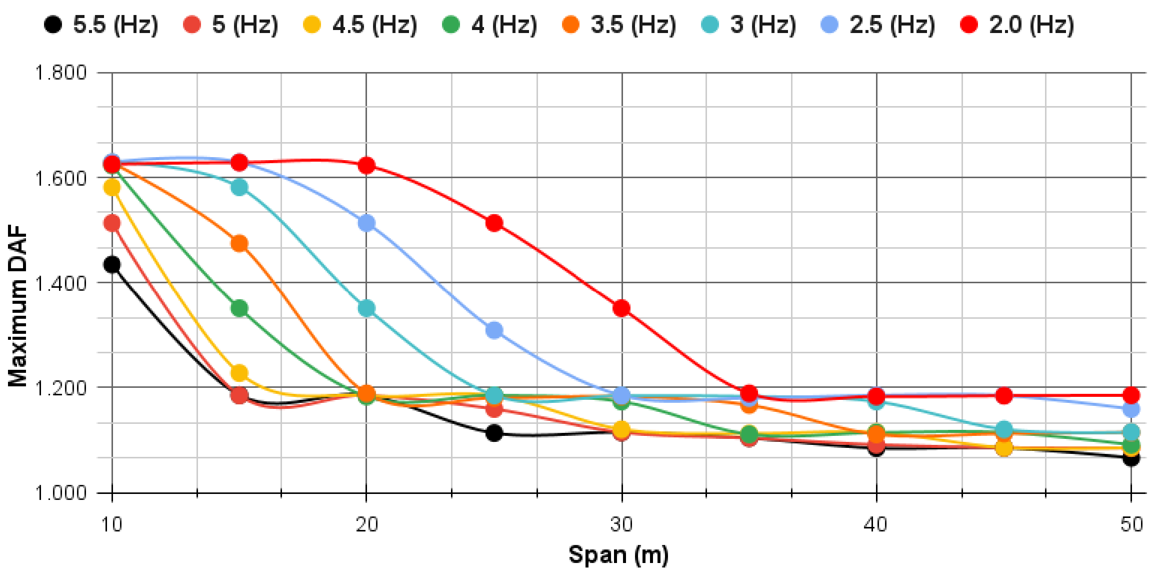

Figure 33 Variation of Maximum DAF values based on bridge span and frequency

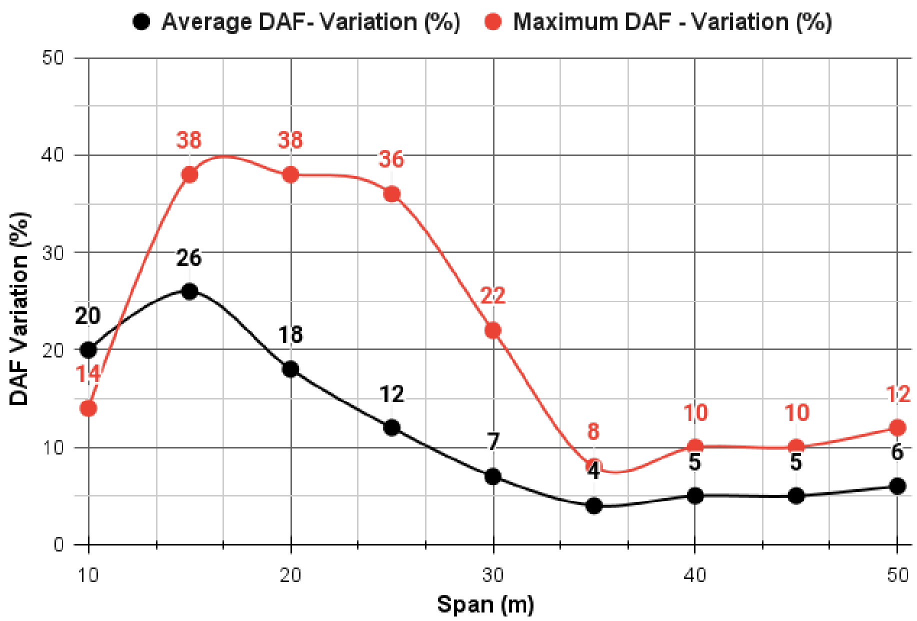

Figure 34 Average and Maximum DAF Variation %

Figure 32 and Figure 33 clearly demonstrate that the variation between the highest and lowest DAF within the frequency range is more pronounced for short to medium-span bridges. However, it is essential to quantify these variations, and it can be comprehended from Figure 34. It can be observed that the impact of frequency is particularly significant for short to medium-span bridges, with the analysis revealing a 26% variation in the average DAF for a 15-meter span. For maximum DAF values, the variations were substantial for both 20-meter and 25-meter spans, with a 38% difference. Beyond 30 meters, however, the variations were minimal, indicating that frequency changes have a negligible effect on DAF for longer spans.

7.3 Inference validation using BWIM Data

From the analytical results, it was inferred that short to medium-span bridges with low frequencies tend to exhibit high DAF values, whereas those with high frequencies generally show lower DAF values. Conversely, frequency variations in long-span bridges have minimal influence on DAF, and their DAF values are typically low. To validate this observation, it is essential to compare it with actual dynamic load testing data obtained from BWIM. For this purpose, this section presents a comparison between the observation from simulation and the BWIM test data (Kalin, 2022).

Table 22 Comparison of BWIM Data with Hypothesis

Site	Bridge span (m)	Bridge frequency (Hz)	Vehicles	Mean DAF	Hypothesis testing
S104a	5.5	9.1	202	1.03	✓
S104b	5.5	8.1	4590	1.04	✓
S107	6.6	14	1850	1.09	✓
S105	6.8	7.1	516	1.08	✓
S101	7.4	5.4	318	1.23	✗
S106a	9.7	5	617	1.1	✓
S106b	9.7	5.4	865	1.19	✗
US02	10.4	8.1	474	1.08	✓
US04	10.4	8.6	746594	1.08	✓
S102	10.5	5.1	432307	1.10	✓
US03	11	8.5	402595	1.05	✓
S103	12	5.8	28533	1.11	✓
US01	12.2	3.5	1,979	1.05	✓
US05	25	1.6	15295	1.17	✓
S110	25.8	3	7398	1.05	✓
S108	34.4	2.4	1608	1.06	✓
S109	35	2.6	25219	1.02	✓

The results from Table 22 clearly indicate that, out of 17 bridge model results, 15 align with the observed trend from the simulation. Two bridge models (S101 and S106b) did not match the observation, while the remaining dynamic load results support it. These discrepancies could be attributed to road surface irregularities, as these bridges were on primary and secondary roads in Slovenia where the BWIM test was done. Additionally, the limited number of vehicle test data for these models, compared to others, may have influenced the results.

7.4 Determination of accuracy of the proposed approach results with BWIM Data

The previous section showed that the inference from the proposed simulation-based approach aligns well with the actual dynamic effects observed on bridges based on the BWIM data. However, the precision of this approach still needs to be verified. In this context, to comprehend whether the results from the new approach are consistent compared to BWIM test data (Kalin, 2022), analysis were conducted to determine DAF values for all bridge models listed in Table 22 based on bridge span and fundamental frequency. The analysis covered a velocity range of 10 to 120 kmph, and the results are shown in Figure 35.

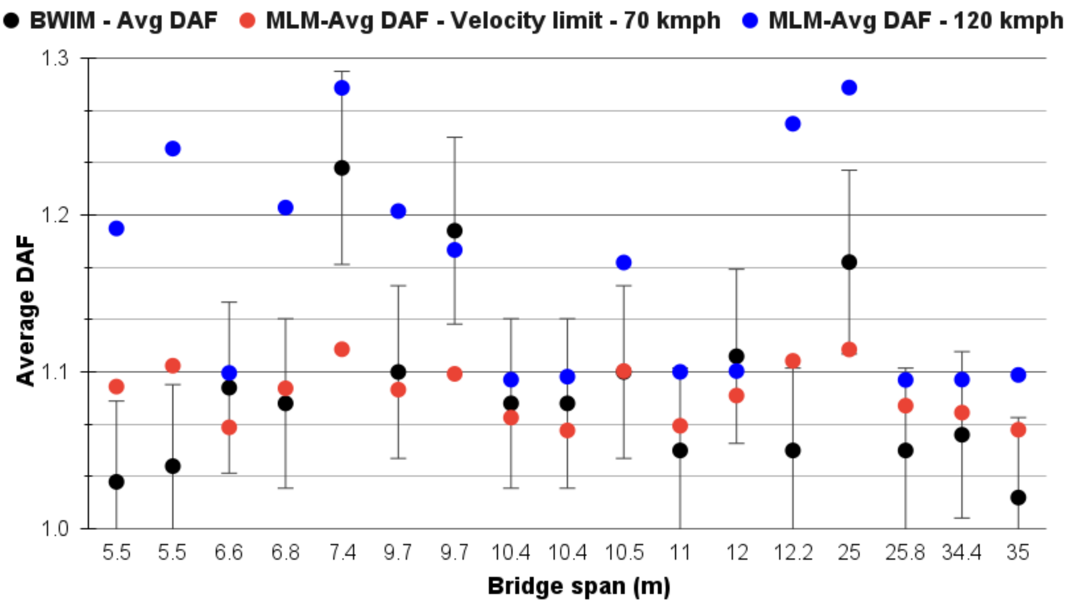

Figure 35 Comparison of BWIM Test data and and analytical model results

Figure 35 shows that the results from the new approach are safe, as the DAF values obtained from the analysis surpass the BWIM test data in most instances. However, upon assessing the accuracy of these DAF values compared to the BWIM test data, it is observed that 8 out of the 17 bridge models exhibit a variation of more than 5%. This discrepancy may be attributed to actual traffic conditions, where the number of vehicles traveling at 120 kmph would be quite less. However, the moving load method of analysis considered velocity range of 10 to 120 kmph and equal weightage was assigned to results across all velocity scenarios, leading to higher DAF values compared to the BWIM data. This issue would be particularly significant for short-span bridges, where the likelihood of vehicles moving at 120 kmph is very minimal.

To assess if adjusting the velocity range would improve the accuracy of the DAF estimation, the velocity range was narrowed to 10 to 70 kmph. This modification aims to verify if the previously observed variations were due to the initial velocity range, and also it demonstrates the effectiveness of the moving load method, in general, and in the velocity range, in particular.

The results from this analysis, shown in Figure 35 clearly indicate that the moving load method aligns closely with the BWIM test data when a velocity range of 10 to 70 kmph is considered. Variations in results were within 5% or less for 15 out of 17 bridge model test cases, confirming the accuracy of the moving load method. These findings demonstrate that the proposed approach to estimate the DAF is both reliable and safe for integration into design.

7.5 Developing new formula for integrating DAF into design

The previous section clearly demonstrates that the insights gained from the new approach for integrating DAF into design is safe and consistent with respect to the actual dynamic load test data. Therefore, the findings from this approach can now be applied to establish DAF values for bridge design based on bridge span and fundamental frequency.

In this context, a formula has been developed, and for this purpose, the results from the moving load analysis conducted for a bridge span range of 10 to 50 m and fundamental frequency of 2 to 5.5 Hz were utilized. The velocity range of 10 to 120 kmph was considered to ensure conservative results, and regression analysis was performed in MATLAB using the analysis data. The regression analyses conducted using the moving load method resulted in a well-fitting model that captures relationship between the Dynamic Amplification Factor (DAF), bridge span, and fundamental frequency. A 2D quadratic polynomial fit was applied to the dataset, yielding strong results with an R-squared value of 0.9087 and an adjusted R-squared of 0.9052, indicating that approximately 91% of the DAF values in the data can be obtained using the formula. The model's root mean square error (RMSE) of 0.0251 further demonstrated its predictive accuracy. To visualize the relationship, both surface and contour plots were generated, highlighting the variation of DAF across the span and frequency parameters. These visualizations confirmed the model's reliability and helped identify key trends. The new formula derived from the regression analysis of the moving load method dataset, incorporating both bridge span and fundamental frequency to account for DAF in design, is as follows:

$$DAF = a_0 + a_1x + a_2y + a_3x^2 + a_4xy + a_5y^2 \tag{19}$$

Where x is the bridge span in meter and y is the bridge fundamental frequency in Hertz. The values of coefficients are a_0 = 1.841, a_1 = -0.02396, a_2 = -0.1485, a_3 = 0.000213, a_4 = 0.001759 and a_5 = 0.008416.

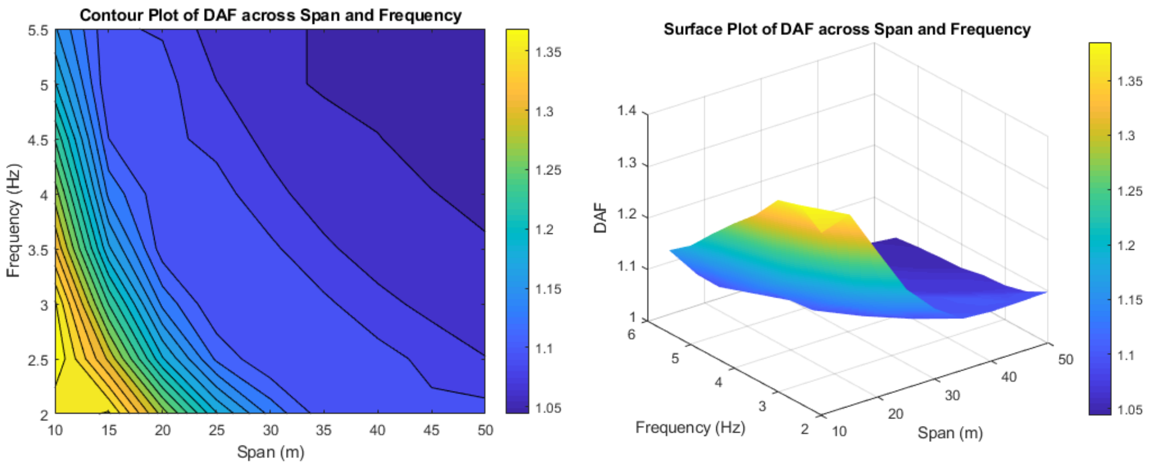

a) b)

Figure 36 Relationship of DAF - bridge span and fundamental frequency a) Contour plots b) Surface plots

7.6 Comparison with Design Codes considering Bridge parameters

Here, the result from the new approach is being considered with two currently used design codes where bridges parameters are considered as the deciding factor for incorporating DAF. The design codes used for this comparison are IRC6:2017 (Indian Road Congress, 2017) and NZTA (2013). The former incorporates DAF based on bridge type, bridge span and vehicle type and later includes DAF based on bridge span as parameters. The comparison between the analysis results and corresponding code values are as shown in Figure 37.a and Figure 37.b.

On comparing these results, it can be easily comprehended that the values incorporated in the codes are higher than the values observed from the analysis. With respect to IRC6: 2017 (Indian Road Congress, 2017), it can be stated that the values are higher than what might be occurring on the bridges. For instance, if a bridge of 10m with 5.5Hz is designed, then the DAF values used in the code might be much higher than what would likely occur on the bridge. But for the combination of 15 m bridge span and 2.0 Hz frequency, the DAF value incorporated in the code is less than what might occur on the bridge. But with respect to the long span bridges, it can be observed that the DAF values in the design code is on the conservative side.

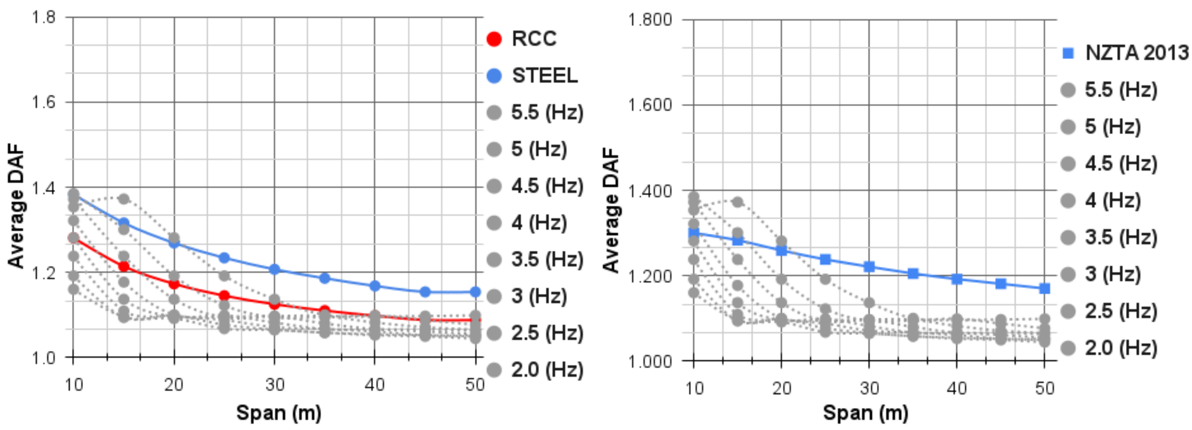

a) b)

Figure 37 Comparison of new approach results with a) IRC6:2017 and b) NZTA (2013)

On considering the NZTA (2013), it can be observed that the DAF values are on the conservative side for long span bridges. With respect to short span bridges, it can be observed that few of the DAF values included in the code are less than the values estimated from the analysis. The maximum value provided in the code is 1.3 but from the analysis it was observed that the highest average DAF value was 1.385 for 10 m span bridge with 2.5 Hz frequency. This trend is observed for spans in the range of 10 to 20 m with low frequencies. The code values are lower for short span bridges with low frequencies but with high frequencies, these values would be sufficient.

7.7 Comparison with Design Codes considering Vehicle parameters

From the literature review, it is evident that only a few design codes account for dynamic amplification factors based on vehicle characteristics and other relevant parameters. Therefore, it is important to compare the values from the new approach with the codes that consider these factors when incorporating DAF into design. For this comparison, CSA-S6-19 (Canadian Standards Association, 2019) and AASHTO LRFD (2012) are used, as the former includes vehicle parameters while the latter applies limit states for DAF integration. The results of this comparison are presented in Figure 38.a and Figure 38.b.

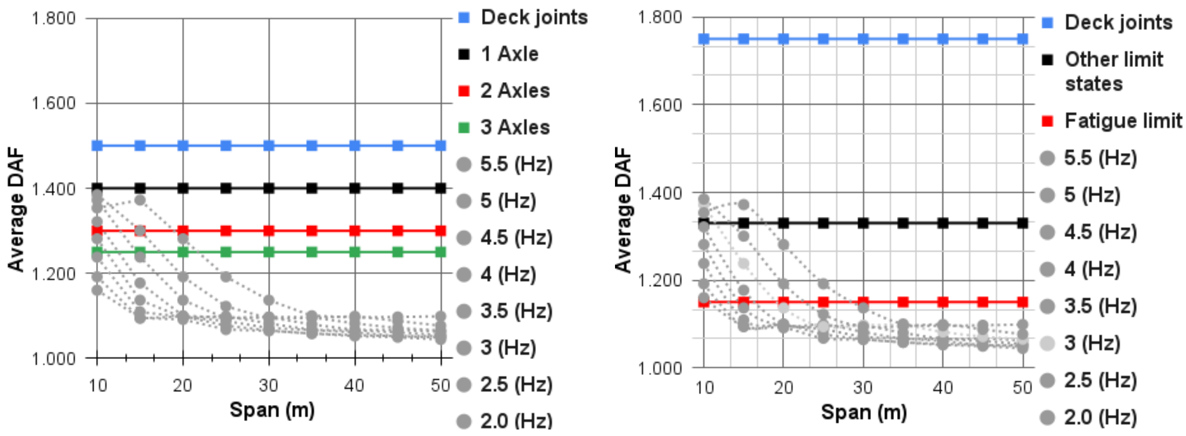

a) b)

Figure 38 Comparison of new approach results with a) CSA-S6-19 b) AASHTO (2012)

When comparing the analysis results with CSA-S6-19 (Canadian Standards Association, 2019), it is evident that the values specified in the code are on the lower side for some bridge models, particularly short- to medium-span bridges with low frequencies. In the case of 2- and 3-axle loads, some DAF values are lower than the dynamic amplification effects that may occur on these bridges. However, all values are on the conservative side for deck joints and single-axle considerations.

For AASHTO LRFD (2012), it is observed that few DAF values in the code are lower than those expected for short- to medium-span bridges. For the fatigue limit state, the values are significantly lower than expected for short- to medium-span bridges, indicating that the allocation for the fatigue limit state might be insufficient. Although most values for other limit states are generally on the safe side, a few for short spans with low frequencies are slightly lower than what might occur. With respect to deck joints, the values incorporated in design are much higher than the analysis results.

In conclusion, comparison of the analysis results with the design codes suggests that the newly proposed method aligns well with the existing codes. The code values are generally conservative for long-span bridges. However, for short- to medium-span bridges, it was observed that the code values may not adequately account for the dynamic amplification in certain cases that could occur under traffic loads.

7.8 Discussion

The fact that dynamic amplification factor is influenced by both bridge and vehicle parameters makes the selection of appropriate parameters for incorporating DAF into design a complex challenge. From the literature review of several bridge design codes, it was found that the codes consider individual factors such as bridge span, frequency, or surface roughness when incorporating DAF. However, none of these codes integrate all these factors simultaneously to fully capture the variations in DAF.

In this section, an approach was explored to determine whether it is necessary to incorporate both bridge span and frequency as parameters for integrating DAF into the design. The analysis was carried out using the moving load method, covering a bridge span range of 10 to 50 meters and a frequency range of 2.0 to 5.5 Hz.

The analysis showed that for a long-span bridge of 50 meters, the highest average and maximum DAF values were 1.099 and 1.186, respectively. In contrast, for a short-span bridge of 10 meters, the highest average and maximum DAF values were 1.385 and 1.625, respectively. These results clearly indicate that DAF decreases as bridge span increases. The reduction in dynamic amplification effects was observed to be significant up to a span of 30 meters, beyond which the decrease in DAF values became minimal.

Regarding bridge frequency, it was observed that DAF values decreased as frequency increased. The highest average and maximum DAF values were recorded at a frequency of 2.5 Hz, with values of 1.385 and 1.629, respectively. In contrast, at a frequency of 5.5 Hz, the highest average and maximum DAF values were 1.16 and 1.354. These results indicate a clear reduction in DAF values at higher frequencies compared to lower frequencies.

Table 23 DAF trend with respect to bridge span and frequency

Description	Low Frequency	High Frequency
Short to medium bridge span	Highest DAF	Lower DAF
Long bridge span	Lower DAF	Lowest DAF

In addition to these key findings, one of the most significant takeaways from the analysis was the pronounced impact of frequency variations on dynamic amplification for short to medium-span bridges, while the effect was minimal for long-span bridges (Table 23). This suggests that for long-span bridges, the influence of frequency on dynamic amplification is negligible. The highest average DAF values were observed for short to medium-span bridges with low frequencies, while the lowest dynamic amplification effects were seen in long-span bridges with high frequencies. The variation in average DAF reached as high as 26% with changes in frequency for a 15-meter bridge span, while for spans over 30 meters, the variations ranged between 4% and 7%. For maximum DAF values, variations were as much as 38% for spans of 15 and 20 meters, with the range decreasing to 8%–12% for spans beyond 30 meters. These results clearly indicate that for short to medium-span bridges, both bridge span and frequency must be considered together to fully understand the dynamic amplification effect under traffic loads. However, for long-span bridges, frequency has little impact on the dynamic amplification factor, as DAF variations across different frequencies were minimal.

While a general trend was observed regarding bridge span and frequency in this study, the preliminary analysis showed minimal variation in DAF values with respect to bridge span and frequency. Significant variations were noted only for a specific span and frequency combinations. These findings suggest that there was not much variation in DAF values based on bridge span or frequency in the preliminary study as the short to medium-span bridges analyzed had high frequencies. Notably, significant variation was observed in a specific model (Bridge-03), as it was the only model that had a combination of short to medium span bridge with a low frequency.

On considering results from Section 5.2, a similar observation was noted, where the average DAF values varied significantly for bridges with nearly identical spans of 6.8 and 7.4 meters. These results clearly indicate that the variations likely arose from differences in the bridge frequencies of the two structures. With respect to the results from the dynamic load tests conducted in Latvia, a similar trend of results was observed. It was seen that for several spans, the dynamic amplification values were varying significantly for the same span. This would have occurred due to the influence of bridge frequency and thus to clearly comprehend the results from dynamic load tests, it is advisable to plot with respect to bridge span and frequency as proved through this analysis. In addition, one of the advantages of using this method would be that this method would make the design more economical, especially for short to medium span bridges. If we consider this method for certain cases of short span bridges, the DAF incorporated can be even reduced by 26%.

Furthermore, to comprehend whether the conclusions from the analysis results align with the actual dynamic effects occurring on the bridges, the results were compared with BWIM data. This comparison revealed that the analysis results matched the BWIM data in 15 out of 17 cases, validating the conclusions. Furthermore, DAF values were also compared with BWIM data to assess result accuracy. The analysis covered a velocity range of 10 to 120 kmph to ensure conservative outcomes, which aligned with BWIM data for 50% of the bridge models. However, when the velocity range was reduced to 10 to 70 kmph, consistency improved, matching 15 out of the 17 bridge models.

When comparing the analysis results with existing design codes, it was found that the results align with the values used in codes that consider bridge parameters for incorporating DAF. The values in the codes tend to be on the higher side for long-span bridges and deck joint designs. However, for short- to medium-span bridges, the comparison revealed that the DAF values in the design codes are lower than what might occur on short span bridges with low frequency. Therefore, this study recommends that further research focusing on short- to medium-span bridges needs to be conducted to produce safer designs.

Hence this section emphasized the importance of incorporating both bridge span and frequency as key parameters for integrating DAF into design. It provided a deeper understanding of how these factors influence the dynamic amplification effect on bridges and offered insights into the limitations of current design codes in addressing dynamic amplification factors effectively.

Chapter 08

8 Summary, Conclusions, and Scope for future works

8.1 Summary

This section provides a summary of the key conclusions drawn from the previous chapters. The study began with a comprehensive review, highlighting various aspects of the dynamic amplification effect on bridges. It focused on factors influencing the Dynamic Amplification Factor (DAF), methods for determining DAF, and how this effect is integrated into standard design codes. This review helped identify research gaps and define the study's objectives. Based on these, a methodology was developed, and the resulting analysis offered new insights into different aspects of the dynamic amplification effect caused by traffic loading. In this section, the overview of the key insights observed from the above chapters would be mentioned and the scope of future works would also be discussed.

The literature review highlighted that the moving load method (Canadian Standards Association, 2019) has the potential to determine the dynamic amplification effect without accounting for vehicle-bridge interaction or other vehicle characteristics. To validate the model's consistency, the results from the moving load method were compared with two complex models—the half-vehicle model (Zhou, 2015) and the lumped spring-mass model (Yang, 2009) as well as a simpler model, namely the coupled model (Sadeghi, 2020). The comparison demonstrated that the moving load method produced results consistent with the two complex models and, moreover, tended to be more conservative. This indicated that the moving load method provides safer, reliable results in comparison to the other models and with respect to velocity, the DAF variations observed in the moving load method aligned well with those from the two complex models.

The comparison between these analytical models also revealed that if the moving load model is simplified further, the accuracy of the model would be reduced considerably. Additionally, when comparing the analytical models, it was evident that the moving load method was the only one capable of incorporating the largest number of bridge parameters. Therefore, the analysis in Section 4 confirmed that the moving load method can effectively be used to determine the Dynamic Amplification Factor, despite neglecting vehicle-bridge interaction and other vehicle characteristics.

8.2 Conclusions

Based on the study conducted in the thesis, the following observations and conclusions are made.

1. After establishing the consistency between the moving load method and other analytical models, the study shifted its focus to a parametric analysis to understand the influence of bridge and vehicle parameters on the dynamic amplification effect. The parameters examined included bridge span, bridge frequency, bridge damping, and vehicle velocity. For the preliminary analysis, eight bridge models were selected from existing literature. Using these models' parameters, the moving load method was applied to determine the average, maximum, and minimum Dynamic Amplification Factor (DAF) values. The bridge spans in the selected models ranged from 14 to 100 meters, with frequencies between 0.75 and 8.03 Hz. These models were chosen to represent a variety of bridges, from short to long spans and from high to low frequencies, to provide comprehensive analysis across different bridge types.
    a. From the analysis, it was found that the Dynamic Amplification Factor (DAF) values did not show significant variation with respect to bridge span, except for one model with a 25-meter span, where notable variations were observed. Aside from this model, no clear pattern emerged regarding the relationship between DAF and bridge span across the short to long span bridges studied. Even though several design codes incorporate the dynamic amplification effect based solely on bridge span, the results suggested this may not always be a reliable approach. To further investigate whether bridges of identical spans would exhibit similar dynamic amplification effects, the DAF values of two bridge models with the same spans were considered. The analysis revealed variations in DAF values between these two bridges, highlighting once again the limitations of using bridge span as the sole parameter for incorporating DAF into design.
    b. Although the bridge frequency range in the study spanned from 0.75 to 8.03 Hz, the analysis did not reveal significant variations in Dynamic Amplification Factor (DAF) values, except for one bridge model. Notably, among the models, two of them had identical frequencies but it was observed from the analysis that they produced significantly different DAF values, further emphasizing the limitations of relying solely on bridge frequency as a parameter for incorporating DAF into design.

c. Regarding the bridge damping parameter, the results aligned well with existing literature. The analysis was conducted for two scenarios: one with no damping and the other with 3% damping. The findings demonstrated that increasing bridge damping led to a reduction in the magnitude of dynamic amplification. When 3% damping was applied, the maximum dynamic amplification values decreased by 4%, while the average values showed a 3% reduction.

d. With respect to vehicle velocity, the analysis revealed that dynamic amplification values were lower at low speeds. This can be attributed to the fact that at very low velocities, the moving load behaves similarly to a static load, resulting in minimal dynamic amplification effects. The analysis of the eight models confirmed that the moving load method produced results consistent with the literature, showing both increases and decreases in DAF as vehicle velocity changed. The variations in velocity were not uniform as the DAF values rely significantly on other bridge parameters. However, a key insight regarding velocity was that the highest amplification values consistently occurred at higher velocities.

2. In Chapter 4, the moving load method results were only compared with those from analytical models. However, to develop an approach based on the moving load method, it was essential to also compare these results with dynamic load test results from the Bridge Weigh in Motion (BWIM) data. This comparison aimed to better understand the relationship between the moving load method's results and the actual effects of traffic on bridges. The analysis revealed consistency between the moving load method and BWIM results. Additionally, the BWIM data showed variations in DAF for bridges with nearly identical spans, further highlighting the limitations of relying solely on bridge span as a parameter for incorporating DAF.
3. On considering the skew angle, this was one parameter which could not be incorporated into the moving load method. Therefore, the concept was extended to a 3D finite element model in Abaqus CAE. The bridge was modeled within the Abaqus environment, and the moving load was applied using the Vdload subroutine. The skew angles analyzed included 0°, 15°, 30°, and 45°. The DAF values remained relatively stable up to a skew angle of 30°, but at a skew angle of 45°, the DAF values varied by approximately 20% compared to the case with a 0° skew angle. This result suggests that if the bridge deck has a skew angle of 45°, a factor of 1.2 should be applied to the values obtained from design codes.

4. From the literature review and the analysis in Chapter 5, it became evident that using either bridge span or bridge frequency as a determining parameter has its limitations. Consequently, an approach was developed to consider both parameters together for incorporating the Dynamic Amplification Factor (DAF) into design. The analysis included 72 bridge models with spans ranging from 10 to 50 meters and frequencies from 2.0 to 5.5 Hz. The following observations are made from the study.

    a. The results indicated that the dynamic amplification effect decreases with increasing bridge span, but this reduction also varies with bridge frequency. This variation was particularly significant for short to medium span bridges. The findings showed that maximum dynamic amplification occurs when there is a combination of a short span bridge and low frequency. This observation explained the dynamic amplification noted in a specific case during the preliminary analysis, as it was the only model exhibiting this combination.

    b. The analysis results clarified why no clear patterns were observed in the variation of DAF with respect to bridge span in the earlier phase: the short span models considered in the preliminary analysis had high frequencies, while long span bridges exhibited lower values, with frequency having minimal impact. It was only Bridge Model 03 that had a medium span with low frequency resulting in significant amplification. Ultimately, the final analysis demonstrated that while frequency variation does not lead to significant changes in DAF for longer spans, it plays a crucial role for short to medium span bridges.

    c. A comparison of the analysis results with the BWIM data showed that both the conclusions and DAF values were consistent. The results are aligned with actual dynamic load test data for 15 out of the 17 bridges tested. These clearly indicated the feasibility of using the analytical results for incorporating dynamic amplification effect into design.

    d. To integrate the DAF values derived from the proposed approach, it was essential to develop an empirical formula to determine DAF values for the purpose of design. Using the results from the analysis of 72 bridge models with the moving load method, a new formula has been suggested in the thesis through regression analysis

e. Finally, the analysis results from the 72 bridge models were compared with currently used design codes to determine if they are aligned with these standards. Since design codes incorporate both bridge and vehicle parameters for DAF, the analysis results were compared against two codes that utilize bridge parameters (Indian Road Congress, 2017) and NZTA (2013) and two that rely on vehicle parameters (Canadian Standards Association, 2019) and AASHTO LRFD (2012). The comparison with CSA-S6-19 (Canadian Standards Association, 2019) and AASHTO LRFD (2012) revealed that the design values provided were safe for deck joints and long span bridges. However, for short span bridges, some values from the analysis exceeded those specified in these codes.

f. When comparing the results with IRC6: 2017 (Indian Road Congress, 2017) and NZTA (2013), it was found that the values for long span bridges were conservative. However, for short to medium span bridges, several values from the analysis exceeded those specified in these design codes. Additionally, these codes only considered bridge span as a parameter, which led to the limitations previously mentioned. In contrast, the new approach was able to address these limitations while remaining consistent with the existing codes. It is important to note that when applying these values, a factor of 1.2 should be multiplied if the skew angle exceeds 30^0.

5. Thus, this study offered a clear understanding of the variation of DAF with respect to different bridge parameters and proposed an approach for integrating DAF into design overcoming the limitations of the existing codes, resulting in safer and more economical designs.

8.3 Scope for future research

This thesis conducted a parametric study and was able to propose an alternative approach for incorporation of DAF into design. However, it is also vital to comprehend the limitations of the study, and they are as follows:

1. The models do not incorporate the effect of road surface irregularities which can significantly contribute towards the dynamic amplification effect.

2. The comparison of the results from the proposed approach was compared only with 17 bridge models and thus more comparisons are required to validate the potential of the approach.
3. The study considered constant velocity for each case but under real traffic conditions, the velocity of vehicles tends to change frequently. In addition, the effect of acceleration is also not considered in the study.
4. With respect to variation of DAF with skew angle, only 1 bridge model was considered. To accurately evaluate the effect of skew angle on DAF, more studies are required.
5. The moving load method did not incorporate the vehicle parameters and vehicle bridge interactions and thus bridges with road surface irregularities, the values predicted by the model might be inaccurate.

To address these limitations, more in-depth studies are essential. Potential areas for future research include the following:

1. This study focused on bridge span and frequency in the proposed approach; as a next step, incorporating road surface irregularities into the moving load methodology would enhance accuracy.
2. The FEA model used a single point load to determine the dynamic amplification effect. Future research could explore the impact of multiple point loads, as actual vehicles typically have multiple axles.
3. Since the analysis utilized only a moving point load, incorporating a half-vehicle model along with surface irregularities in future FEA models could provide deeper insights into vehicle-bridge interaction.
4. Finite element modeling could also be expanded to include wind loading effects, offering a broader understanding of variations in the Dynamic Amplification Factor (DAF) in the presence of wind load.
5. The moving load method was applied only to straight simply supported bridges; extending this approach to curved bridges in future research could reveal variations in DAF for different bridge geometries.

9 References

American Association of State Highway and Transportation Officials. (2012). *LRFD bridge design specifications* (6th ed.)

American Association of State Highway Officials. (1962). *The AASHO Road Test [report].: Pavement research* (No. 816). National Academy of Sciences-National Research Council.

Australian Standard, A. (2004). 5100: Bridge Design. *Standards Australia International (SAI): Sydney*.

Azimi, H., Galal, K., & Pekau, O. A. (2011). A modified numerical VBI element for vehicles with constant velocity including road irregularities. *Engineering structures*, *33*(7), 2212-2220.

Bakht, B., & Pinjarkar, S. G. (1989). Dynamic testing of highway bridges--a review. *Transportation Research Record*, (1223).

Billing, J. R., & Green, R. (1984). Design provisions for dynamic loading of highway bridges. *Transportation research record*, (950).

Brady, S. P., O'Brien, E. J., & Žnidarič, A. (2006). Effect of vehicle velocity on the dynamic amplification of a vehicle crossing a simply supported bridge. *Journal of Bridge Engineering*, *11*(2), 241-249.

Cai, C. S., Shi, X. M., Araujo, M., & Chen, S. R. (2007). Effect of approach span condition on vehicle-induced dynamic response of slab-on-girder road bridges. *Engineering Structures*, *29*(12), 3210-3226.

Campbell, T. I., Agarwal, A. C., & Csagoly, P. E. (1971). Bridge vibraiton study. *MTC Research and Development Rep*, *172*.

Canadian Standards Association. (2019). *Canadian highway bridge design code* (CSA S6-19). Mississauga, ON: Canadian Standards Association

Cantieni, R. (1983). Dynamic load tests on highway bridges in Switzerland. *Rep*, *211*.

Cebon, D. (1999). *Handbook of vehicle-road interaction*.

Chang, D., & Lee, H. (1994). Impact factors for simple-span highway girder bridges. *Journal of Structural Engineering*, *120*(3), 704-715.

Congress, I. R. (2017). Standard specifications and code of practice for road bridges. In *Indian Roads Congress* (pp. 1-89).

Cook, R. D., Malkus, D. S., Plesha, M. E., & Witt, R. J. (2002). *Concepts and applications of finite element analysis* (4th ed.). John Wiley & Sons.

Deng, L., Yu, Y., Zou, Q., & Cai, C. S. (2015). State-of-the-art review of dynamic impact factors of highway bridges. *Journal of Bridge Engineering*, *20*(5), 04014080.

EN 1991-2. (2003). Eurocode 1: Actions on structures–Part 2: Traffic loads on bridges. *CEN-European Committee for Standardization*.

Frýba, L. (1972). *Vibration of solids and structures under moving loads*. Noordhoff International.

González, A. (2010). *Vehicle-bridge dynamic interaction using finite element modelling*. Sciyo.

Hossain, K. A., & Amanat, K. M. (2011). Effect of span length on the dynamic amplification factor in the deck of concrete box girder bridges. *Journal of Civil Engineering (IEB)*, *39*(1), 59-75.

Kalin, J., Žnidarič, A., Anžlin, A., & Kreslin, M. (2022). Measurements of bridge dynamic amplification factor using bridge weigh-in-motion data. *Structure and Infrastructure Engineering*, *18*(8), 1164-1176.

Kalin, J., Žnidarič, A., & Kreslin, M. (2015). Using weigh-in-motion data to determine bridge dynamic amplification factor. In *MATEC Web of Conferences* (Vol. 24, p. 02003). EDP Sciences.

Liu, C., Huang, D., & Wang, T. L. (2002). Analytical dynamic impact study based on correlated road roughness. *Computers & structures*, *80*(20-21), 1639-1650.

Ludescher, H., & Brühwiler, E. (2009). Dynamic amplification of traffic loads on road bridges. Structural engineering international, 19(2), 190-197.

Malekjafarian, A., Corbally, R., & Gong, W. (2022, October). A review of mobile sensing of bridges using moving vehicles: Progress to date, challenges and future trends. In *Structures* (Vol. 44, pp. 1466)

Manning, D. G. (1981). Effects of traffic-induced vibrations on bridge-deck repairs. *NCHRP Synthesis of Highway Practice*, (86).

McLean, D. I., & Marsh, M. L. (1998). *Dynamic impact factors for bridges* (Vol. 266). Transportation Research Board.

New Zealand Transport Agency. (2013). *Bridge manual* (3rd ed.). Wellington, New Zealand: New Zealand Transport Agency.

O'Brien, E. J., Znidaric, A., Baumgärtner, W., González, A., & McNulty, P. (2001). *Weighing-in-motion of axles and vehicles for Europe (WAVE) WP1. 2: Bridge WIM systems*. University College Dublin.

Ontario Ministry of Transportation. (1991). *Ontario highway bridge design code* (3rd ed.). Downsview, ON: Ontario Ministry of Transportation

Ontario Ministry of Transportation and Communications. (1983). *Ontario highway bridge design code* (2nd ed.). Downsview, ON: Ontario Ministry of Transportation and Communications.

Organization for Economic Cooperation and Development. (1998). Dynamic interaction between vehicles and infrastructure experiment (DIVINE).

Paeglite, I., & Paeglitis, A. (2013). The dynamic amplification factor of the bridges in Latvia. *Procedia Engineering*, *57*, 851-858.

Patra BK, Pradeep A, Bagchi A. (2024). Seismic analysis of skew deck slab bridges. In: Fourth International Bridge Seismic Workshop (4IBSW); Carleton University, Ottawa, Canada.

Patra, B. K., Kumar, R., & Kumar, V. (2013). Analysis of skew deck slab bridge by analytical methods. Journal of Structural and Transportation Engineering (JSTE), 1(4), 31–35. https://doi.org/10.26634/jste.1.4.2138

Pradeep, A., and Bagchi, A. (2024). Determination of Dynamic Amplification Factor in Bridges using Simple Analytical Models. Canadian Society of Civil Engineering (CSCE) Annual Conference, Niagara Falls, Ontario.

Paultre, P., Chaallal, O., & Proulx, J. (1992). Bridge dynamics and dynamic amplification factors—a review of analytical and experimental findings. *Canadian Journal of Civil Engineering*, *19*(2), 260-278.

Sadeghi Eshkevari, S., Matarazzo, T. J., & Pakzad, S. N. (2020). Simplified vehicle–bridge interaction for medium to long-span bridges subject to random traffic load. *Journal of Civil Structural Health Monitoring*, *10*, 693-707.

Schweizerischer Ingenieur- und Architektenverein. (1988). *Einwirkungen auf Tragwerke: Entwurf* (SIA 160E). Zurich, Switzerland: Schweizerischer Ingenieur- und Architektenverein.

Shokravi, H., Vafaei, M., Samali, B., & Bakhary, N. (2024). In-fleet structural health monitoring of roadway bridges using connected and autonomous vehicles' data. *Computer-Aided Civil and Infrastructure Engineering*.

Wekezer, J. W., & Taft, E. E. (2023). *Dynamic load allowance for reinforced concrete bridges*. *Journal of Structural Engineering*, *45*(2), 123-134.

Wright, D. T., & Green, R. (1964). *Highway Bridge Vibrations: Part II, Ontario Test Programme*. Department of Civil Engineering, Queen's University.

Yang, Y. B., & Chang, K. C. (2009). Extraction of bridge frequencies from the dynamic response of a passing vehicle enhanced by the EMD technique. *Journal of sound and vibration*, *322*(4-5), 718-739.

Zhou, Y., Ma, Z. J., Zhao, Y., Shi, X., & He, S. (2015). Improved definition of dynamic load allowance factor for highway bridges. *Structural Engineering and Mechanics*, *54*(3), 561-577.

10 Appendix A: Fortran code for the Vdload subroutine (for *v* = 5.56 m/s)

```
subroutine vdload (
C Read only (unmodifiable)variables -
1 nblock, ndim, stepTime, totalTime,
2 amplitude, curCoords, velocity, dirCos, jltyp, sname,
C Write only (modifiable) variable - 1 value)
include 'vaba_param.inc'
dimension curCoords(nblock,ndim), velocity(nblock,ndim),
1  dirCos(nblock,ndim,ndim), value(nblock)
character*80 sname
!dimensions of the tyre , length and width respectively
real*8 a,b
!tyre pressure
real*8 p
a=0.3
b=0.3
p=1000
slabWidth=10
vehicleVelocity=5.56
displacement=vehicleVelocity*stepTime
do km = 1, nblock
        ! in width
        if (curCoords(km,1)<(slabWidth+(2*b))/4. .and. curCoords(km,1)>(slabWidth-
(2*b))/4.) then
        ! in longitudinal direction
        if (curCoords(km,3)<displacement+a .and. curCoords(km,3)>displacement) then
               value (km)=p
        else
         value (km)=0.0
          end if
end if
end do
return
end
```

11 Appendix B: List of Publications

Journals

1. Pradeep, A., Patra, B. K., and Bagchi, A. Effect of Vehicle velocity and Skew angle on Dynamic Amplification Effect on Bridges - ASCE Bridge Engineering Journal – *Submitted, Under Review*
2. Pradeep, A., Sarkar, A., and Bagchi, A.A Novel Approach for Incorporating Dynamic Amplification Factor into Bridge Design – *In progress*

Conferences

1. Patra BK, Pradeep A, and Bagchi A. (2024 Aug). Seismic analysis of skew deck slab bridges. Fourth International Bridge Seismic Workshop (4IBSW); Carleton University, Ottawa, Canada.
2. Pradeep, A., and Bagchi, A. (2024). Determination of Dynamic Amplification Factor in Bridges using Simple Analytical Models. Canadian Society of Civil Engineering (CSCE) Annual Conference, Niagara Falls, Ontario.
3. Sankar, S. N., Pradeep, A., and Bagchi, A. (2024). Study on the Performance of Structures Located above Underground Metro Tunnel. Canadian Society of Civil Engineering (CSCE) Annual Conference, Niagara Falls, Ontario.
4. Pradeep, A., Solaimalai, G. D., Sankar, S. N., and Sabamehr, A. (2024). Anomaly detection in SHM of pipelines using statistical models. 11th European Workshop on Structural Health Monitoring (EWSHM), Germany.
5. Sarkar, A., Pradeep, A., Patra, B. K., and Bagchi, A. (2025, July 2-4). Vibration-based damage detection in RCC T girder bridges: Assessing the impact of age and span on structural integrity - (EVACES 2025), Porto, Portugal. – *Abstract Accepted*

Posters

1. Pradeep, A., and Bagchi, A. (2024). Seismic effect on skew bridges [Poster presentation]. Annual meeting of CEISCE Network, University of Sherbrooke.